N 120215

FIRST PANORAMAS OF THE LUNAR SURFACE ACCORDING TO THE MATERIAL FROM THE AUTOMATIC STATION LUNA-9

GPO PRICE $ _____

CFSTI PRICE(S) $ _____

Hard copy (HC) 3.00

Microfiche (MF) .65

ff 653 July 65



FACILITY FORM 602

N68-24855 (ACCESSION NUMBER)

130 (PAGES)

CR 94656 (NASA CR OR TMX OR AD NUMBER)

(THRU)

(CODE)

(CATEGORY)

LIBRARY COPY

SEP 1966

LANGLEY RESEARCH CENTER
LIBRARY, NASA
LANGLEY STATION
HAMPTON, VIRGINIA

National Aeronautics and Space Administration
Goddard Space Flight Center
Contract No. NAS-5-9299

ST- LPS- 10503/Sp

FIRST PANORAMAS OF THE LUNAR SURFACE ACCORDING TO THE MATERIAL FROM THE AUTOMATIC STATION LUNA-9

N68 24855

Edited by the
USSR Academy of Sciences

LIBRARY COPY

SEP 9 1968

LANGLEY RESEARCH CENTER
LIBRARY, NASA
LANGLEY STATION
HAMPTON, VIRGINIA



29 JUNE 1966

TABLE OF CONTENTS

Chapter — Page

SUMMARY 2

PREFACE 3

PART I — DESCRIPTION OF THE APPARATUS AND THE CONDITIONS OF FLIGHT 4

INTRODUCTION 4

I. CONSTRUCTION AND ON-BOARD SYSTEMS 6

1. The Lunar Rocket 6
2. The Automatic Station Luna-9 10
3. Television System 14

II. DYNAMICS AND CONTROL IN FLIGHT 20

1. Flight Trajectory 20
2. Flight Control 24
3. Correction 26
4. Deceleration 30

PART II — RESULTS OF THE STUDY OF LUNAR PANORAMAS . . . 41

INTRODUCTION 41

I. CONSTRUCTION OF THE PLAN OF THE LANDING SITE . . 43

1. Photogrammetric Method of Panorama Processing . . . 43
2. Orientation of the Panoramas 51
3. Construction of the Topographic Plan of the Locality . . 56
4. Topographic Peculiarities of the Landing Site of ALS Luna-9 63

II. MORPHOLOGICAL PECULIARITIES OF THE LUNAR SURFACE 67

1. Craterlets 69
2. Linear Structures 73
3. Stones 81
4. Generalized Model of the Landing Site 87

PART III — PANORAMIC PHOTOGRAPHS OF THE LUNAR SURFACE 95

TOPOGRAPHIC PLAN AND SCHEME OF THE LANDING SITE

*

* * *

*

ST - LPS - 10503/Sp.

FIRST PANORAMAS OF THE LUNAR SURFACE ACCORDING TO THE MATERIAL FROM THE AUTOMATIC STATION LUNA-9

(*)

Monograph, 101 pp.
50 photographs,
3 Panoramas
2 Topographic maps,
MOSCOW, 1966.

Edited by the
USSR Academy of Sciences

SUMMARY

This is the official presentation by the Presidium of the USSR Academy of Sciences of the panoramic photographs obtained by the station LUNA-9, and reproduced with documented precision. The preliminary results of their analysis are also presented here, alongside with the description of the experiment itself.

The report consists of three parts. The first part is devoted to the description of the apparatus and of flight conditions. The second part deals with the results of the study of lunar panoramas: at first, the construction of the landing site is discussed; then the morphological peculiarities of the lunar surface are examined in detail.

The third part of this report is the presentation itself of the panoramic photographs of the lunar surface, with a topographic plan and a sketch of the landing site.

*
* *

(*) PERVVYE PANORAMY LUNNOY POVERKHNOSTI PO MATERIALAM AVTOMATICHESKOY STANTSII "LUNA-9"

- Original approved for publication on 4 May 1966 and printed in 5000 copies.
- The present draft translation is printed in 200 copies for release on 1 July 1966.

PRECEDING PAGE BLANK NOT FILMED.

PREFACE

The soft landing of the automatic station Luna-9 on the surface of the Moon is an outstanding scientific and technical achievement. First of all, it became possible to investigate the microsculpture of the lunar surface distinguishing in it details of dimensions in millimeters.

Soviet cosmonautics covered a long path. On 4 October 1957, the era of space investigations was opened by the flight of the first artificial satellite of the Earth, and on 12 April 1961, man flew in space for the first time. Three lunar rockets resolved new problems in the year 1959. The first artificial planet of the solar system was created, measurements of the magnetic field and of cosmic radiation were conducted at great distances from the Earth, the surface of the Moon was reached, the magnetic field near it was investigated alongside with the radiation setup and the part of the Moon, visible from the Earth, was photographed. Later, in 1965, photographs of the still noninvestigated part of the Moon, its far side, were obtained with the aid of the interplanetary station Zond-3. Finally, on 3 February 1966, the automatic station Luna-9 effected the soft landing.

The panoramic photographs transmitted by the station Luna-9 provide material for direct scientific conclusions on the structure of the lunar surface. Near the station, inside a small crater, there is no noticeable dust layer. The soil is sufficiently hard to withstand the weight of the station. Linear structures, visible on the surface, are apparently formed by matter more resistant than the surrounding formation, while separate stones, visible in great numbers near the station, not only fail to show any evidence of having ever been covered up by drifting dust, but, to the contrary, look as if they were "outgrown" from the surface of the soil as a result of gradual disintegration.

The launching of Luna-9 and the materialization of the soft landing are the result of great labor of Soviet scientists, engineers and all the workers of the production and experimental collectives having participated in the present work.

In this work, the USSR Academy of Sciences published the panoramic photographs of the station Luna-9, reproduced with documented precision, the preliminary results of their processing and the description of the experiment itself. This is done with the view of acquainting wide circles of readers with the major success in the field of space mastering, as well as to provide all the possibilities for Soviet and foreign scientists to utilize the obtained data for the further progress of science.

Presidium of the USSR Academy of Sciences

The insufficiency of data hindered the solution of a series of technical questions, linked with the soft landing on space probes on the Moon's surface.

Because of the absence of characteristics of lunar soil, it was necessary, in particular, to build the station Luna-9, basing it on the feasibility of its landing on a soil with most different characteristics, from dust-like to rocky.

Another difficulty stems from the absence of atmosphere on the Moon, thus making it necessary prior to landing to orient the rocket relative to the lunar vertical with great precision, and then to decelerate it with the aid of jet engines. The velocity must then be decreased from 2.6 km/sec to a few meters per second.

In order to effect a soft landing the automatic station must descend on the lunar surface in a region exactly preassigned. This required trajectory correction.

This part of the work is devoted to a brief description of the setup of the lunar rocket, of the automatic station Luna-9 and its television system. Expounded also are the basic principles of flight dynamics and guidance, complemented by a diary of the flight and of the station's operation.

*

* *

CHAPTER I

CONSTRUCTION AND ON-BOARD SYSTEMS

1. THE LUNAR ROCKET

The lunar rocket is designed for the conveyance to the Moon of the automatic station Luna-9 and the assurance of its soft landing on the lunar surface.

The composition of the on-board devices and the construction scheme of the lunar rocket are determined by the problems that must be resolved by the rocket and the station from the moment of its bringing to the flight trajectory to the Moon and up to the end of the transmission of the lunar landscape's television pictures and of the results of scientific measurements.

These problems amount to the following:

—determination of the true flight trajectory after the end of the operation of the last stage of the carrier rocket, determination on the ground of adjusting data by trajectory measurements and their transmission on-board for effecting the correction;

—obtaining from the lunar rocket of telemetric information on the systems' operation and, in case of necessity, modifying by the command radioline of these systems' regimes of operation;

—trajectory correction, at which rocket orientation in space is performed with great precision, switching the motive installation on, stabilization of the rocket during engine operation, switching it off after correction and restoration of the required orientation of the rocket in space;

—determination of the true flight trajectory after correction, calculation on the ground and transmission on-board of the adjusting data for the conducting of the braking session near the surface of the Moon;

—braking and landing on the Moon's surface;

—assurance of bilateral radiocommunication with the automatic station after landing and of the transmission to the Earth of the television picture of the lunar landscape and of the surface microrelief, and also of the results of scientific measurements.

In order to resolve the previously enumerated problems the following complex of lunar rocket systems was worked out: motive installation, the orientation system, the radiotelemetering system, the guidance system by the engine and the rocket stabilization system during engine operation, the radioaltimeter, the antenna-feeder device, the systems of thermoregulation, of power feed and of on-board automation.

Design of the Lunar Rocket— The construction scheme of the lunar rocket and the completion of the design of its separate systems and devices were chosen on the basis of the requirement to assure the maximum reliability of the soft landing and to obtain the greatest possible weight of the station.

The lunar rocket (Fig. 1) consists of the automatic station Luna-9 (ALS) 1, of the motive installation, of the guidance system compartment 2 and of various instrumentation 3, 4, installed on the rocket's body.

With the view of reducing fuel consumption on the deceleration near the Moon and obtaining the maximum weight for ALS, the entire apparatus and the aggregates, required only for the flight to the Moon, are placed in compartments separating prior to deceleration. The appropriateness of it is obvious, since for full braking a substantial amount of fuel is required.

In order to ensure the minimum weight of the jettisonable compartment, their hermetic bodies are computed for only a 100 mm Hg pressure drop. Prior to blast-off, the compartment pressure on the ground is near that of the atmosphere. After lift-off, the pressure in both compartments drops gradually owing to a valve, especially opened to that effect, as the rocket rises. When it descends to 100 mm Hg, the valves close and the pressure is maintained in the course of the entire flight time to the Moon. At that pressure, a sufficient heat transfer is assured between the devices and the walls of the container.

In ALS and in the guidance system compartment, where a more intense heat sink from functional aggregates by way of convective heat exchange is required, the pressure is much higher, that is, about 1.2 atm.

The motive installation of the lunar rocket consists of a liquid-fuel rocket engine 5, of guiding engines 6 and of fuel tanks.

The tank block of the motive installation consists of a spherical tank 7, of an oxidizer and of a toroidal fuel tank 8, made of aluminum alloy. Such a form of tanks allowed to obtain for the motive installation the minimum weight and the minimum moment of inertia of the whole lunar rocket.

Two operations are required for the landing on the Moon: the correction of the trajectory and the deceleration (braking) at the surface with the aid of a retrorocket. The greatest weight of the lunar station is achieved when applying for the correction and deceleration of a unique motive installation with a rocket engine.

The engine and the fuel feed system assure a two-time switching on, in weightlessness and in operation in two regimes: at correction with constant thrust and at deceleration with a wide range of thrust regulation. Rocket engines with low thrust serve as guidance engines. They are designed for the creation of guidance moments preserving the preassigned rocket orientation in space.

The main powerstructure of the whole lunar rocket is the spherical tank 7 of the motive installation's oxidizer. All the systems and the engine are installed on that tank. This allows to coordinate the directions of their mutual installations with a precision to several minutes of arc and to maintain this precision during the entire flight, despite pressure fluctuations in the tank on account of temperature variation.

Besides, such a scheme allows to reduce to a minimum the number of coupling construction elements, and consequently to diminish the weight of the lunar rocket.

The Systems of the Lunar Rocket-- The orientation system is designed for orienting the engine in the direction given from the Earth when effecting the correction and for the orientation along the lunar vertical prior to braking near the Moon. The orientation system consists of an optical block of angular velocity counters and of computing equipment.

The complementary parts of the orientation system consist of microengines 9, operating on compressed gas, and of balloons 10 with gas reserve. The radioaltimeter 11 has its own narrow directional parabolic antenna 12.

As already stated, the astroorientation system imparts to the lunar rocket a preassigned position prior to engine operation at correction and braking. As the command is given to switch on the engine, the astroorientation system is switched off. Subsequently, during the entire time, the guidance by the lunar rocket and its stabilization are assured by a special system consisting of gyroscopic devices. Moreover, there is a device for regulating the engine thrust during braking.

During the flight to the Moon, the thermal regime of the lunar rocket and of all the systems is assured by imparting to the design ele-

ments specific optical properties, which is achieved by appropriate painting and the creation of a specific rotation regime of the rocket relative to the Sun.

The guidance by the lunar rocket in flight is materialized by both, the radioline command from Earth and by the on-board program-temporal and logical devices. The guiding by the processes, which are fundamental for the delivery of the station on the Moon and which have a sufficiently rapid course, for example, the correction or the deceleration, is conducted autonomously. Only the initial data for these processes are preassigned from the ground for they are dependent on the true trajectory parameters. On the other hand, guidance by numerous processes (in particular, all the sessions of radiocommunication in flight, designed for trajectory measurements, for telemetering the information and for the reception on-board of the adjusting data) is assured on command from Earth or on that of the airborne program device.

The radiotelemetric systems of the lunar rocket and of ALS Luna-9 assure not only the transmission of scientific information, but also the control of apparatus' operation and of the state of the various construction elements.

The temperature and pressure are measured in all the hermetic compartments. The temperature is also measured at various spots of the envelopes and inside numerous devices. The electric voltages are controlled either directly at the feed sources or upon conversion by various transformers. Transmitted with the aid of telemetry are also the signals confirming the materialization of different operations, for example, opening of antennas, separation of either parts, wear and tear of mechanisms.

Such a careful investigation of the entire apparatus' complex and more particularly of the station Luna-9 itself is necessary since one of the most important scientific problems of the experiment is the study of the character of the functioning of the apparatus under entirely new and complex conditions on the Moon, where, for example, the soil temperature in the vicinity of the station must vary during its operation by some one hundred fifty degrees as the height of the Sun increases.

The power feed of the apparatus on the lunar rocket and on ALS Luna-9 is materialized by chemical batteries. For an operation time of 3—5 days such a system is more advantageous in respect to weight than the power feed by solar cells. Besides, it is simpler and more reliable which is particularly important when materializing the first experiment of landing on the Moon.

The greater part of source of electric power feed is situated in jettisonable compartments, and only those current sources that assure the apparatus' operation over the deceleration portion of the trajectory and the operation of the station Luna-9 after landing are respectively installed in the guidance system compartment 2 and on the ALS.

2. THE AUTOMATIC STATION LUNA-9

The fundamental systems of ALS Luna-9 are situated inside the hermetic container of near spherical shape. The body of the lunar station consists of two half-envelopes.

A frame with the receiving-transmitting apparatus, radioline command devices, electronic program-temporal installations, chemical batteries, automation devices, scientific and telemetric apparatus is installed inside the body. Fastened in the lower-half-envelope are a fan, an electrovalve and a radiator of the thermoregulating system, and in the upper envelope—the television system and the cosmic radiation counters.

As may be seen in Fig. 2, there are installed outside the body four lobe antennas 1, four pivot bolt antennas 2 with brightness standards 3 suspended over them and three dihedral mirrors 4. At landing, the lobe and pivot bolt antennas are in a position allowing the transmission of the stereoscopic images of six narrow parcels of the lunar surface, and the brightness standards, having a different coloring with known reflection factors are designed to estimate the albedo of lunar formations in the landing region.

Together with the landing installations, the lunar station is fastened to the guidance system compartment of the lunar rocket.

The folded antenna lobes impart to the ALS an ovoid shape; its center of gravity is located nearer the base. Thanks to that, the lunar station acquires upon separation of the landing facilities a preassigned position on the lunar surface (lobes upward). At the same time, the lobes protect the television camera, the pivot bolt antennas, the mechanisms and the mirrors from casual damage and dusting.

About four minutes after landing, a mechanical device, designed to open the antenna lobes is triggered on command either from the program-temporal device or the clockwork (this command may be emitted from the Earth). As the antenna lobes open up, the station itself, the

pivot bolt antennas and the mirrors are brought into the operational position.

The weight of the ALS Luna-9 after landing corresponds to weight on the Earth of about 100 kG.

The station's dimensions are: from the base to the center of the television camera lens—58 cm; total height, including the pivot bolt antennas—112 cm, diameter of the circumference described along the open lobes—160 cm.

During the flight and after landing, prior to bringing up the station into its operational position, the folded lobes functions as the transmitting and receiving antennas of the meter band. The shape of the lobes is so chosen that the antenna system's radiation pattern be near circular.

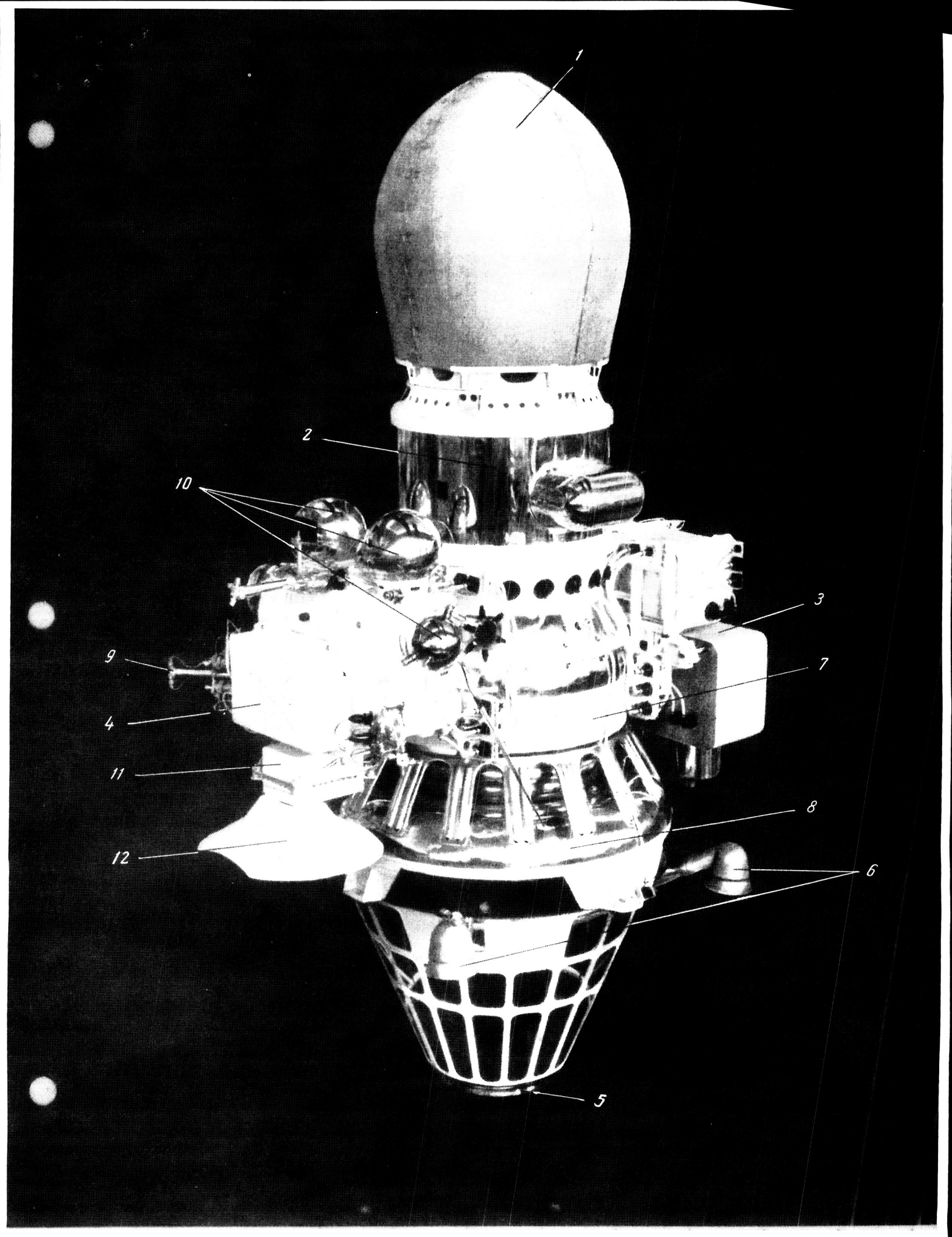
After landing and bringing up the station into the operational position, the open lobes serve only as transmitting antennas, while the four pivot bolt antennas are utilized for reception; these antennas open up after the unfolding of the lobes. The chosen placement and antenna utilization scheme assures the communication with the lunar station after landing in the case, when the lobes fail to opne up for one reason or another, as well as if the station did not assume its normal position on the Moon.

To assure the temperature regime of the lunar station after landing, the thermoregulating system is chosen such that the station be isolated to the maximum extent from the external thermal fluxes and the outside discharge of the heat emitted by the devices be assured. The protection of the station from thermal fluxes emitted by the lunar surface and the Sun is realized by a special thermic insulation on the station's body.

The thermoregulation system consists of radiators, consisting of small tanks with water of the automation block, a fan and an electrovalve.

The fan assures the heat transfer from the devices to the gas and the gas to the radiators. The automation block triggers the command for the opening or closing of the electrovalve according to the gas' factual temperature. When the valve is open, the tanks unite with the external medium and water evaporation takes place in the vacuum, which assures the diversion of heat from the radiators and the resulting lowering of the gas' and the devices' temperature. When the valve closes up, the evaporation of water and heat elimination ceases.

The thermoregulation system may operate normally at any


1
2
10
3
9
7
4
11
8
12
6
5

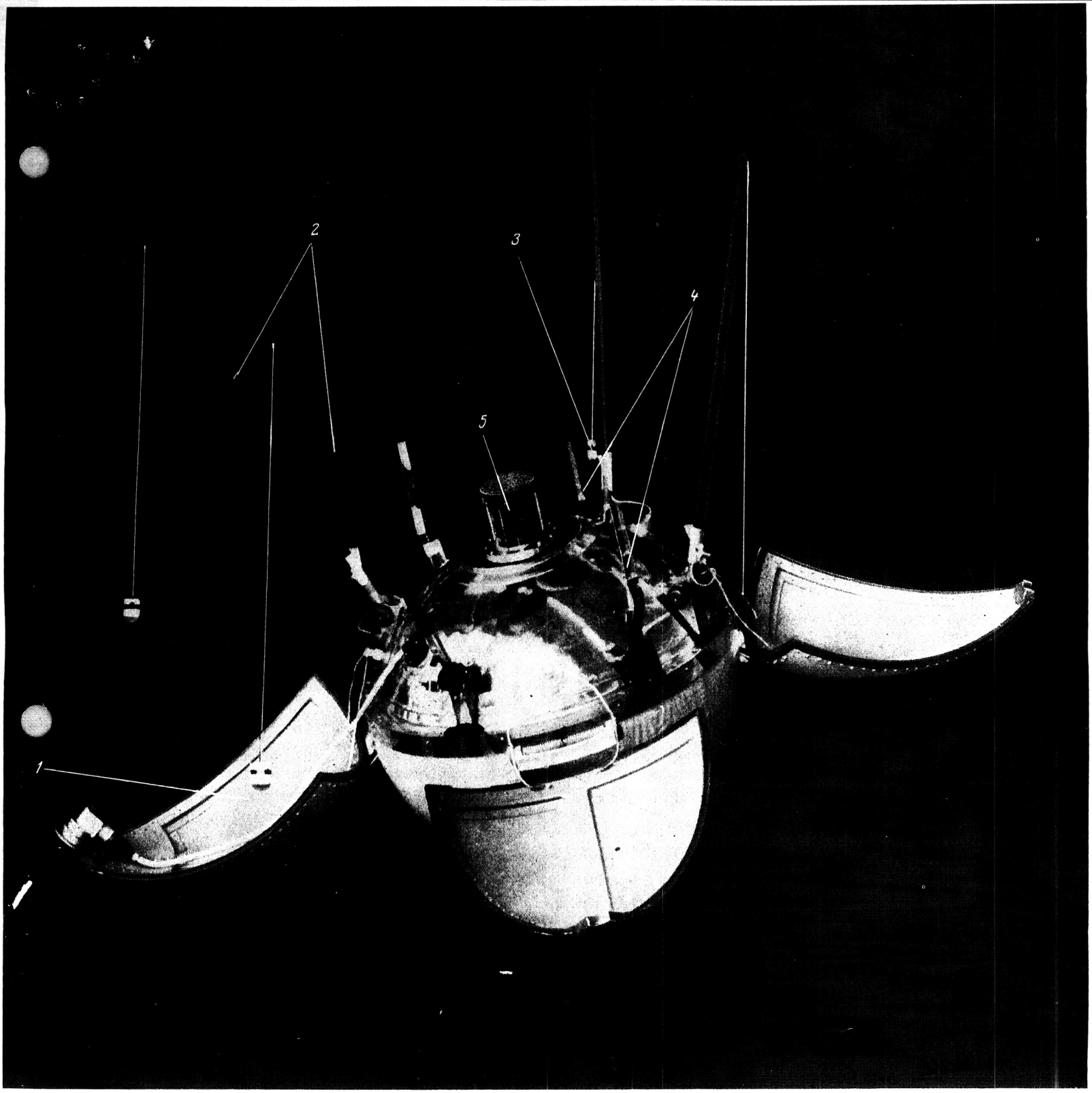


Fig. 2

The Automatic Station Luna-9

station's position relative to the Moon. To assure the thermal regime of the television camera, emerging outside the outline of the station's hermetic body, the external surface of the camera has been gold plated. This excludes the camera heating on account of the heat emitted by the lunar surface and the Sun. Moreover, for the protection from direct solar rays, a heat-insulating screen is installed in the upper part of the television camera.

3. TELEVISION SYSTEM

The image of lunar landscape was transmitted from the station Luna-9 with the aid of a special panoramic television camera installed at the center of the upper part of the ALS.

The lunar panorama, as the object of television transmission, is characterized by a series of peculiarities that have to be taken into account when working out the camera.

The characteristic trait of lunar landscape is its immobility. Only shadows from surface irregularities vary their length as a function of the height of the Sun, but this takes place relatively slowly: the duration of the day on the Moon constitutes nearly 15 terrestrial days, and that is why the height of the Sun varies only by 0.5° per hour. It is thus possible to speak in terms of immobile image transmission.

The conditions of illuminance on the Moon are well known, for in the absence of atmosphere the incident solar light flux reaches the lunar surface without absorption. However, the wide range of possible brightness of the details on the surface of the Moon, the ignorance of light reflection characteristics, determined by the microrelief, and the possibility of the station's landing under different conditions are all factors creating a substantial uncertainty. Moreover, the light flux, reflected from the surface of the Moon, depends strongly on the height of the Sun and on the direction of observation.

Both mirror shifts are effected with the help of engine 4, of which the rotation velocity is stabilized. The profile of the hammer, inducing the vertical swinging of the mirror is made such that the linear angular displacement of the mirror be assured for the line scanning period and its rapid return to initial position during a time constituting about 10% of the period. The application of the mechanical system allowed to have a scanning linearity, high and stable in time, owing to which the device could be used for measurement purposes.

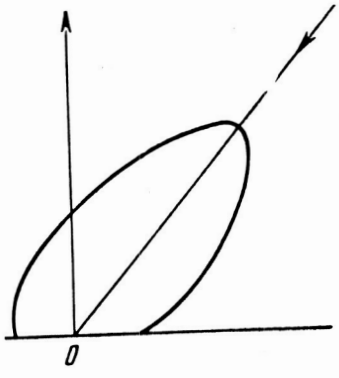


Fig. 3

Scattering indicatrix of the light diffused by the lunar surface, according toground observations

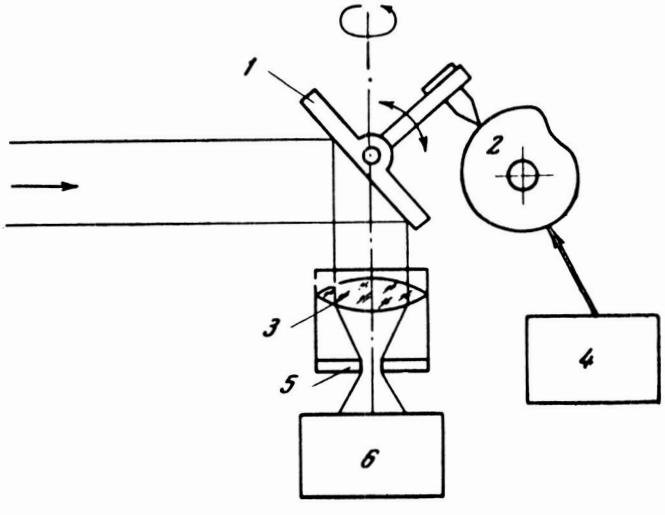


Fig. 4

Scheme of the television camera

The choice of the value of the vertical visual angle of the camera is a compromise between the striving for having the required angular resolution and yet the assurance of covering the field of vision of a sufficiently large part of the surface. The accounting of these factors and of a whole series of additional considerations allowed us to pause at the value of the vertical angle of about 29°. This angle is asymmetrically disposed relative to the plane perpendicular to the axis of rotation of the camera (18° downward, 11° upward, Fig. 5), so that the preferential transmission of precisely the Moon surface's image may be assured. For the chosen vertical angle, the ratio of the sides of the circular panorama is obtained close to 1:12.5.

One of the peculiarities of the station is the inclination by a certain angle, foreseen in its design. The base of the station and the mechanism of its lobes are made such that at their opening up, the axis of the station and alongside with it, the axis of the television camera, be inclined by about 16° to the local vertical on a sufficiently smooth horizontal. This ensures the hitting by the visual field of the camera of one of the nearest parcels of the lunar surface, and creates favorable conditions for the transmission of the microrelief image from the minimum distance to the camera. Such a parcel, with the best possible resolution on the surface, is disposed in the eastern sector of the portion of lunar surface observed from Luna-9.

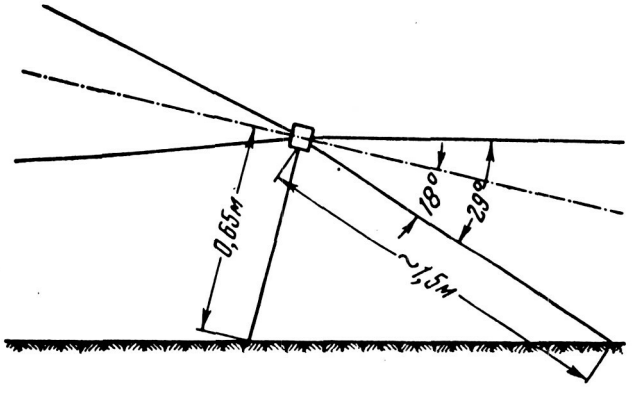


Fig. 5. - Visual field of the television camera

From the images, it may be seen that the selected vertical angle of the field of vision is near optimum. It provides the necessary representation of the general structure of the landscape and ensures the reception of high quality, easily-decipherable rendering on which microrelief details, measured in millimeters, are recognized.

The television camera of Luna-9 has the shape of a small metallic

cylinder, inside of which are placed all the required blocks and mountings (Fig. 6). It is partly installed in the body of the ALS. To ensure the thermal regime, specific steps are taken, which were already mentioned above.

In connection with the fact that the operation conditions of the camera on the Moon's surface are difficult to determine beforehand with sufficient completeness, and taking into account the limited power possibilities of the ALS, it has been necessary to assure a flexible operational guidance of the camera. With this in view camera operation has been foreseen in all regimes assigned on command from the Earth.

The scanning of the camera has the following operational regimes:

1. - Image transmission with a speed of one line per second with clockwise survey.

2. - Image transmission with the same speed at counterclockwise sweep.

3. - Accelerated transmission regime, that is, rapid swing in direct or reverse directions.

The presence of various regimes facilitates the guiding of the device, so as to be in the position to concentrate over the most interesting areas of the image with minimum time loss. The third regime is auxiliary and is not designed for image reception, but for the operational choice of the required panorama sector according to videosignal observation. The switching on of this regime may also be possible at the time when information telemetering takes place. At the same time, there is generally no time loss for the selection of the panorama area of interest to us.

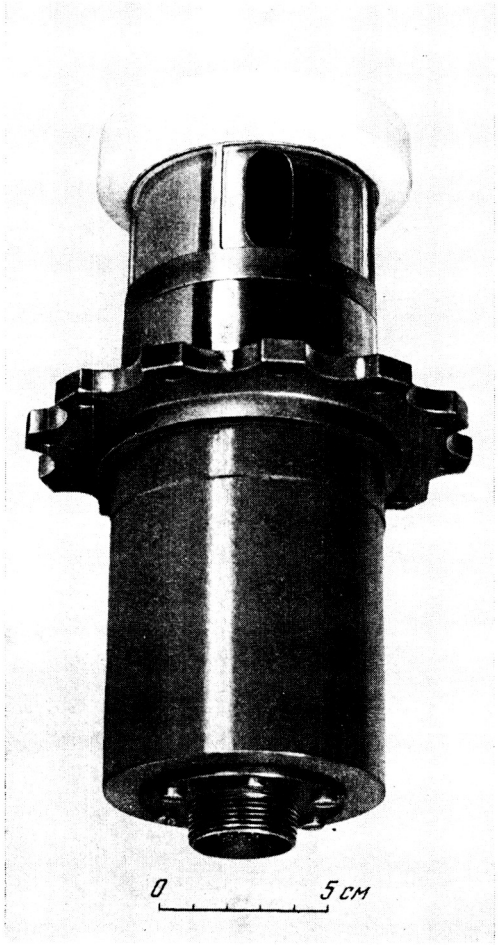


Fig. 6. Television camera

As may be seen from the optical sketch of the camera (Fig. 4), the light flux from the transmitted object hits the mirror 1 and then the diaphragm 5 forming the image element after having passed through the lens 3.

The dimensions of the diaphragm determine the resolution of the de-

vice, which in the Luna-9 variant constitutes 500 elements in one line, or about 0.06° per single television element; this is controlled during ground tests of the device with the aid of a special experimental table, that is, a dash black and white target. The errors of the mechanical scanning device do not exceed one third of a single television element. The camera has the capability of distinguishing details of 1.5 — 2 mm dimensions from a distance of 1.5 m. With available panorama side ratio, 600 lines are transmitted to the full circular panorama in order to obtain an identical resolution in the vertical and horizontal directions.

When the orientation of the ALS is normal, the nearest portions of the lunar surface will be located at a distance of about 1.5 m from the camera. This is why the camera objective is focused to ensure sharp image transmission from the distance of 1.5 m to infinity. As may be seen from the images obtained, even the nearest objects, that is, the parts of the lunar station itself, are sufficiently clearly transmitted.

After the diaphragm, located in the focal plane of the objective, the light flux from the object is registered by the light receiver 6 (Fig. 4), which converts it into an electric signal. This signal, determined by the brightness of the object, hits the ALS transmitter after a series of transformations, and is then transmitted to Earth.

The transmission took place in the frequency of 183.530 Mc with the use of radiosignal frequency modulation method. For optimum tuning of the communication channel, the depth of frequency modulation could be varied on command from the Earth.

The radiosignals of the station Luna-9 were received by a special radiocommunication center from which was separated the image signal registered on a film and magnetic tape. The registration on film in the form of panorama image was conducted on drum-type photo-telegraph equipment in which one revolution of the cylindric drum, covered by a photofilm, corresponded to one line of the image, whereas the displacement of the registering light-optical head along the drum's generatrix corresponded to the panoramic scanning.

Special devices assured synchronous and inphase operation of the ground registering equipment and of the television camera of Luna-9. The errors of registration, introduced at image reception, in parts of geometric distortions and resolution, were neglectingly small.

The uncertain luminosity condition of operation of the device has compelled us to work out a system of automatic regulation of camera sen-

sitivity (ASR). A photoresistor, ahead of which a limiting blind is installed, serves as the ARS system's sensor. The photoresistor is situated in the upper part of the optical-mechanical scanning device and it rotates with it. It reacts on average illuminance in a 10^{o} by 10^{o} visual field, about coinciding with the lower part of the panorama. The sensor's visual field limitation is rendered necessary for diminishing the experimental errors, of which the most important sources are the "black" lunar sky and the solar shine.

In connection with ASR system's tuning being performed in terrestrial conditions, which obviously differ from lunar, and to exclude a possible error while increasing the reliability of the device, ground control of ARS system's operation has been introduced. One of the commands improves the device's sensitivity by comparison with the nominal, the other diminishes it.

The camera with ASR assures the transmission of a quality picture in the illuminance range from 80 to 150 000 lux.

The ASR justified itself in practice; this may be seen from the pictures received, which are characterized by uniform density about the entire panorama. At the same time, the influence of reflection properties of strongly dug up surface is well noticeable by the darkening of parcels situated on the horizon by comparison with the forward plane.

During transmission the Luna-9 camera did not have to interfere with ASR system's operation. The command for sensitivity increase was conducted for experimental aims during the first session and for a limited time: on the first panorama $\gamma = 69 \div 133$, shadowed at Sun's 7^{o} height, was transmitted with increased sensitivity during the first session.

CHAPTER II

DYNAMICS AND CONTROL IN FLIGHT

1. FLIGHT TRAJECTORY

The general flight scheme consists of several fundamental stages. In the first stage, the lunar rocket, together with the accelerating stage, are put into a near-terrestrial orbit with the help of the carrier rocket. After engine switch-off, both the rocket and the satellite envelop the Earth. The guidance system is prepared for starting from orbit. The accelerating stage is switched on at the preassigned moment of time. At the end of the portion of trajectory, when the rocket attains the required velocity, the engine is cut off and the lunar rocket separates from the accelerating stage. Thus begins the portion of passive flight to the Moon. The telemetric control of on-board systems is achieved from ground points and measurement of rocket motion parameters is conducted. The measurement data flow into the computing centers, where by way of mathematical processing of trajectory measurements, the parameters of the actual motion trajectory are determined.

When the trajectory is determined with sufficient precision, the magnitude and the direction of the correcting impulse are computed. The tuning of the on-board system of lunar rocket guidance is materialized by the command radioline. Trajectory correction is achieved at the given moment of time: the engine is switched on as a result of which motion parameters are modified.

After correction the trajectory assures the rocket's hitting the preassigned region of the Moon. Over the trajectory following the correction trajectory measurements, checking of correction's completion and refinement of actual motion parameters are carried out. At rapprochement with the Moon the on-board guidance system is prepared for carrying out the deceleration. The flight is completed by rocket braking and by landing of the automatic station on the surface of the Moon.

When projecting the lunar rocket, one must resolve entirely new problems in outer space practice: the deceleration and braking near the Moon's surface and the station's soft landing. The requirement of reactive braking of the rocket is obvious, for there is no atmosphere on the Moon.

Analysis of the different variants of deceleration has shown that most reliable and therefore desirable for the first experiment is the vertical deceleration variant. In such a case, it was required that at the time of approaching the Moon the relative velocity of the station be directed approximately toward the center of the Moon. This allowed a simplification of the landing system.

Choice of Power-Optimum Trajectories— The distances from the Earth to the Moon for its various positions in the orbit constitute 360 to 407 thousand km. To attain these distances in conditions of passive flight directly after after its bringing into the flight trajectory to the Moon, the velocity of the rocket must be greater than a specific minimum value.

If the velocity exceeds this threshold, the trajectory of the rocket intersects the sphere of radius equal to the distance to the Moon from the center of the Earth. When the blast-off time of the carrier rocket from the Earth varies, this intersection point shifts parallelwise to the terrestrial equatorial plane, for at that time, the trajectory, as a hard line, turns together with the Earth around its axis of rotation. On the other hand, the variation of blast-off time from the AES orbit, leads to trajectory rotation in the plane of that orbit. At the same time, the point of intersection of the sphere by the trajectory shifts along the arc of the great circle, constituting an angle i with the equatorial plane, equal to the inclination angle of the AES orbit to the equator. This is why the fulfillment of conditions for hitting the Moon can be arrived at by properly choosing the take-off time from the ground and the time of acceleration rocket blast-off from the AES orbit. Then too, by varying the initial velocity, it is possible to obtain trajectories with different flight times to the Moon. The selection of flight is mainly determined from the condition of power expenditure optimization.

In the simplest case of a one-stage rocket, the fuel consumption increases exponentially with the rise of the velocity, which is imparted to the rocket by the engine. For multi-stage rocket systems, the initial to final weight ratio is more complex to determine, whereas the power difficulties of the space flight may always be estimated by the aggregate velocity that must be imparted to the payload to the engine over all flight stages.

In the problem under consideration, the engines impart the velocity to the rocket several times: at placing into the orbit of an AES, at firing from that orbit, at trajectory correction and at deceleration prior to landing.

Compiled in Table 1 for illustration are the respective values of

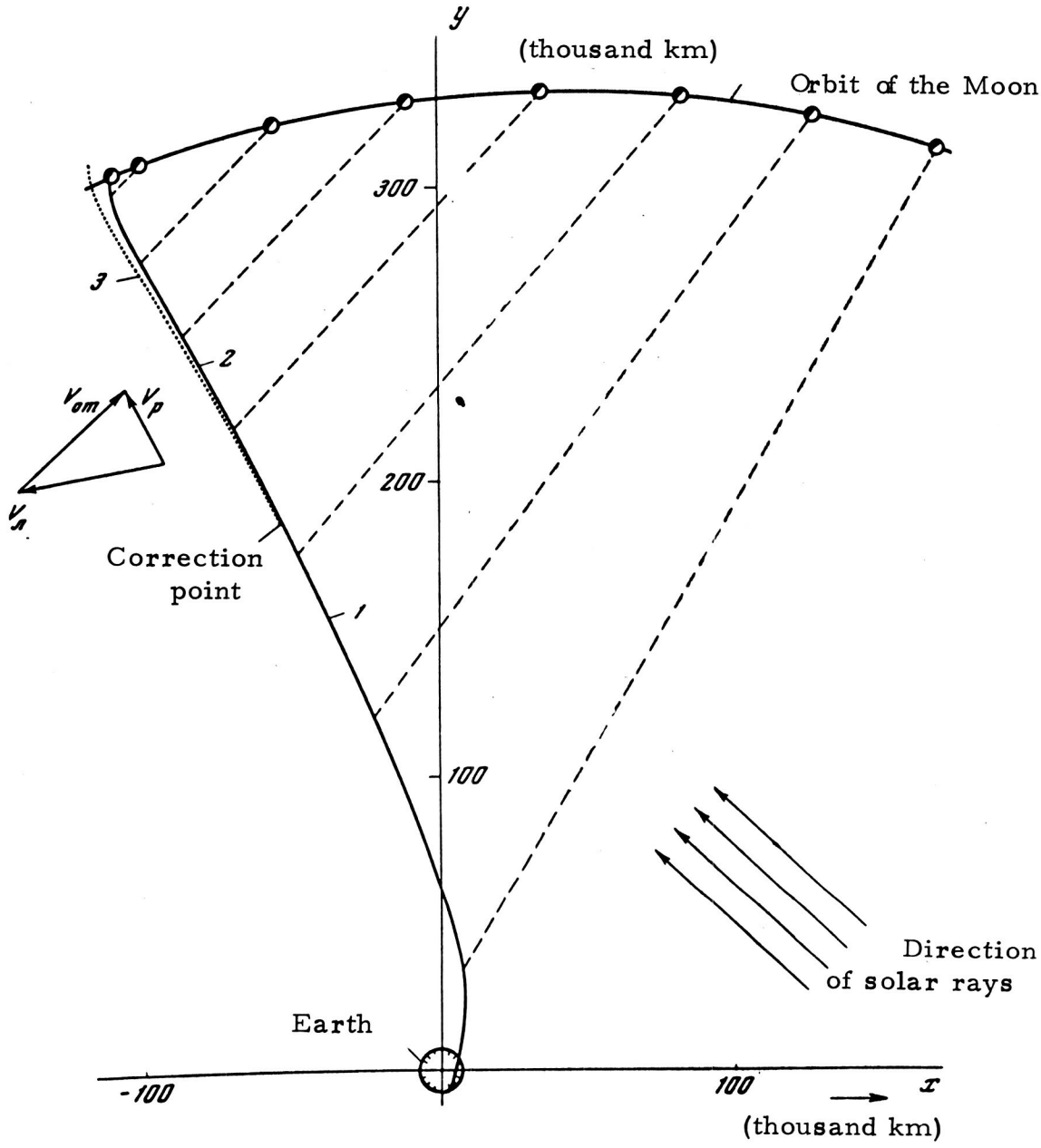


Fig. 7

Projection of Luna-9 trajectory on the plane of the terrestrial equator

Table 1

T days	v m/sec	v_T m/sec	$\frac{\Delta d \text{ km}}{\text{m/sec}}$
2	10 995	2900	380
	10 920	2625	1000
	10 907	2540	1800

the velocity v at the beginning of the passive portion near the Earth and the deceleration velocity v_T near the Moon as functions of the flight time T to the Moon.

With the decrease of the flight time both quantities v and v_T increase. If we disregard the requirement of motion correction, the trajectories with maximum possible flight time require a minimum fuel expenditure. However, with the increase of flight time to the Moon, the influence of bringing out errors on the magnitude of the miss increases notably. The values of failure Δd near the Moon for an error of 1 m/sec are shown in the last column of Table 1. The accounting of fuel expenditure for the correction, which should rectify the bringing out of errors, has shown that most advantageous from the energetic viewpoint are the trajectories with flight time to the Moon equal to 3—4 days and nights.

At final selection of the trajectory, the condition of favorable visibility of the Moon from specific points, located over the territory of the Soviet Union, during the deceleration time of the rocket and immediately upon the station's landing, was also taken into account.

Landing Region on the Moon and Date of Take-Off—The flight trajectory of Luna-9 and a portion of the orbit of the Moon are shown in Fig. 7 in projection on the terrestrial equatorial plane. The positions of the rocket and of the Moon for the same moments of time are joined by dashed lines. The latter just about coincide with the direction along which the rocket rapprochement with the Moon took place, that is, with the direction of the relative velocity v_{rel}. At greater distances from the Earth, the rocket shifts by about the radius, traced from the center of the Earth. The angle of that relative velocity with this radius depends mainly on the magnitude of rocket velocity v_r, as well as on the velocity v_M of the Moon, which is about 1 km/sec and which is directed perpendicularly to the radius traveled from the Earth to the point of rapprochement. As to the magnitude of rocket velocity v_r at its rapprochement with the sphere of action of the Moon, where the lunar attraction only begins to manifest itself notably upon the rocket, it is determined by the initial velocity. For a trajectory with flight time to the Moon of the order of three and one half days, it is about 0.5 km/sec. This is why for such trajectories the relative rapprochement velocity is directed at nearly a 60—70° angle to the direction Earth-rocket.

The condition for nearly vertical landing requires that at rapprochement with the Moon the relative velocity vector be directed approximately at the center of the Moon. The lunar attraction then modifies the value of relative velocity but does not practically change its direction. This is why the final rapprochement with the Moon takes place at an angle of 60—70° to the line Earth-Moon.

Hence, it follows that for trajectories with flight time to the Moon of the order of 3 and 1/2 days under conditions of nearly vertical deceleration the angle between the directions from the center of the Moon to the point of landing and to the Earth will constitute some 60—70°, that is, for the terrestrial observer the landing point must be situated at the western part of the visible disk of the Moon. Depending upon the Moon's position on the orbit on account of the Moon's libration and the eccentricity of its orbit, the point of landing shifts even at precise vertical deceleration, remaining in a region with selenographic coordinates 50—79° east longitude and 0—16° north latitude. Other coordinates may also be obtained for an inclined deceleration.

In order to obtain the most favorable photographing conditions for the lunar surface and for the solution of the problem of assuring the thermal regime of the automatic station, the landing was planned in the region of the morning terminator.

Hence, it follows that the angle between the radii, traced from the center of the Moon to the landing region and to the Sun, must be near 90°; at the same time, in the landing region the Sun must be to the East. Consequently, the angle between the directions from the center of the Moon to the Earth and the Sun must constitute about 20—30°. This determined in its turn the position of the Moon in its orbit for the given month at the moment of time of rapprochement with the rocket, and consequently, the date of arrival to the Moon and that of carrier rocket blast-off.

The relative disposition of the Earth, the Moon and of the Sun recurs with a period equal to the synodic lunar month, that is, approximately every 29.5 days. Consequently, the take-off dates, satisfying the enumerated conditions recur with the same periodicity.

2. FLIGHT CONTROL

General Orientation—Program-temporal, logical and computing devices have been installed on-board the rocket. These devices automatically controlled a whole series of operations required for the solution of flight problems. Their operation was coordinated with the lunar rocket and Luna-9 guidance according to the flight scheme and on command from the Earth.

The communication session was switched on from the control center according to a program worked out beforehand. During these sessions telemetric control of the state of on-board devices and the correctness of the on-board automation was carried out.

For conducting the preassigned operations, separate systems of automatic rocket guidance could be switched on by the command radioline. The tuning of on-board systems was made with the aid of the same radioline. In case of necessity, such a scheme would allow the intervention in the operation of the on-board systems.

Trajectory Measurements and Orbit Determination— The refining of the actual flight trajectory after bringing out the spacecraft is a problem which is resolved systematically starting from the first Earth satellite. This is usually required for controlling the precision of bringing out into orbit the forecast of further motion, or the tying of scientific measurement data to the spot in space. The solution of this problem for landing the automatic station on the Moon's surface was a factor of flight control. The magnitude and the direction of the correcting impulse, designed to modify the flight trajectory in such a way as to guarantee the preassigned rocket's rapprochement with the Moon, were determined according to the trajectory refined after the bringing out. Starting from the motion parameters determined by the refined trajectory, the tuning of the on-board automation was also carried out. The commencement time for the session of the rocket's preparation for deceleration near the Moon was assigned according to the trajectory, defined after correction.

The flight trajectory refinement after bringing out the rocket and after correction was mainly conducted according to radioengineering measurement data. Special radiocommunication sessions from a few points situated on the territory of the Soviet Union, were devoted to measurements of the distance to the rocket, of the radial motion relative to the point, of the angular coordinates of the rocket relative to a specific system of coordinates, linked with the given point. These data were transmitted automatically by special telegraphic lines to the computing centers. Measurements were included into the mathematical processing which was carried out with the aid of electronic computers.

Besides radioengineering measurements, parameters, measured by optical means, were also utilized in the problem of trajectory determination. The photographing of the lunar rocket against the stellar background allowed an independent determination of the rocket's angular coordinates.

3. CORRECTION

The first flights of Soviet rockets to the Moon were conducted without trajectory correction. The precision in the bringing out into orbit the second cosmic rocket for the purpose of hitting the Moon as well as for flying past it and photographing its surface was sufficient for conducting these experiments.

For direct hitting of the preassigned region of the Moon and a nearly vertical rapprochement with its surface, substantially higher precisions were required. It was not then deemed appropriate to set forth to the control system any too severe requirements for bringing out the rocket near the Earth but rather to conduct over the initial flight stage the determination of the actual trajectory according to measurements, and then to materialize with the aid of the orientation system and the motive installation the required trajectory correction, that is, to correct the bringing out errors.

The trajectory correction may be viewed as a jump-like variation of the velocity vector. Three velocity vector components of the correction velocity are three control parameters that could be used for the materialization of the preassigned rapprochement with the Moon. With the aid of a single correcting impulse (three free parameters) it was possible not only to assure the rocket's rapprochement with the preassigned region of the Moon but also to modify the duration of the flight to the Moon. The latter was not foreseen, since the possible variations of flight duration on account of bringing out errors near the Earth are rather small.

Analysis of the problem has shown that the optimum vector of the correcting impulse must be near the plane perpendicular to the ray rocket-Moon. This property was found to be convenient for the instrumental materialization of engine orientation at correction.

Choice of Correction Time—In unison with the program of flight, the trajectory correction was effected on 1 February 1966 at 22 29 hours Moscow time, when the station was at the distance of 233 000 kilometers from the Earth and 190 000 km from the Moon.

Several considerations determine the choice of the correction point on the trajectory. After bringing out into orbit, it is necessary to determine the actual flight trajectory with sufficient precision and reliability: to conduct measurements of trajectory parameters, processing them on computers, to calculate the correction assignment and to transmit it on-board the rocket. The precision in trajectory determination increases with the length of the portion over which motion parameter measurements are made. If for an ideal completion of correction the preci-

sion for rapprochement with the Moon cannot be of higher value than that of knowledge of the actual flight trajectory. Another factor, on account of which a later materialization of correction is deemed preferable, is the impossibility of realizing a computed correction with ideal precision. The influence of errors resulting from the correction of errors in velocity variation in magnitude as well as in direction on the miss near the Moon decreases as the rocket gets nearer to the Moon.

An opposite requirement brings forth the condition of optimum value of the correcting impulse. For illustration, we compiled in Table 2 the correction velocity vector, rectifying the miss near the Moon by 10 000 kilometers, depending upon the distance of the correction point from the Moon.

It may be seen from Table 2 that the power consumption for the correction of the same bringing out errors increases substantially as the station approaches the Moon.

TABLE 2

Distance from the Moon, in 1000 km	Correction velocity for a 10000 km miss in m/sec
300	28
200	46
100	140
50	200

The performing of the correction at the distance of 190 km from the Moon was the result of a compromise decision in which besides the indicated causes, others too were taken into account.

Engine Orientation—In order to realize the preassigned engine direction in space at correction as well as the end of the flight prior to deceleration, an astronavigation system was installed on-board the rocket. Optical visors, logical and computing devices, angular velocity sensors and microengines operating on compressed gas were part of the system; with their aid the moments of forces for the materialization of the required orientation and stabilization of the rocket relative to its mass center could be obtained.

The Sun, the Moon and the Earth were chosen as the supporting luminaries. Up until now the Sun and the star Canopus, that is, sufficiently remote objects served as supporting luminaries in the flights of Soviet and American space probes to Venus and Mars. The orientation by close luminaries, such as the Earth and the Moon, has certain advantages. A greater reliability should be noted when performing the operation search for luminaries: this is linked with the greater brightness of these objects. Besides, the astronatigation systems, operating with comparatively close heavenly bodies, allow not only to realize the required engine orientation, but also to measure the coordinates of the rocket relative to the planet to-

ward which it flies.

The preparation to effecting the correction began by automatic orientation at the Sun of one of the rocket's axes. The signals from sensor systems disposed on the rocket, entered the computing-resolving device, which materialized the control of the microengine operation.

A rough orientation insured the penetration of the Sun into the optical visor of precise solar orientation. After one of the rocket axes was stabilized at the Sun, the search for the Moon began by rocket rotation near the axis.

Tuning-in of the Orientation System— The tubes of the optical sensors have comparatively small visual fields from one to several degrees. In order to obtain that the Moon hit the visual field of the lunar sensor during the rotation around the axis directed at the Sun, the required angle between the solar and lunar visors must be insured beforehand.

The preliminary tuning in of the astronavigational system is conducted on the ground. The mutual disposition of luminaries is determined by the computed trajectory for the planned orientation times, and the tubes are installed on the basis of these calcualtions.

The final system's tuning-in is materialized in flight. The orientation system's operational scheme is such that its retuning by some parameters is always required, whereas only its possibility is foreseen by other parameters. After the actual trajectory has been determined according to measurement data, a new computation is performed. If the position of the rocket relative to luminaries is found to be essentially different from that, on the basis of which the ground tuning-in of the system was computed, a retuning is carried out with the aid of the command radioline.

The required tube axis rotation, determined by calculation, is coded to the Earth in the form of a dual number. This number is transmitted to the rocket and is memorized by the airborne counter. Then, on command from Earth (or with the aid of the computing-resolving device), the tube rotation is realized on-board.

During the flight of Luna-9, in particular, the angle between the lunar and solar visor, established on the Earth, was not subject to modification, for the correction was performed at a prearranged time, and the rocket's bringing out near the Earth was achieved with sufficient precision. However, the possibility of the astroorientation system's retuning was there,

which allowed, in case of necessity, to conduct the correction under conditions of rougher bringing out or at another moment of time.

When the Moon hits the visual field of the sensor and the rocket is stabilized, the system allows the measurement on-board of the actual angle between the Moon and the Sun. This angle is transmitted to Earth in coded form. The coincidence of its value with the precomputed one allows the verification of both, the correctness of astronavigation system's operation and the accuracy in the determination of the actual flight trajectory.

The orientation at the Moon and the Sun of tubes, whose position relative to the rocket is known, permits the tying of the rocket's axis to the absolute system of coordinates at any moment of time. The astronavigation system relative to the rocket was installed in such a way that at the m9ment of time, when the Sun and the Moon were both in the visual fields of the respective visors, the engine be directed nearly perpendicularly to the direction toward the Moon.

To realize the given direction in space of the correcting engine, it was necessary to materialize its turn relative to the axis rocket-Moon. The mangitude of the turn was determined on the ground by the refined flight trajectory and it was also transmitted on-board.

Control of Engine Operation— To materialize the rocket orientation relative to its mass center in conditions of passive flight, only small moments of forces are required of microengines. At engine switching on there appear disturbances linked with the impossibility of obtaining an ideal coincidence of the engine's line of thrust and of the rocket's mass center. This is why, prior to engine switch on, the astronavigation system transfers the stabilization functions to another system. The system of coordinates and the position of the rocket are memorized by gyroscopic devices. The moments of forces, with the help of which the required rocket orientation is maintained, are created by special, rather small rocket engines.

Simultaneously with engine switch on began the operation of a device which integrates the acceleration. When the acceleration integral (imaginary velocity) along the rocket's axis has reached the preassigned value, the engine switch off takes place. The computed value of the imaginary velocity was determined on the ground by the actual flight trajectory and was transmitted on-board beforehand prior to the correction session in the form of a coded number.

4. DECELERATION

Upon correction, several sessions of trajectory measurements have been conducted. The mathematical processing of these measurements on electronic computers permitted the verification of the precision of correction performance, and to determine the motion parameters over the portion of rocket rapprochement with the Moon. The tuning-in of the system's parameters for further automatic control of landing were determined with the aid of computers.

Six hours prior to landing the respective initial data of the installation were transmitted on-board the station by means of the radioline.

The session of the rocket's preparation to deceleration was begun on radioline command about two hours prior to rapprochement with the surface of the Moon. The order of subsequent operations was determined by the automation of the on-board devices. The first stage of rocket orientation was analogous to the one during correction. As a result, the rocket was found to be stabilized at the Moon and the Sun.

Then, a special optical visor began the search for the Earth. After the $E_a$rth had hit the visor's visual field, the logical device of the system controlled the constant tracking of the Earth by this visor over the extent of the subsequent motion.

These operations were completed about ten minutes prior to the passage of the lunar rocket at a point situated at the distance of 8 285 km from the center of the Moon.

The problem of deceleration consisted in decrease practically to zero of the rocket's motion velocity relative to the Moon. Let us recall that at rapprochement the velocity was about 2600 m/sec. This could naturally be obtained only on the condition of engine orientation along the direction of the relative velocity.

Analysis has shown that at deceleration the rocket is oriented in space by the computed trajectory, the magnetude of the lateral velocity component at the end of the deceleration is likely to be found very great. It will be about proportional to the deflection of the actual point of the Moon's surface crossing by the trajectory from the calcuated one; at the same time, a lateral velocity of the order of 40 m/sec corresponds to a 100 km deflection; this means that such a deceleration scheme would be subject to very high requirements as regarding the precision of trajectory knowledge after correction.

The solution of this problem is linked with the utilization at deceleration of the method of engine orientation along the lunar vertical. Fig. 8 represents schematically the surface of the Moon of which the center is at the point O. The line AMO represents the computed trajectory, approaching the Moon perpendicularly to its surface. The curve SS' is the actual trajectory for which the point of intersection with the lunar surface is the distance l from the computed, which is equal to the length of the arc MN. The arrow NV points at the direction of the relative velocity near the surface of the Moon.

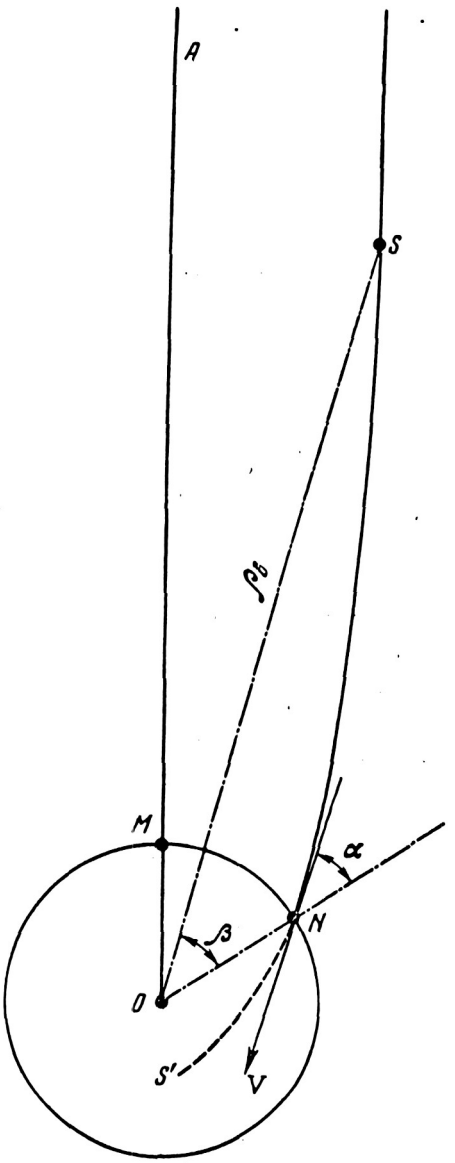


Fig. 8
Explanation of the deceleration scheme.

The picture of Fig. 8 is a plane picture. However, the point N may be displaced in any direction from the computed point M. The combination of the possible trajectories with various positions of the point N forms a pencil of trajectories, which in the first approximation has for small values of the miss, an axial symmetry with the axis AM.

Analysis has shown that for a pencil of trajectories with a specific selenocentric energy h it is possible to indicate a particular distance from the Moon ρ_b, a function of h. For any pencil trajectory and significant values of the miss l the direction from the point S distant by to the center of the Moon O will be in practice little dependent on the direction NV of the relative approach velocity when moving over this trajectory. This property was put to use for the orientation of the rocket at deceleration. The fundamental idea consists in engine orientation toward the center of the Moon over a distance computed beforehand and in the maintenance of this orientation till the beginning of deceleration. In the case of the flight of Luna-9, it was assumed $\rho_b = 8285$ km. For illustration, we compiled in Table 3 the values of the angles $\alpha, \alpha - \beta$

TABLE 3

l, км	α, deg	$\alpha-\beta$, deg	v_6, m/s
60	1,1	0,006	0,3
100	2,2	0,012	0,5
200	4,5	0,026	1,1
300	6,9	0,054	2,5
500	11,4	0,103	4,7

and the value of the lateral velocity v_l at the end of deceleration as a function of the miss l. These quantities are computed for $\rho_b = 8285$ км.

After passing the given height φ_4 the tracking of the Moon ceased and the orientation of the rocket was maintained with the help of the tracking of the Earth and of the Sun with the aid of the respective optical sensors.

In order to obtain the required orientation by the moment of time of the beginning of deceleration, it was necessary to maintian the orientation at the time of fixing the lunar vertical in the absolute system of coordinates. Inasmuch as the Earth shifts in this system of coordinates during the flight time prior to deceleration, it was found to be necessary to take these effects into account in the form of corrections relative to optical visors during engine installation.

Prior to engine switch on and for a timely beginning and conducting of the deceleration, it is necessary to be aware of the rocket altitude above the Moon with high precision over the last portion of the trajectory.

To that effect, a radioaltimeter was placed on-board the rocket, the antenna axis of which being oriented parallelwise to the axis of the engine.

The radioaltimeter fixed the moment of passage of the preassigned altitude of about 75 km above the landing point. This measurement constituted the signal for the beginning of the deceleration cycle.

The engine was switched on after altimeter signal according to a precalculated time. Just as for the correction, the guidance and the control of rocket stabilization in the process of engine operation was realized by a special gyroscopic system. At the very outset of engine operation, the apparatus, already not required for further flight, was separated from the rocket. Its weight was thus alleviated by 300 kg. This allowed to deliver to the Moon a station of greater weight.

At correction the guidance system must have insured only the preassigned velocity variation in magnitude and direction. At landing, it was necessary to realize not only the computed resulting velocity at the end of

the deceleration i. e. the integral of acceleration, but also the law of variation of that velocity. At the end of deceleration this requirement was the consequence of the necessity to emerge at the preassigned height above the surface of the Moon with sufficient precision.

The time-table of operations performed by the automatic station Luna-9 is compiled in Table 4, in the following pages, and it is illustrated in Figures 9 and 10.

END OF PART 1

TABLE 4

No.	Date and Time	Operation
	31 January	
1	15 h. 53 min. 21 sec.	End of operation of the last stage of the carrier-rocket; separation of the lunar rocket from the last stage; switching on the program-temporal device.
2	16 h. 46 min. 16 h. 56 min.	First session of trajectory measurements and recept. of telemetry data. Switch on of receiving-transmitt. radio-apparatus, of the ventilation system and of telemetry blocks. Trajectory measurements (determination of remoteness and of topocentric coordinates by radioengineering means, i. e. azimuth and spot angle. of the lunar rocket and telemetering of scientific data and of the information on temperature and pressure inside the various compartments of the lunar rocket and the operation of its equipment.
3	17 h. 57 min.	Imparting rotation to the lunar rocket so as to insure a normal thermal regime for all its components.
4	18 h. 19 min.	Trajectory measurements and reception of telemetric data; switching on the astroorientation system and the control of its work.
5	23 h. 15 min.	Trajectory measure, emts and reception of telemetric data.
1	1 February	
6	4 h. 45 min.	Trajectory measurements and reception of telemetric data
7	15 h. 36 min. 15 h. 52 min.	Radiocommunication session, in which, besides the carrying out o of the same program, on board time control took place.
8	20 h. 09 min.	Radiocommunication session. Tuning the on-board systems for correction. Control of the correctness of data introduction into the on-board program-temporal device. Reception of temetered information on the state of the main systems of the lunar rocket.
9	21 h. 16 min. 23 h. 14 min.	Session for trajectory correction Checking the on-board time. Measurements of radial velocity. Rough and then precise solar orientation. Opening of lunar rocket's blinds and orientation at the Moon.

TABLE 4 (continued)

No.	Date and Time	Operation
		Heating of the control system Operation of the motive installation in the regime for correction. Automatic engine switching off on command from the acceleration integrator. Measurement of the radial velocity after the of operation of the motive installation. Control of the completion of operations and of the state of on-board devices for the entire session.
	2 February	
10	01 h. 36 min. 01 h. 46 min.	Session of trajectory measurements and of reception of telemetric information.
11	16 h. 16 min. 16 h. 31 min.	Radiocommunication session, trajectory measurements, telemetry control and brief tentative switching of ALS television apparatus.
12	22 h. 42 min. 22 h. 59 min.	Trajectory measurements, and reception of telemetry data.
	3 February	
13	01 h. 22 min. 01 h. 28 min.	Ibidum.

No.	Date and Time	Operation
14	15 h. 34 min. 16 h. 31 min.	Tuning the on-board systems for deceleration. Control of the state of the on-board systems and of the accuracy of data introduction into the program-temporal device.
15	19 h. 28 min.	Beginning of the last radiocommunication session prior to landing - deceleration session. Switching on the apparatus assuting the control of the lunar rocket at deceleration time. On board time checking and also of initial data transmitted during the preceding session. Trajectory measurements. Turn of the lunar rocket. Orientation of one of the rocket's axes at the Sun. Orientation of the other axis at the Moon. Orientation of the optical visor toward the Earth. Construction of the lunar vertical at a distance of about 8300 kk from the center of the Moon and switching the control gyroscopic system on.

../..

TABLE 4 (end)

No	Date and Time	Operation
		Continuous control of operation of all on-board devices by means of telemetry. Signal of the radioaltimeter of preassigned altitude (about 75 km) having been attained and switching the deceleration motive device on.
16	21 h. 44 min. 42 seconds	Switching the astroorientation system off, control transmission to the autonomous gyroscopic system. Firing the engine. Jettisoning the compartments. Preparation of the landing systems.
17	21 h. 45 min. 30 seconds	ALS Luna-9 accomplishes the soft landing.
18	21 h. 49 min. 40 sec. — 22 h. 06 min.	First radiolink with ALS on the surface of the Moon. Switching on the rec.-transm. radioapparatus and of ventilation, and also of service and scientific apparatuses. Transmission of scientific data and telenetric control of the on-board systems. Switching the thermoregulation system on. Unfolding of the lobe and dod antennas. Reversal of receivers from lobe to rod antennas Antenna opening duplicated by the mechanical-time device.

No	Date and Time	Operation
	4 February	
19	0 h. 00 min. 0 h. 15 min.	Second radiocommunic. session
20	04 h. 50 min. 06 h. 37 min.	Transmission of the first lunar panorama and telemetry data. Switching ALS TV apparatus on. Sweep of lunar landscape and panorama transmission to Earth. Reception of telemetry data on the state and operation of the on board systems and apparatus.
21	17 h. 00 min. 19 h. 54 min.	Transmission of the second lunar panorama and of telemetry data.
	5 February	
22	04 h. 00 min. - 04 h 04 min.	Third radiocommunication sess.
23	19 h. 00 min. - 20 h. 41 min.	Transmission of the third lunar panorama and telemetry data.
24	21 h. 47 min. - 21 h. 56 min.	Fourth radiocommunic. session
25	22 h. 28 min. - 22 h. 45 min.	Fifth radiocommunic. session.
	6 - 7 February	
26	23 h. 37 min. - 01 h. 55 min.	Complementary session for transmission of separate areas of the lunar surface and telemtry data.

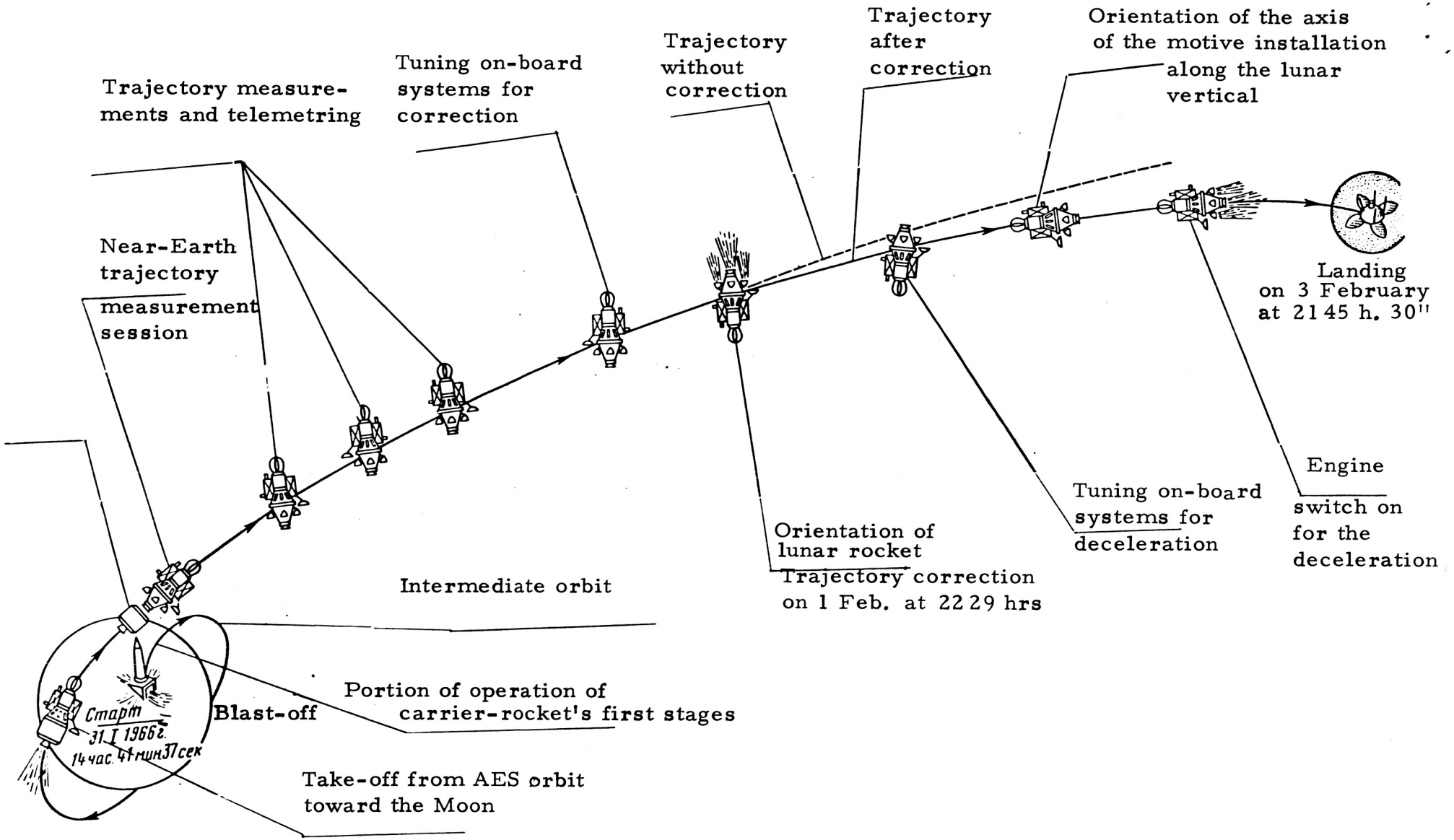


Fig. 9.- Flight Scheme of the Lunar Rocket

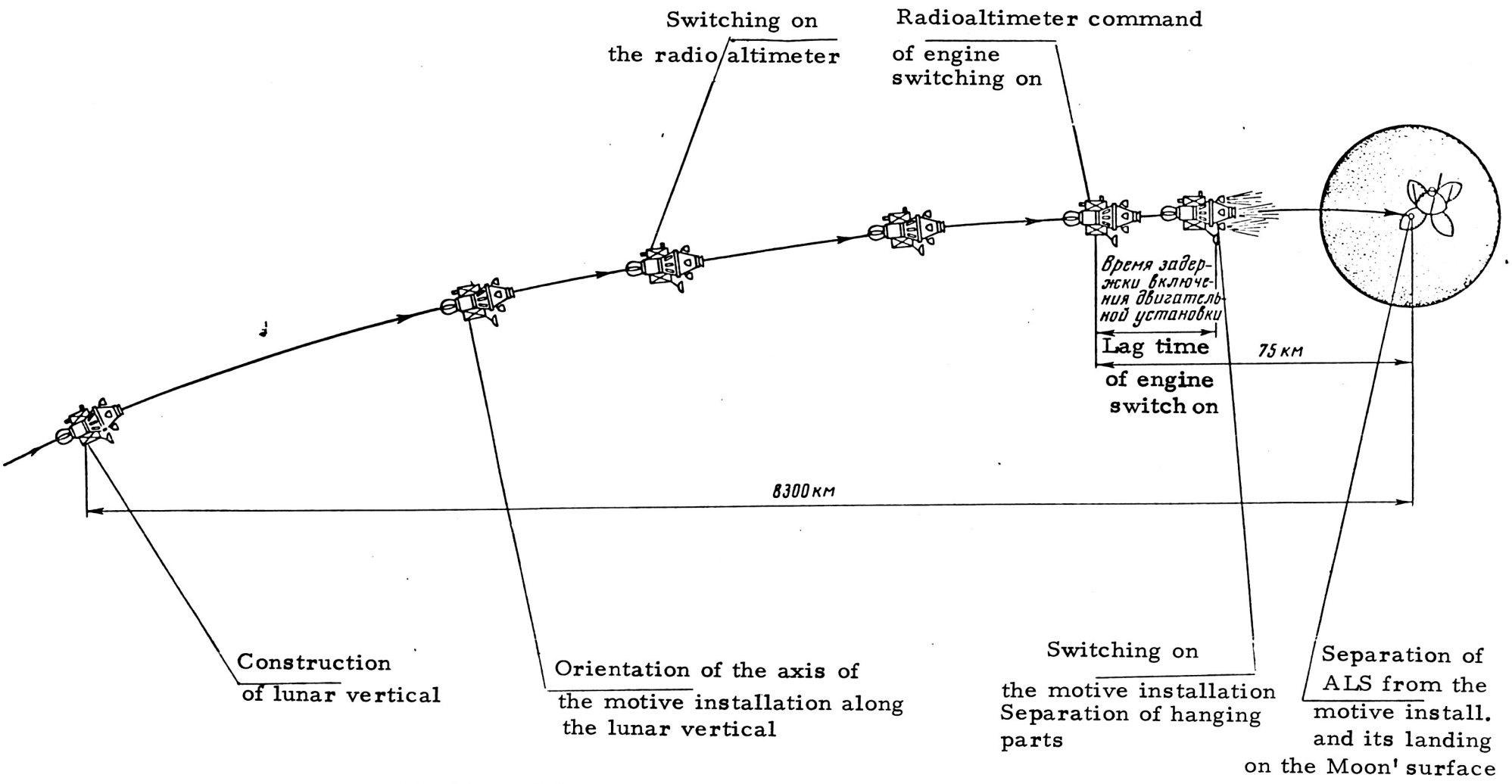


Fig. 10. - Scheme of the near-lunar portion of the trajectory of the lunar rocket

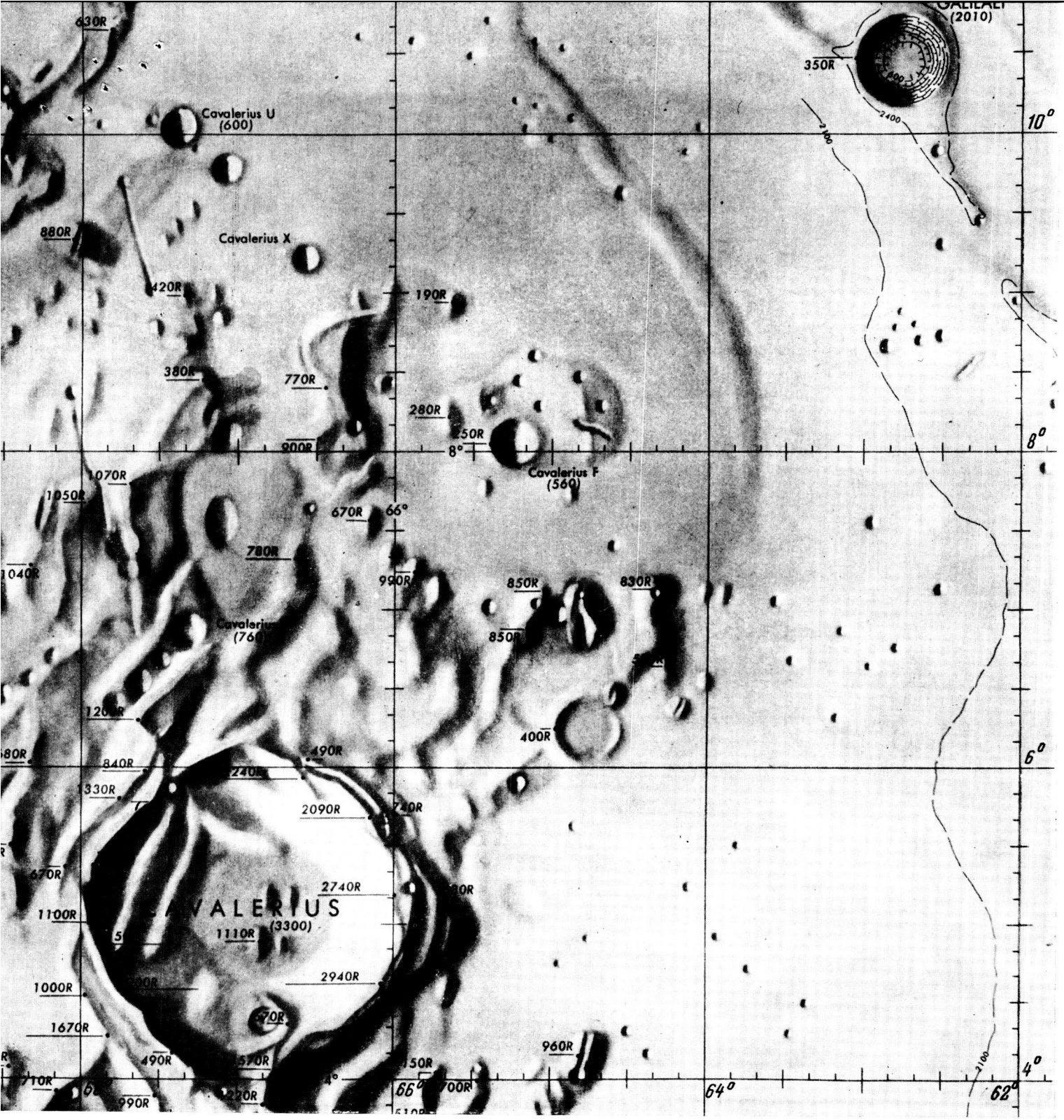


Fig. 11

Map of the landing region of Luna-9

Fig. 12

Photographic Map of the Moon
The cross indicates the landing site.


C
3
10

PART TWO

RESULTS OF THE STUDY OF LUNAR PANORAMAS

INTRODUCTION

The landing region of the station Luna-9 was selected in the equatorial region, near the morning terminator, on the illuminated part of the lunar surface; in other words, at a spot, where the Sun has just begun to rise, its height increasing by about 12° per terrestrial 24-hour day.

Such a choice of landing place creates favorable conditions for obtaining pictures of the lunar surface. In the morning hours all the objects have long shadows, which shorten comparatively rapidly as the Suns rises above the horizon. Owing to this, it is possible to obtain in a comparatively short time a series of panoramas with shadow lengths varying nearly in geometric progression. In fact, for the first two days of station's operation, program-foreseen panoramas have been obtained at heights of the Sun of respectively 7, 14 and 27 degrees, and moreover, after one more day, during a complementary session when the Sun was at 41 degrees above the horizon, fragments A and B were obtained, which encompass part of the panorama in the range from 330 to 55 degrees. Photographs with sufficiently different shadow lengths provide material for the determination of the shape of hollows as well as of protrusions.

Three full panoramas are attached to the third part of this work, where they are also represented in the form of 22 fragments and 12 stereopairs, printed by the phototype method, thus assuring the most accurate documentary reproduction of the originals. Separate impulse interferences, having on the panoramic photographs the characteristic aspect of small white or black circles, have been retouched. The fragments A and B are brought out in Fig. 27.

In order to facilitate the indications on the location of details in the panoramas and on their fragments, a graduated scale has been plotted in the abscissa with the angle γ, counted from the plane of panning (see 1 of Ch. 1)

from an arbitrary point situated more or less to the North. The scale has not been plotted along the ordinate axis, but, in case of necessity, we shall indicate the value of the angle $\xi = \beta - 18°$, counted from the lower edge of the panorama in the scale 1 = 5.5 mm (on fragments).

The station landed near the western edge of the Ocean of Storms, in the vicinity of the point with coordinates 7° North latitude and 64.5° West longitude. Although this region is indeed located within the bounds of the Ocean of Storms, admitted in the selenography, it apparently cannot be considered as purely mare region. Somewhat to the West and to the South of the landing place large craters are located, such as Cavalieri (diameter 60 km) and Hevel (diameter 120 km), surrounded by a well developed network of rims and spurs, reminding us of half-flooded mountain ranges. The distance from the landing place to the rim of Cavalieri crater is comparable with the diameter of the crater itself. This is essential for the interpretation if we take into account that secondary craters usually emerge at distances comparable with the diameter of the primary crater. In the landing region itself there is a group of hills (Cavalieri system γ) with flat declivities (their steepness not exceeding 10 - 15 degrees), rising over the surrounding region by some 500 – 800 meters.

Apparently, all the surrounding region is also somewhat lifted relative to the region of the Ocean of Storms, adjacent to the East. The area of the landing region is shown in the map of Fig. 11, in the scale of 1 : 1,000,000 (Lunar Chart U. S. Air Force and Nasa, N 56, May 1963), and in Fig. 12 shows the photographic chart of the visible hemisphere of the Moon with the indication of the landing spot by a cross. It is possible that Luna-9 actually landed in a region, intermediate in its properties between the purely maria and continental regions, suggesting in this regard the "Mare Cognitum" region, of which large-scale pictures were obatined with the aid of Ranger-7.

In the region considered the continental and maria areas are mixed up to the extent that it is difficult to determine on the basis of flight dynamics where the landing place belongs.

It is impossible to determine even directly, whether or not the landing place is in the maria or continental area by the simple view of the panorama, for the region encompassed by the visual field is small by comparison with the details distinguishable from the Earth. However, on the basis of detailed study of the photographs, not only the microrelief properties, but also a series of characteristics of the landing place can be recognized.

*

* *

CHAPTER I

CONSTRUCTION OF THE PLAN OF THE LANDING SITE

1. PHOTOGRAMMETRIC METHOD OF PANORAMA PROCESSING

The pictorial surface, upon which the special panoramic television camera constructs the image, constitutes a sphere (Fig. 13). The scanning ray of the telecamera performs two angular motions in mutually perpendicular planes, rotating near the center S of panning, which is the point of reflection of the projecting ray on the surface of the scanning mirror. We shall denominate one of the above planes as the panning plane. It passes through the point S and is perpendicular to the panning axis Sc (rotation axis of the telecamera head). The panning plane is fixed relative to the ALS. We shall designate the other as the scanning plane. It passes through the panning axis and rotates around it (line scanning). The scanning ray is deflected in this plane as a consequence of mirror swinging (vertical sweep) within the limits of the angle β_0 determining the transverse angle of the field of vision. The position at any moment of time of the sighting ray relative to the ALS is characterized by the angles γ and β. The first, γ , is counted in the panning plane from a certain initial direction to the trace of its intersection with the scanning plane. The direction toward any part of the ALS design, hitting the visual field of the telcamera (for example, the antenna) is taken for the origin of the count. The second angle β is determined in the scanning plane from the trace of its intersection with the panning plane to the sighting ray.

The center of panning, the panning and the scanning planes, coinciding with the initial direction, form the panoramic system of coordinates. The angles β and γ are the panoramic latitude and longitude of a point of the locality M, of which the image is marked in Fig. 13 by the point m. When registering the panorama on the phototelegraphic device, the line sweep is obtained as a result of drum rotation in such a way that to its single revolution corresponds one line. The vertical sweep is created by the motion of the writing photohead along the drum's generatrix. The distance counted on the photograph along the line is directly proportional to the angle β , and in the direction perpendicular to the lines—by

the angle γ. Knowing the angle β_0, the length of the line on the film and the step of the vertical scanning, it is easy to determine the transverse and longitudinal proportionality factors. In this way, it is possible to take down the counts of β and γ directly from the photograph.

One panorama gives the directions from the center of panning to the points of the locality, but does not allow the determination of their spatial position. In order to resolve this problem, it would be necessary to have two panoramas obtained from various points of space and properly oriented relative to one another. Then, having found the directions β, γ to the same points of the locality by way of two panoramas, and having restored the orientation of the latter, it is possible to resolve the so-called spatial cut. Shown in Fig. 14 is the sketch of the general case of the spatial panoramic cut.

The captions for Fig. 14 are as follows: X, Y, Z is a certain horizontal system of coordinates; S_1, S_2 are panning centers for the first and second panoramas respectively: C_1c_1, C_2c_2 are the panning axes S_1N_1, S_2N_2 are the verticals, N_1 N_2, n_1, n_2 are the nadir points in the locality and on the panoramas, $S_1n_1c_1v_1$, $S_2n_2c_2v_2$ are the planes of the main vertical, S_1v_1, S_2v_2, N_1C_1, N_2C_2 are the traces of their intersection with the panning planes and the plane XY, S_1o_1, S_2o_2 are the initial directions. Heavy lines indicate the so-called outer orientation elements, limiting all the degrees of freedom of the panoramas and determining their orientation relative to the system of coordinates X, Y, Z. This is X_{N_1}, Y_{N_1}, H_1 that is the coordinates of the first panning center; α_1, α_2 are the panoramas' inclination angles, $\varkappa_1$, $\varkappa_2$ are the angles between the initial directions and the lines Sv of the panoramas, B is the base of panning, α_B is the angle of inclination of the base relative to the horizontal plane, φ_1, φ_2 are the angles between the lines N_1C_1, N_2C_2 and the projection of the base B' on the plane XY, A_B is the azimuth of the basis' projection. Given the elements of outer orientation and the panoramic coordinates of the point of the locality $o_1m'_1 = \gamma_1$, $m_1m_1 = \beta_1$, $o_2m_2 = \gamma_2$, $m'_2m_2 = \beta_2$ (see Fig. 14), the coordinates X_M, Y_M, h of the locality point M are determined unilaterally. When the external orientation of the panoramas is unknown, it is possible to construct a nonoriented model of the locality. To that effect one must know the elements of the mutual orientation of the panoramas. These are: $o_1b'_2 = \gamma_{b_2}$, $b'_2b_2 = \beta_{b_2}$, $o_2b'_1 = \gamma_{b_1}$, $b'_1b_1 = \beta_{b_1}$, τ is the angle between the basic planes $S_1c_1b'_2b_2$ and $S_2c_2b'_1b_2$. . The points b_1 and b_2 are the images of the panning centers of the neighbroing panoramas. Denoted in Fig. 14 are also D_1 and D_2, which are the distances from the nadir points N_1 and N_2 to the point M', which is the projection of the point of the locality on the horizontal plane, λ_1, λ_2 are the angles between the projection of the base and the directions N_1M' and N_2M'.

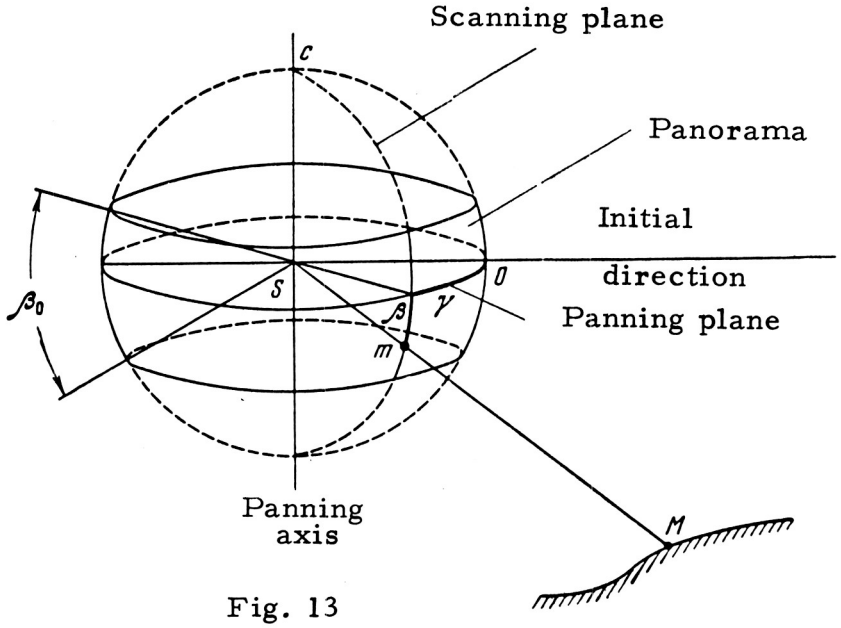


Fig. 13
Panoramic projection

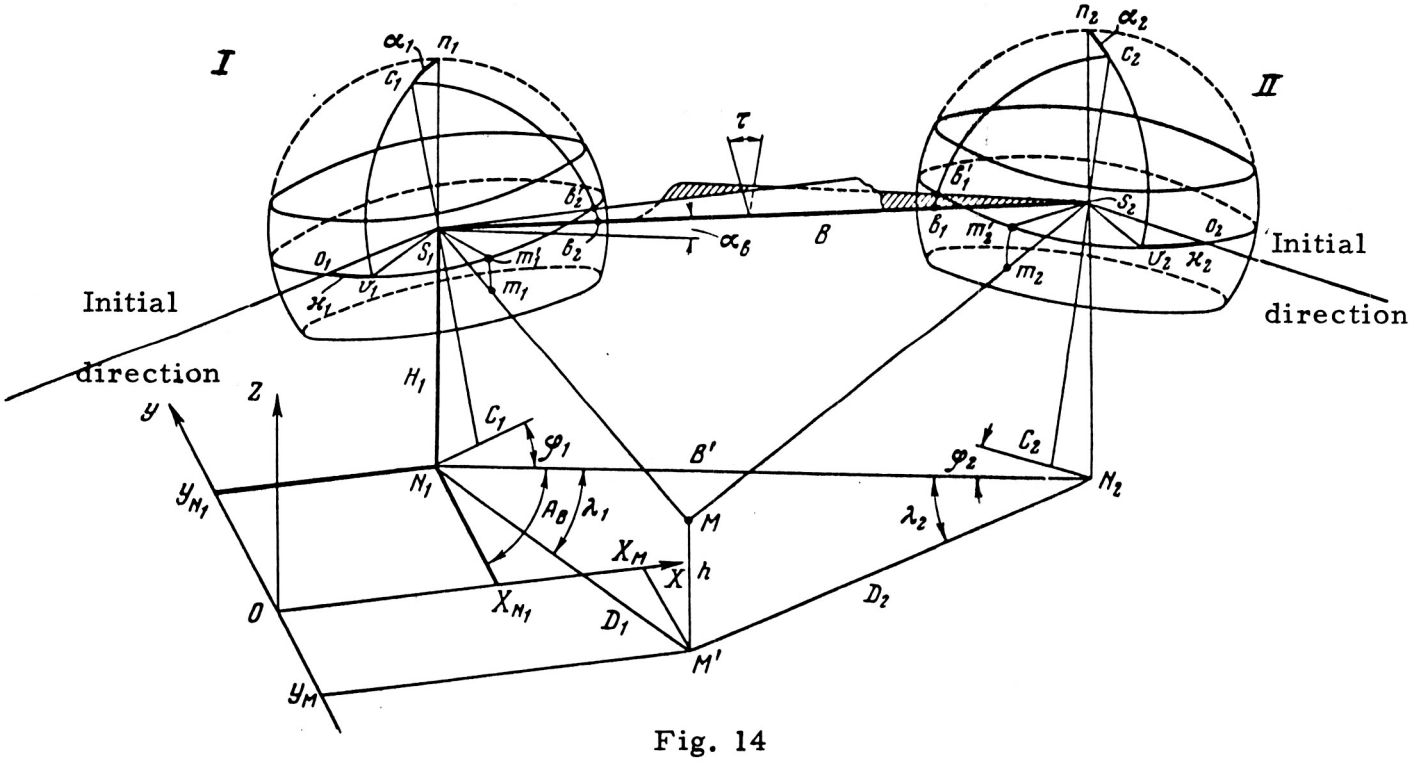


Fig. 14
Spatial panoramic cut

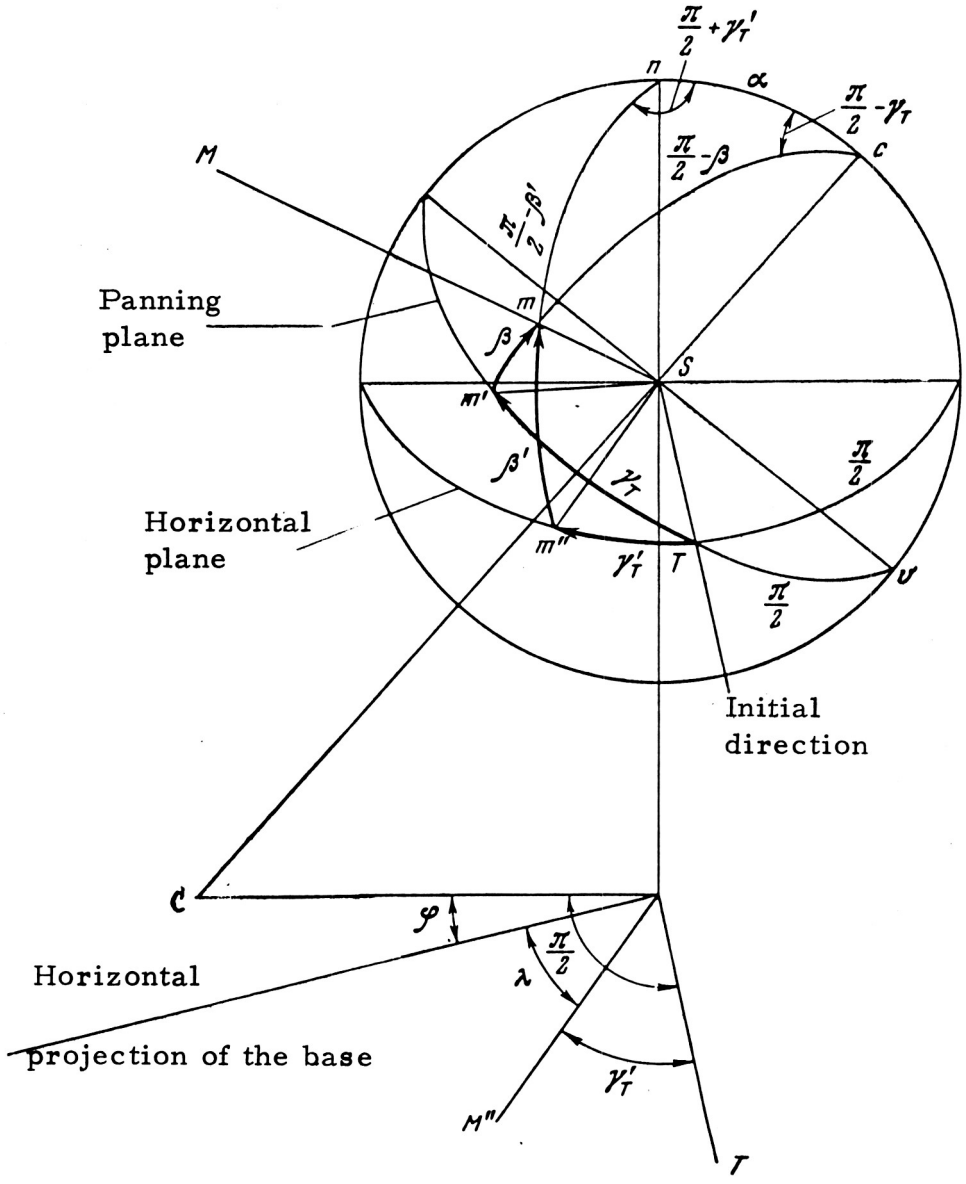


Fig. 15

Reduction scheme of panoramic latitudes and longitudes

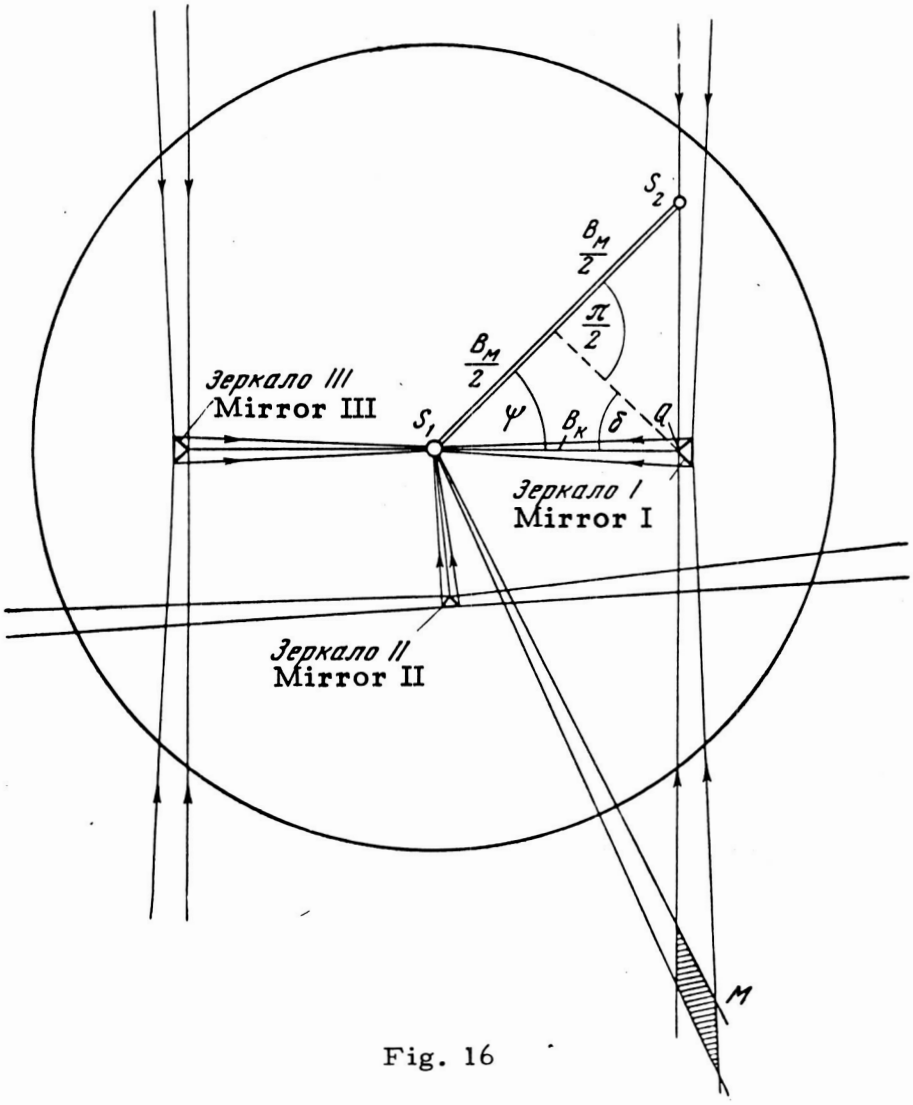


Fig. 16

Mirror installation scheme

The panoramas forming a spatial cut allow the stereoscopic viewing of the locality's image.

The spatial panoramic cut can be practically resolved by parts, separately for the determination of the position of the points of the locality in the plane and separately by altitude. To that effect, we must reduce the angles β and γ, measured by the panorama in the vertical and horizontal planes.

Shown in Fig. 15 is a geometric scheme of such a reduction. For the sake of simplicity we took for the initial counting direction of panora-

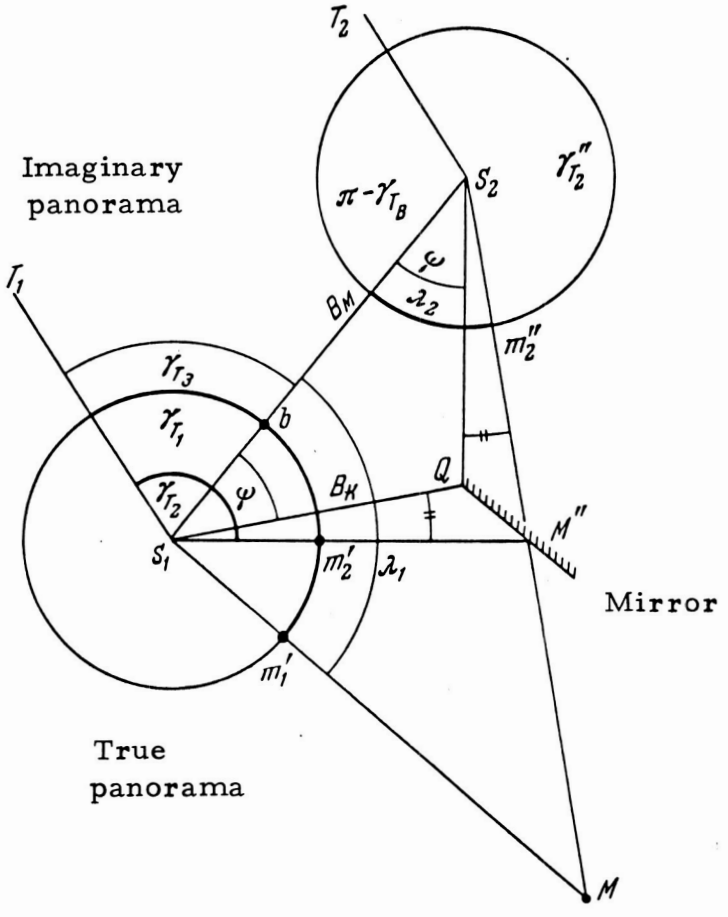


Fig. 17

Scheme of panoramic cut construction
with the aid of the mirror

mic longitudes, the line of intersection of the panning plane with the horizontal plane $\left(\varkappa = \frac{\pi}{2}\right)$. — The denotations are: $m'm = \beta$, $Tm' = \gamma_T$ which are measured, and $m''m = \beta'$, $Tm'' = \gamma'_T$ the reduced panoramic latitudes and longitudes of the point M of the locality. From the spherical triangle mnc, we find

$$\sin\beta' = \cos\alpha \sin\beta + \sin\alpha \cos\beta \sin\gamma_T, \qquad (1)$$

$$\cos\gamma'_T = \frac{\cos\beta \cos\gamma_T}{\cos\beta'}. \qquad (2)$$

Knowing the angle φ (see Fig. 14), it is easy to find the angle λ:

$$\lambda = \frac{\pi}{2} - \gamma'_T - \varphi.$$

Having thus obtained λ_1, λ_2, and taking into account that $B' = B \cos \alpha_B$, we resolve the cut in the plane XY (the triangle N_1N_2M' in Fig. 14) and we determine D_1, D_2, X_M, Y_M. Having D_1, H_1, β'_1, it is

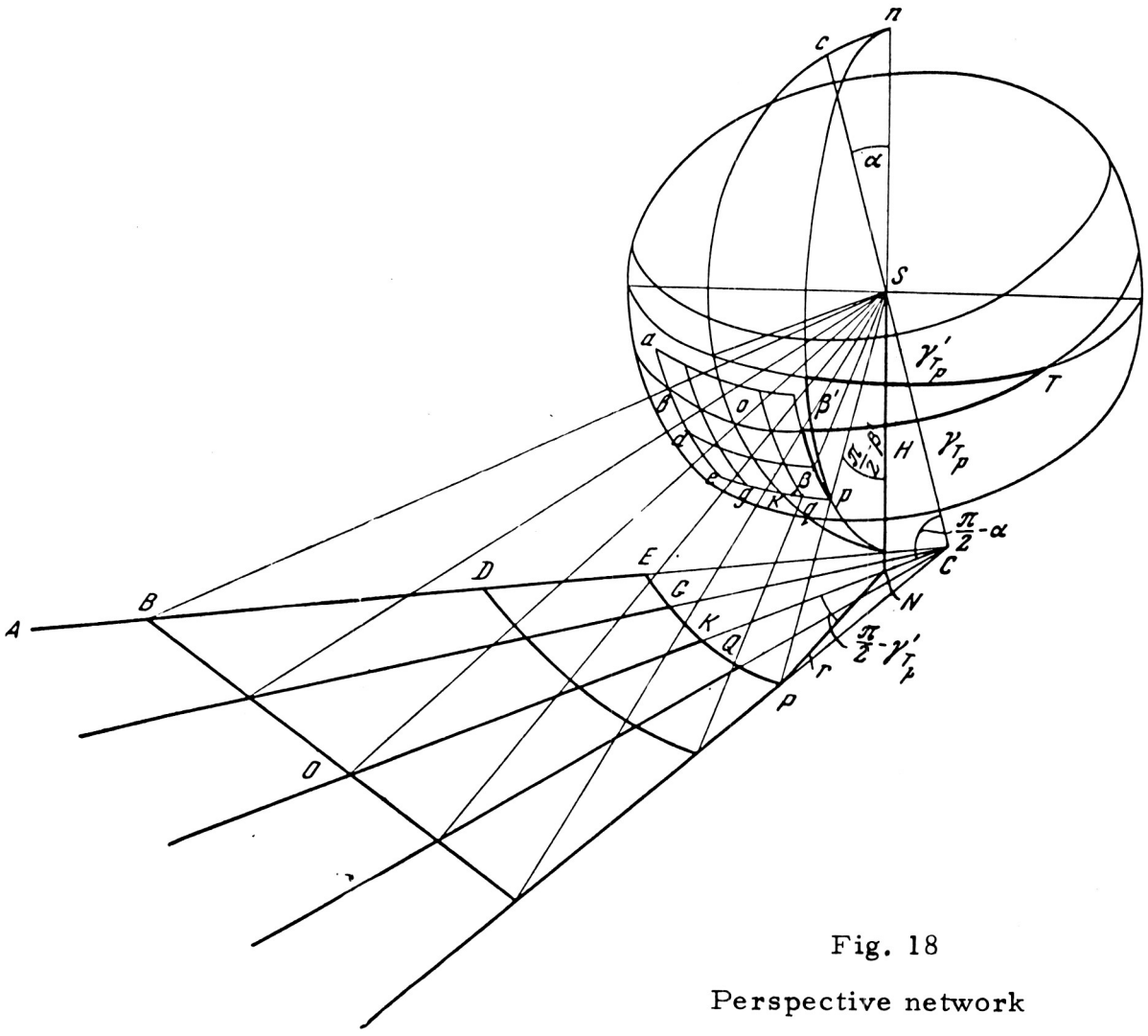


Fig. 18

Perspective network

easy to find h.

In order to obtain a spatial panoramic cut on Luna-9, two dihedral mirrors were installed. A scheme of mirror installation is shown in Fig. 16 (the ALS being viewed from above). In this way, the bounded portions of the locality are scanned by the telecamera twice, directly and after reflection in the mirrors. At the same time, in the first case, the panning takes place from the true center S_1, and in the second case—from the imaginary center S_2. Thus forms the imaginary base B_M. The mirrors are installed perpendicularly to the panning plane. The denotations of Fig. 16 are: Q for the rib, $B_k = S_1Q$ for the adjustable basis of the mirror, δ is the angle between its facet and the direction S_1Q, Ψ is the angle between S_1Q and the imaginary base. Evidently,

../..

$$B_M = 2B_k \sin\delta, \quad \psi = \frac{\pi}{2} - \delta.$$

Drawn in Fig. 17 is the construction of the panoramic cut with the aid of the mirror. The locality point M, taken for simplicity as lying in the panning plane, is figured on the true panorama at the points m'_1 and m'_2. They have the panoramic γ_{T_1} and γ_{T_2}, which are counted from the inclination axis of the panning plane S_1T_1. The panoramic longitude of the image m''_2 of the point M'' on the imaginary panorama is counted from its inclination axis S_2T_2 parallel to S_1T_1 and is equal to

$$\gamma''_{T_2} = \pi + 2\gamma_{T_B} - \gamma_{T_2},$$

where γ_{T_B} is the longitude of the point b on the true panorama (direction of the base relative to the line S_1T_1). Further, we obtain the cut angles

$$\lambda_1 = \gamma_{T_1} - \gamma_{T_B}, \quad \lambda_2 = \gamma''_{T_2} - \gamma_{T_B},$$

with the aid of which it becomes possible to find the position of the point M in the panning plane.

If we reduce B_M, γ_{T_1} and γ_{T_2} to the horizontal plane, this problem may be resolved in the plane XY.

If the point of the locality does not lay in the panning plane, its panoramic latitude in the imaginary panorama is equal to the latitude of the image of that point in the mirror in the true panorama.

Another possibility of constructing a spatial panoramic cut according to Luna-9 panoramas stems from the fact that because of the station's rotation, the panoramas were obtained from various points of space. If we take two panoramas (for example, the first and the third) they form a panoramic stereopair. (See Fig. 14.)

The direction, close to the base, provides cuts at a very sharp angle. Such cuts are of low precision. In the cases when the locality is near the plane, the contour plane may be constructed in the zones of poor cuts with the aid of a perspective network of equal latitudes and longitudes shown in Fig. 18. The panoramic coordinates of the junction points of the network are reduced in the horizontal plane by the formulas (1) and (2). Then, the distance of the junction points from the nadir point N is found from the formula $r = H \operatorname{ctg} \beta'$. The position of the junction points on the plane may be determined by constructing the directions $\frac{\pi}{2} - \gamma'_T$ (see Fig. 18) and by plotting along them the distance r.

The lines of the perspective network, corresponding in the plane to the panoramic meridians, are figured by straight lines and they intersect at the point C. The panning plane is figured by a straight line, and the other lines of equal latitudes by conical cross sections.

2. ORIENTATION OF THE PANORAMAS

The area of the locality encompassed by the panoramas is not great and this is why the topographic plan of the landing site of Luna-9 is constructed in the local rectangular horizontal system of coordinates. It is practical to take for its origin the panning center of one of the panoramas, while orienting the axes of the abscissa and of the z-axis coordinates along the selenographic meridian and the local vertical. The coordinates of one of the panning centers are given in the same fashion (see Fig. 14).

To determine the inclination of the panning axis we shall utilize the line of visible horizon. If the latter is identical to the line of imaginary horizon the rotation axis of the panning plane passes in the panorama through the point of intersection of its trace with the horizon line (Fig. 19).

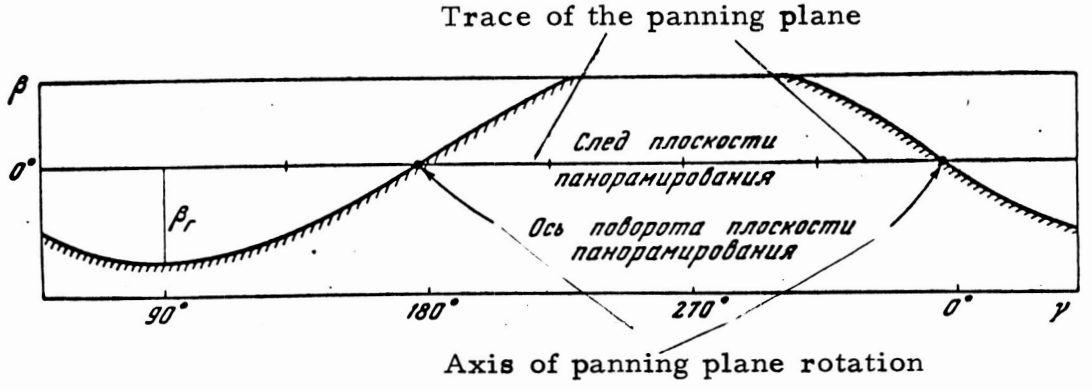


Fig. 19

Sketch showing the image of the horizon on the panorama.

Let us assume one of them to be the origin of the count. In this case, the point of greatest distance between the horizon and the panning plane's trace has the longitude $\gamma_r = 90°$. Evidently, the reduced latitudes β'_r of all the points of the horizon are zero, since they lay in the horizontal plane passing through the panning center because of the low

altitude of the ALS above the site, we neglect here the lowering of the horizon). Then, we shall find from the expression (1) that $\alpha = -\beta_r$. In other words, the panorama inclination takes place in the scanning plane where the panoramic latitudes of the horizon line β_r are extreme.

Since the lines of the visible and true horizons differ from one another because of the relief, we utilize for the determination of the greatest possible number of horizon points, rejecting the clear protrusions and the dips. Let us transform the equation (1), bearing in mind that $\beta'_r = 0$, and let us resolve it for a series of points of the horizon relative to α_i

$$\operatorname{tg}\alpha_i = -\frac{\operatorname{tg}\beta_{r_i}}{\sin\gamma_{r_i}}. \qquad (3)$$

Then, γ_r will be each time counted from the intersection point of the visible horizon line with the trace of the panning plane. From the thus found values of α_i we shall find the average and we shall take it for the first approximation. We shall resolve the equations (3) relative to γ_{r_i} for the same points of the horizon, substituting in it α'_{cp}:

$$\sin\gamma_{r_i} = -\frac{\operatorname{tg}\beta_{r_i}}{\operatorname{tg}\alpha'_{cp}}.$$

Having plotted in the panoramas the values of γ_{r_i}, corresponding to the various points of the horizon, we shall obtain a certain scattering of counting origins relative to that chosen originally at the intersection of the line of visible horizon by the trace of the panning plane. We shall find the average deflection by the formula

$$\Delta\gamma'_r = \frac{\sum(\gamma_{r_i} - \gamma_r)}{n},$$

where n is the number of measurements. We shall transfer the origin of the count of panoramic longitudes to the point with the coordinate $\gamma_r + \Delta\gamma'_r$ and take it for the new origin of count γ_{r_i}. Analogously we shall find the subsequent approximations α''_{cp}, α'''_{cp} ... and $\Delta\gamma''_r$, $\Delta\gamma'''_r$ ... and we shall extend them until $\Delta\gamma_r$ will differ from zero by no more than one order of magnitude with the measurement precision by the panorama. The thus found final point of panning longitude count lies on the rotation axis of the panning plane relative to the horizontal plane, that is, on the line ST (see Fig. 15), and is identical to the point T. The value of α_{cp} found from the last approximation is taken for the inclination angle α of the panorama. However, inasmuch as the relief of the horizon is unknown to us, the obtained inclination angle must be plotted in the quasihorizontal plane.

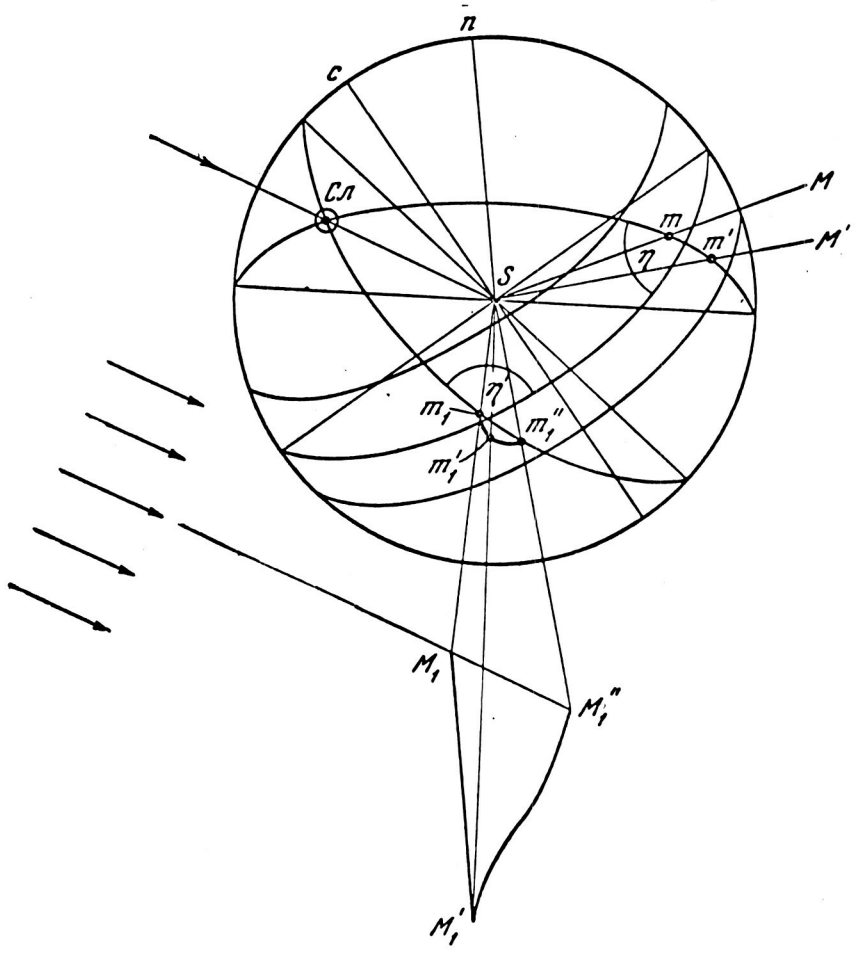


Fig. 20

Construction scheme for the image of the object and its shadow

The azimuthal orientation of the panoramas will be found by the shadows of local objects. A scheme of such a distribution is shown in Figures 20 and 21.

We shall find the azimuthal orientation of the panoramas of local objects. The scheme of such a determination is conveyed in Figures 20 and 21. The denotations of Fig. 20 are: M_1, M'_1 is the local object; M'_1, M''_1 is its shadow (of whic h the shape is dependent on the relief of the locality where the shadow is incident); m_1 m'_1 are the images of the object and of the shadow, M, M', m, m' are the analogous points corresponding to another object; $C_л$ is the image of the Sun in the panorama if it covered the entire sphere. Evidently, the identical points of the object and of the shadow lay on the line passing through the Sun and parallel to the line $C_л S$. Therefore, the projecting rays SM_1 and SM'' lay in the plane containing the line $SC_л$. This plane intersects the panorama by the arc of the great circle m_1 m''_1 on which are lying the Sun's

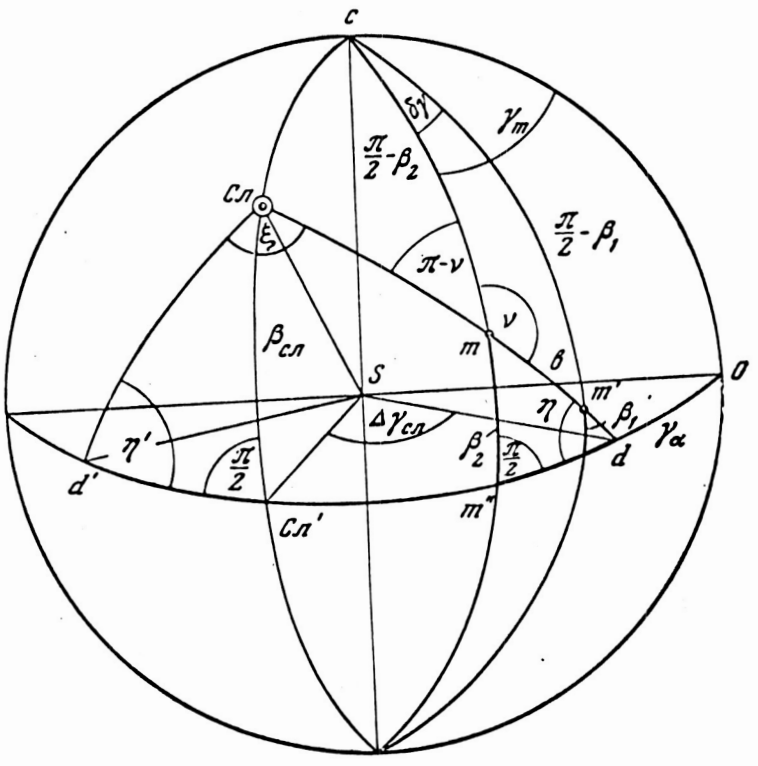


Fig. 21

Scheme for the determination of panoramic latitudes and longitudes of the Sun's image on the panoramas

images Cл , the points of the object M_1 and the points M''_1 of its shadow.

The arcs of the great circles, linking the identical points of several objects and of their shadows intersect at the point of the Sun's image C Consequently, having found such an arc in the panorama, one may determine the panoramic coordinates of the point of the Sun. Let us perform this as follows.

From the spherical triangle mcm' (Fig. 21), we obtain

$$\cos b = \sin\beta_1 \sin\beta_2 + \cos\beta_1 \cos\beta_2 \cos\delta\gamma.$$

Evidently, $\delta\gamma = \gamma_m - \gamma_{m'}$, where γ_m and $\gamma_{m'}$ are the longitudes of the points m and m',

$$\cos\nu = \frac{\sin\beta_1 - \cos b \sin\beta_2}{\sin b \cos\beta_2}.$$

From the triangle mm''d, we shall determine the inclination angle of the plane C л m m'd with the panning plane

$$\cos\eta = \cos\beta_2 \sin\nu,$$

and also

$$\sin\delta'\gamma = \mathrm{tg}\beta_2 \,\mathrm{ctg}\eta,$$

where $\delta'\gamma = dm''$. We shall obtain the longitude of the intersection line between the plane C m m'd and the panning plane by the formula

$$\gamma_d = \gamma_m - \delta'\gamma.$$

The values of γ_m, $\gamma_{m'}$, β_1, β_2 are measured directly by the panorama.

The angle η and the point d with the longitude γ_d determine the position in the panorama of the arc of the great circle passing through the point of the Sun and the image of a certain object and of its shadow. The angle η' and the point d' may be found similarly for another object.

Therefore, known in the spherical triangle $dC\text{л}d'$ (Fig. 21) are the angles η, η' and the side $dd' = \Delta\gamma$, equal to the difference of the panoramic longitudes of the points d and d'. Consequently,

$$\cos\xi = -\cos\eta\cos\eta' + \sin\eta\sin\eta'\cos\Delta\gamma.$$

From the same triangle, we shall obtain

$$\cos a = \frac{\cos\eta' + \cos\eta\cos\xi}{\sin\eta\sin\xi},$$

where $a = C\text{л}d$.

From the right triangle $C\text{л}\,d\,C\text{л}'$ we shall find

$$\mathrm{tg}\Delta\gamma_{C\text{л}} = \cos\eta\,\mathrm{tg}\alpha,$$

$$\mathrm{tg}\beta_{C\text{л}} = \sin\Delta\gamma_{C\text{л}}\,\mathrm{tg}\eta.$$

The quantity β_{C_Δ} is the panoramic latitude of the Sun. The panoramic longitude of the Sun γ_{C_Δ} will be determined by adding to the longitude of the point d the quantity

$$\gamma_{C_\Delta} = \gamma_d + \Delta\gamma_{C_\Delta}.$$

Reducing γ_{C_Δ}, β_{C_Δ} to the horizontal plane, we shall find the height of the Sun above the horizon $\beta'_{C_\Delta} = h'_\odot$ and the horizontal panoramic longitude γ'_{C_Δ}.

When the coordinates of the landing site and the panning time become known, the azimuth of the Sun $A_\odot$ and its computed height $h_\odot$ may be determined. The convergence of $h'_\odot$ and $h_\odot$ constitutes the control of local vertic al determination and of constructions on the panorama. Knowing $A_\odot$, it is possible to compute the azimuth of the inclination axis of the panorama

$$A_T = A_\odot - \gamma'_{C_\Delta}.$$

For construction of the spatial cut by stereopairs, having formed as a result of the ALS Luna-9 inclination, it is necessary to find the base which is the distance between the panning centers. This may be performed graphically constructing by the reduced panoramic longitudes the planes of the points having been materialized in the mirrors of both panoramas. If we superimpose these planes one upon the other by making the identical points coincide, the panning centers plotted on the planes will not coincide. The line, linking them, is the projection of the base B' of the panoramic stereopair on the horizontal plane. The vertical component of the base may be found by way of computing the excesses of locality points, having been materialized in the mirrors of both panoramas according to reduced panoramic latitudes. Taking the averages of excess differences of identical points, we shall obtain the excess (surpassing) of one panning center over the other. The same problem may be resolved analytically by applying the well known formula of inverse spatial cut.

3. CONSTRUCTION OF THE TOPOGRAPHIC PLAN OF THE LOCALITY

To construct the plan, the first and third panoramas were used. Recognized and denoted were the locality's identical points, of which the identical points' images materialized on the true and imaginary panoramas (by reflecting in the mirrors). It was then found that several identical points materialized in mirrors on both panoramas. Then the overlapping parts of the panoramas were examined with the aid of a stereoscope and such characteristic formations as craters, stones, strata and structurally different smooth portions of the locality's surface were de-

ciphered. Certain deciphering signs of formations, which were utilized at the study of those portions of the panoramas where the stereoeffect is absent or insufficient were exposed in the process of stereoscopic analysis.

Following are the characteristic formations found to constitute such signs:

— for craters: ellipsoidality of the contour, shadow inside it, characteristic contrast variation relative to the surrounding locality if we understand by contrast the ratio $K = D_1 / D_2$, where D_1 is the photographic density of the diapositive image outside the limits of the crater contour, D_2 is the same inside the contour, we shall have for the illuminated crater rim $K > 1$, and the shaded rim $K < 1$);

— for stones: irregularity of the contour, deep shadows outside the contour, shines, which are areas with quite low photographic density of the diapositive picture (the clear ones being nearly white spots from the side opposite to the shadow);

— for ridges; stretching of the contour, absence of deep shadows, low image density on the side turned toward the Sun, and somewhat higher on the op osite side, coarse structure inside the contour;

— for smooth areas with fine structure: generally rather low mean density of the image because of the absence of deep shadows from tiny roughnesses, absence of noticeable image divisibility;

— for smooth areas with coarse structure: more or less regular alternation of clear spots against the dark background or, to the contrary, a comparatively high mean density of the image because of shadows and roughnesses, presence of separate impregnations noticeably differing in size from the fractional elements of the general background.

Because of image perspectiveness and rapid scale decrease from the nearest to the far edge of the panoramas, these signs cannot be considered absolute.— They require a logical interpretation for the various portions of the panorama, taking into account their disposition and the direction of the illumination. The reliability of the deciphering is correspondingly heterodynamic too. It may be deemed sufficient for the forward

plan areas in the zones of good stereoeffect, where tiny elements of surface structure are examined volumetrically. As we are drawn away from these zones, the deciphering acquires a more and more hypothetical character. The results of deciphering are represented on the panorama a of Fig. 22.

Simultaneously with the deciphering on the characteristic points of the relief and situation, pickets of the total number exceeding 200 were denoted; they are required for the composition of the topographic plan. The pickets were chosen on noticeable crests of the relief, on crater lips, at the base and, wherever possible, on summits of stones or ridges. In view of the deep shadows in the first panorama, we succeeded in choosing pickets at crater bottoms only in a few cases.

Scales of panoramic latitudes and longitudes were broken down in the panoramas according to construction data, and the coordinates of all the denoted locality points were determined by them.

The panorama orientation was determined by the horizon and the shadows of the local objects described in paragraph 2 of the present chapter. The obtained heights of the Sun, the inclination angles of the panoramas and of the azimuth axes are compiled in Table 5.

TABLE 5

Panoram No.	Date and time of photographing	Height of the Sun	Absolute Inclinat. angle	Inclinat. axis azimuth
1	4 February 04 50 hrs to 06 37 hrs	7°30'	16°30'	169°
3	5 February 19 00 hrs to 20 41 hrs	26°18'	22°40'	173°

The panoramic latitudes and longitudes of the locality points were reduced to vertical and horizontal planes after these data. The required computations were performed with the aid of computers.

All measurements were made after the original panoramas. The scale of their images is such that one line has about 0.4 mm thickness. This predetermined the appropriateness of performing panorama measurements graphically. (As is well known, the precision of graphical measurements is of 0.08 mm.) For the same reason, the pickets were plotted on the plan by graphical-mechanical method with the aid of a gadget, constructing the cut mechanically. Following is the sequence of the work.

The true and the imaginary centers of panning of the third panorama were plotted on the drawing board of scale 1 : 10 (1cm of the plan corresponds to 10 cm on the locality). The meridian was marked; the axes of the panning plane inclination relative to the horizontal plane, corresponding to the true and imaginary centers of panning, were traced. The reduced longitudes of identical locality points, having materialized on the true panorama and in the mirrors, were plotted from these centers. Plane cuts were constructed by the method described in paragraph 1 of this chapter, and the plane disposition of these points was found. The distances from the panning centers to all the points were taken down from the plane, and the excesses of the locality points over the quasihorizontal plane passing through the true panning center of the third panorama have been determined with the aid of the reduced panoramic latitudes (vertical angles). This plane was taken for the plane of the plan, to which are referred also the excesses of all the remaining points of the locality. When determining the excesses, we took also into account the heights of the imaginary panning centers relative to the true one, which were found during the reduction of the imaginary bases to the above referred to quasihorizontal plane.

The described construction was performed for the images reflected by one rib of the first mirror, by two ribs of the second and one rib of the third. Two ribs were dropped from the processing as the sky was found to be reflecting in them.

In this way, four lines of direction points were obtained in the plan (Fig. 23). An inner control was available when constructing the lines of direction. It consisted in that the point excesses were determined twice by each line of direction—relative to the true and imaginary panning centers respectively. The discrepancies in the excesses did not exceed 4 cm for a root-mean-square error of ± 1.5 cm. Moreover, the first and second mirrors are so oriented that two lines of direction did not intersect in the plan. Several identical points were recognized in the intersection zone. This allowed to perform the control of the position of such points in the plan and in height. The deviations in the plan did not exceed 1 cm in the locality (1 mm on the plan), those in height have the same order as inside a single line of direction. Inasmuch as the construction principle of all lines of direction is identical, the other two lines of direction must evidently have an identical precision.

The described lines of direction were taken for the geometric frame in the construction of the plan of the locality as a whole.

Subsequently, the position of the panning center of the first panorama and the base of the panoramic stereopair were found by the me-

thod described in paragraph 2 of the present chapter, the inclination axis of the first panorama was entered on the plan, the picket cuts were constructed by the reduced panoramic longitudes, the planar distances to the pickets from the first and the third panning centers were taken down and the excess of the locality points, corresponding to them over the above quasihorizontal plane, was found by the reduced latitudes of the pickets. The value of the base B in nature was found to be equal to 9 cm, the inclination angle of the base was $\alpha_B = 6°20'$, and the excess of the panning center of the first panorama over the quasihorizontal plane was 1 cm.

The convergence of excesses found from either panning centers constitutes an intrinsic control. The order of discrepancies was found to be the same as for the lines of direction.

In view of the fact that the picket intersection in the plan took place at quite sharp an angle (for the forward points near 5°, for the more remote to 10'), picket tying up was effected according to the position relative to the line of direction points.

For the sake of control, some of the pickets were constructed twice: by the described graphic mechanical and analytical methods. The convergence obtained was of the same order as the above-indicated.

In the sector near 60°, located on the extension of the base to the east of the panning centers, the obtained stereocuts were unsatisfactory. In this zone (see Fig. 23), the situation was entered on the plan by a perspective network. In the sector near 100° from the western side, we did not succeed in constructing the plan, for the simple reason that no locality was obtained in that part of the panoramas (the telecamera was looking into space). Besides, there are seven narrow sectors in which the details of the station (the lock, the antenna and the mirrors) shielded the region. These sectors did not practically interfere with the composition of the plan for the layout clsoded by them is easily interpolated by the neighboring sectors.

Then, by way of interpolation, contour lines with cross sections at every 5 cm in height were traced in the plan between the pickets. The laying of the contour lines was corrected by photo observation under the stereoscope.

The obtained topographic plan is quite uneven in precision on account of both the rapid decrease of cut angles and the perspective, hindering a reliable determination of formation contours. This is why, in its final form, it is presented in two variants. The first variant includes the central part

of the area encompassed by the panoramas. This area is given in the scale of 1 : 20 and is characterized by an average root-mean-square error of the point position in the plan of the order of ± 10 % and $\pm 2 - 5$ cm in height. The second variant encompasses the entire area subject to photogrammetric processing. It is given in the scale of 1 : 40 and it must be viewed as a scheme. There is no possibility of appraising its accuracy. Both variants are represented in the third part.

By comparison with the plan, the scheme is somewhat generalized and the tiniest craters in particular are shown in it.

A mosaic photoplan of the locality in the scale of 1 : 6 consistint of separate transformed photographs, has been prepared in the limitted area shown in the scheme of Fig. 23. To that effect, fragments of the third panorama were utilized. With this in view, small areas, bounded by lines of equal latitudes and longitudes and forming a network of rectangles, have been marked on the panorama. Using the method described in paragraph 1 of the present chapter, this network was reduced to several intermediate planes inclined at different angles relative to the panning plane. Separate portions of the panorama were transformed on a phototransformer in such a way that the boundary of these areas coincide with the corresponding lines of the first network established on the screen of the transformer. The photographs obtained at each such operation were again transformed according to the following network, and so forth, so long as the image did not become planar. The mosaic, thus made, has been mounted jointly on the board, on which the planar perspective network was plotted, this one being identical to the network laid out on the panorama. At the same time, each element of the mosaic is established along the network as follows. In view of the fact that the area of the locality on which the photoplan is composed has an insignificant relief, a satisfactory convergence of contours has been obtained along the cuts (the discrepancies do not exceed 1.0 mm).

Examining the transformed photographs brought out in the third part, one must bear in mind that inclination angles of the panorama areas referred to relative to the plan vary from 54 to 70°. This is why separate microelements of the relief, protruding above the lunar surface, create a sort of tiny "dead" areas (areas that have not been considered). At transformation into plan these elements behave as if they lay sideways; as a consequence, their shape is distorted. This is particularly noticeable at the edges of the referred to photoplan.

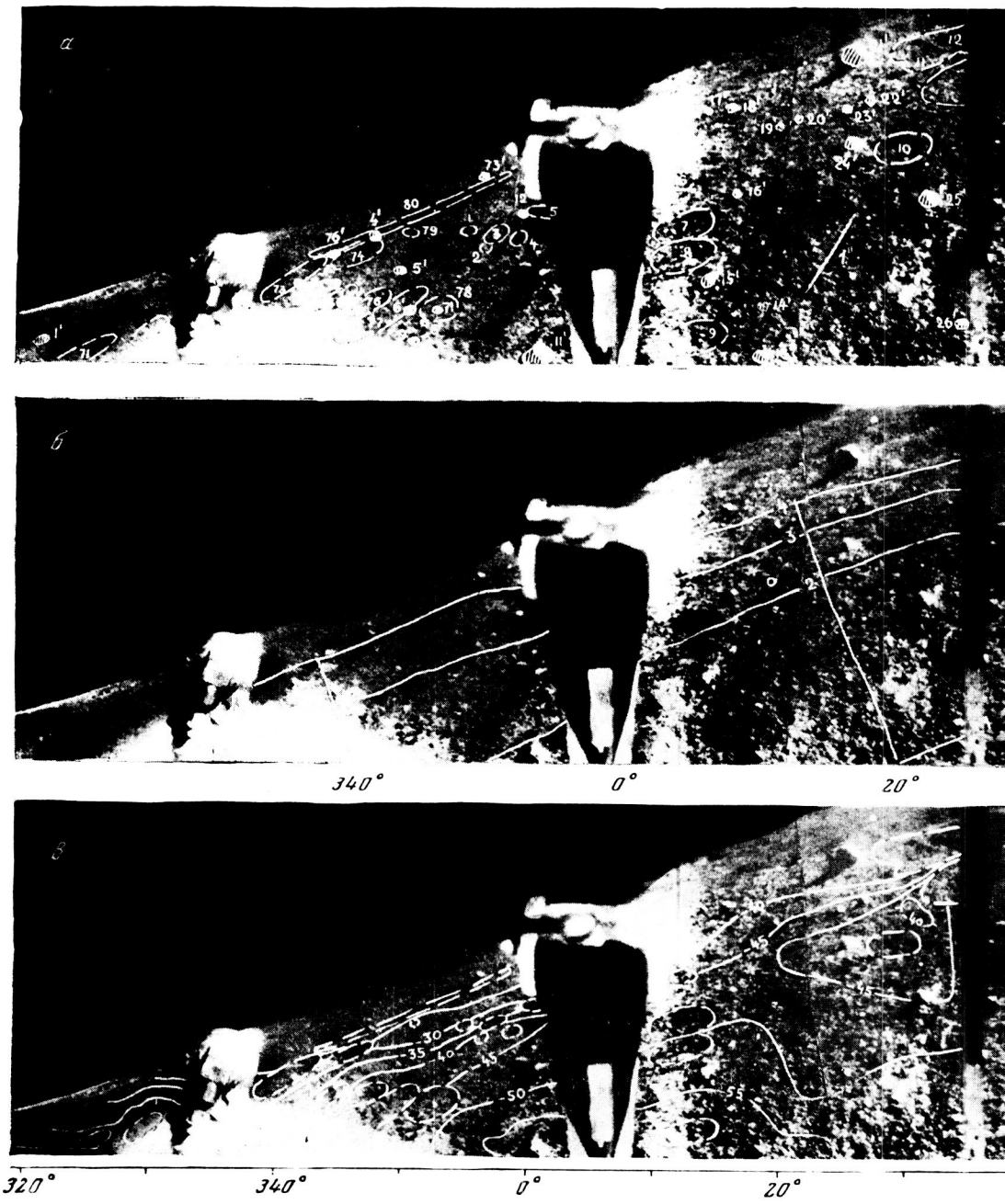


Fig 22 A

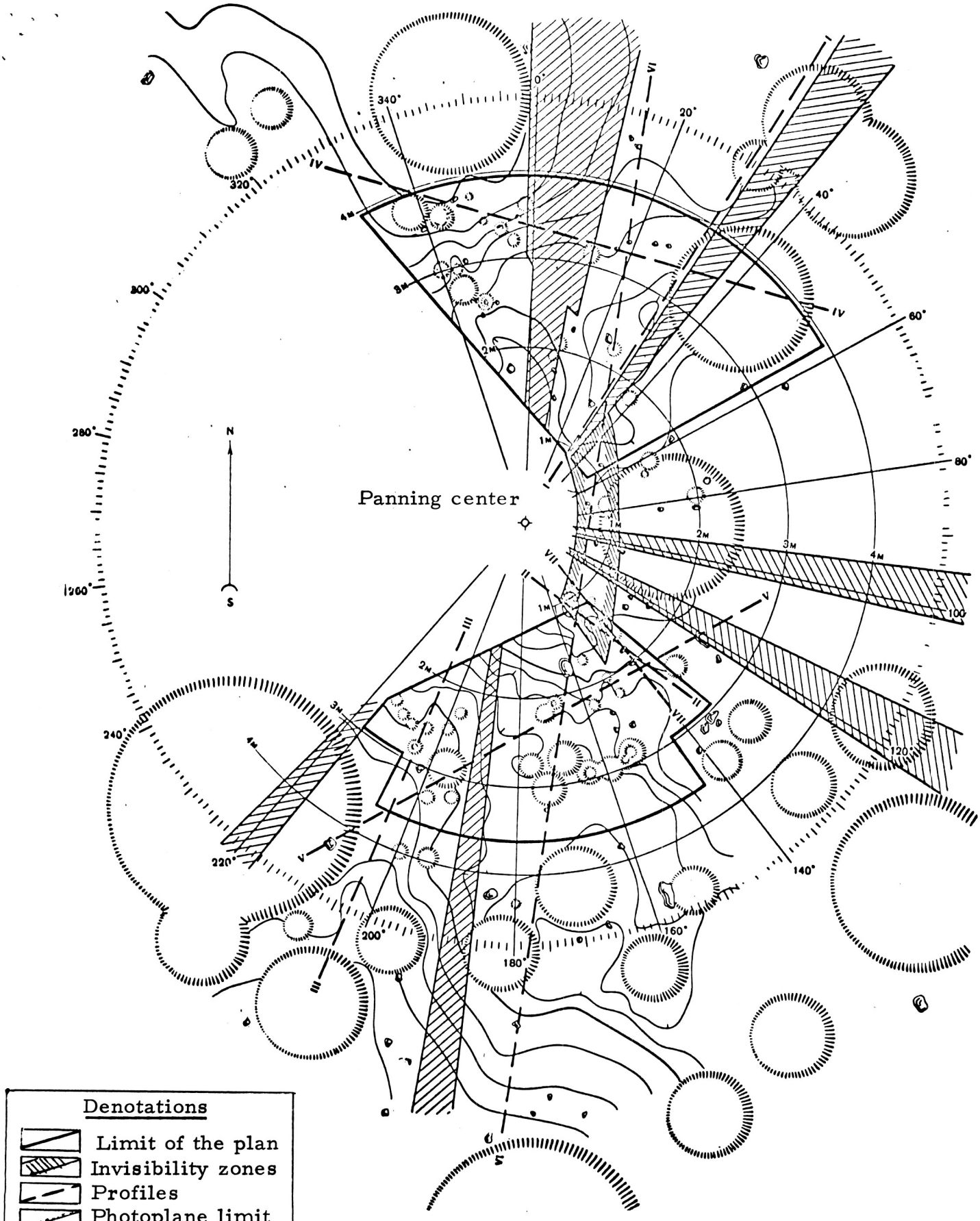


Fig. 23

Disposition of the processed areas

4. TOPOGRAPHIC PECULIARITIES OF THE LANDING SITE OF ALS LUNA-9

The initial material serving for the topographic analysis consists of panoramas with networks entered upon them of ranges and contour lines of the above described plan and of the scheme and profiles of the locality.

The range and the contour lines were transferred to the panorama (Fig. 22, б, в) from the plan and on the panorama. The range lines correspond to circumferences traced on the plan every 1 m, concentrically to the projection of the panning center of the third panorama.

The locality points (Fig. 24) are constructed with the aid of the topographic plan. Three profiles correspond to the lines of direction referred to the above, three others are laid out along the directions most interesting from the standpoint of surface morphology. The disposition of profiles on the plan is shown in the scheme in Fig. 23. For greater clarity the vertical scale of profiles was taken twice as large as the horizontal.

The landing site constitutes a fairly smooth surface with a well expressed relief, with hills noticeable on the line of visible horizon.

The most characteristic form of mesorefief is constituted by craterlets and craters, that is, rounded depressions—pits of quite variable dimensions. No system of any kind is observed in the disposition of these depressions. Some of them are disposed in an isolated manner, and others —by groups; some overlap one another and there are tiny craterlets inside coarser ones and on their slopes. Small tubercles are noticed at the center of some tiny hollows.

The character of the contour lines provides the basis to assume that the ALS lies on the western slope of a small depression, that may possibly be a lunar crater; owing to its dimensions and the limitedness of the television system's visual angle, the latter can only be partially glanced over in the panoramas. At stereoscopic viewing the "brow" of this crater is observed as the boundary of the surface uplift behind which follows a lowering in the northern part of the panorama and a terrace-like surface in the southern part. If the crater brow is extrapolated in the plan, considering it as a circle, its diameter is found to be equal to about 14 - 15 meters. Analyzing the profiles, it is possible to establish that the depth of the crater is about 60 - 70 cm. All the craters and craterlets visible in the panorama have lesser dimensions: from 3 m to 10 cm in diameter and from 20 to 2 cm in depth.

In the zone under review, steep folds and cracks of the surface, hindering the motion under terrestrial conditions, are entirely absent. On the whole, the relief is comparatively smooth, through its structure is sufficiently complex; the sinuosity of the contour lines is evidence of that. Encountered on the slopes of the large crater, referred to above, are slanting mounds, depressions, ravines and saddle points.

In view of the fact that the excesses are given relative to the quasihorizontal plane, the general dip of the locality cannot possibly be determined. The local dip of the slopes of the large crater is of about 0.09 (5°).

As was indicated in paragraph 3 of the present chapter, we could not succeed in pointing out the internal parts of the craters by contour lines because of deep shadows and of image perspective. It is thus not possible to judge about their cross section and the true distribution of dips on the basis of only stereophotogrammetric data. The distribution of dips inside the large crater may be traced by the profile.

Another widespread element of the landscape is constituted by clot-like and stone-like objects, emerging above the topographic suface, which for the sake of simplicity, we shall denominate as simply stones. There is observed in their seemingly chaotic distribution a certain regularity, which is manifest in that the stones are often seen near the brows of craters. The dimensions of the stones fluctuate in the plan as well as in height from a few centimeters to several decimeters.

To the formations creating the topographic layout should also be referred the small ridge-like elevations and also portions of the ground with a different microsculpture. Here and below we imply by microsculpture the inequalities of the soil with dimensions in centimeters and less.

A ridge is denoted on the plan, which is stretched in the meridional direction. There possibly exist other ridges, differently oriented and having gone unnoticed because of the absence of distinction in the illumination of their slopes.

On the whole, the microsculpture of the surface of the soil has an "eaten" cellular character. The dimensions of separate roughnesses, observed in photographs, constitute but a few millimeters. It is possible to judge on that by comparing them with the dimensions of the tape, constituting a part of the station, visible on the third panorama at $\gamma \approx 75^{\circ}$ and having a width of 13 mm. The roughnesses are grouped into local associations, already measured in centimeters. They are precisely responsible

for the impression of variegation which is created owing to the conjunction of brightly illuminated and darkened areas.

There are outlined against the background of such a structure areas in which the associations have a nearly linear disposition of a few decimeters' extension. Some of them are noted in the plan.

Appraising the locality of ALS Luna-9 landing site, it should be stated that it is quite complex for orientation. The latter is conditioned by the extrauniformity of the landscape, the absence of notable guiding lines, the shielding of the layout by the relief and by limited visual field, namely at observations from depressions. In this regard, the locality suggests the terrestrial stone deserts.

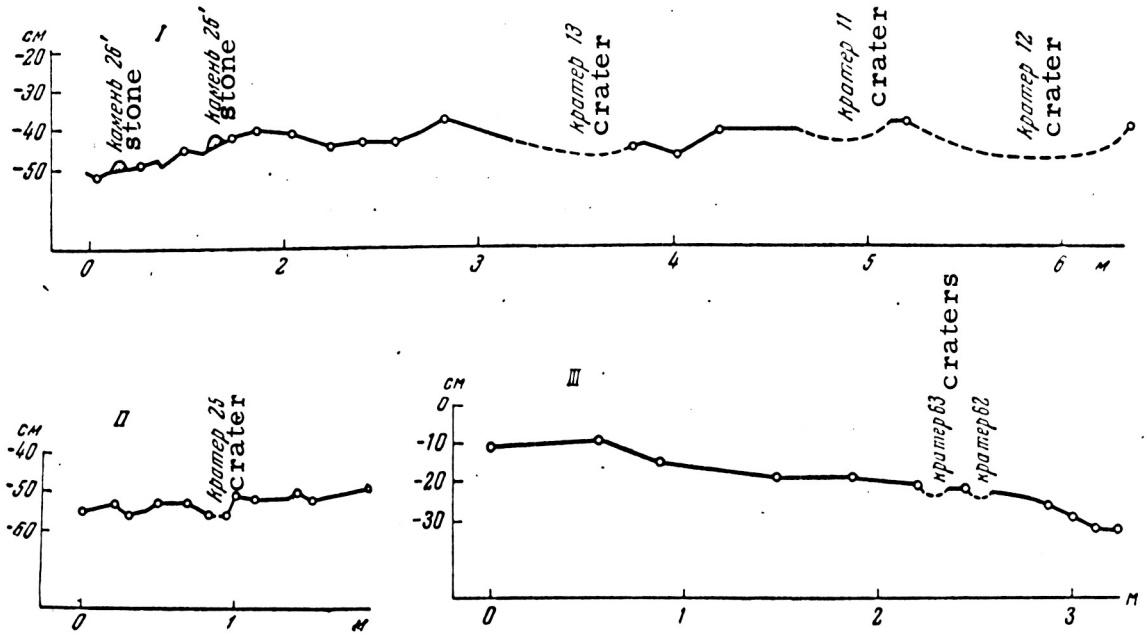


Fig. 24

Profiles of selected directions

Figure continued

Fig. 24 (continuation)

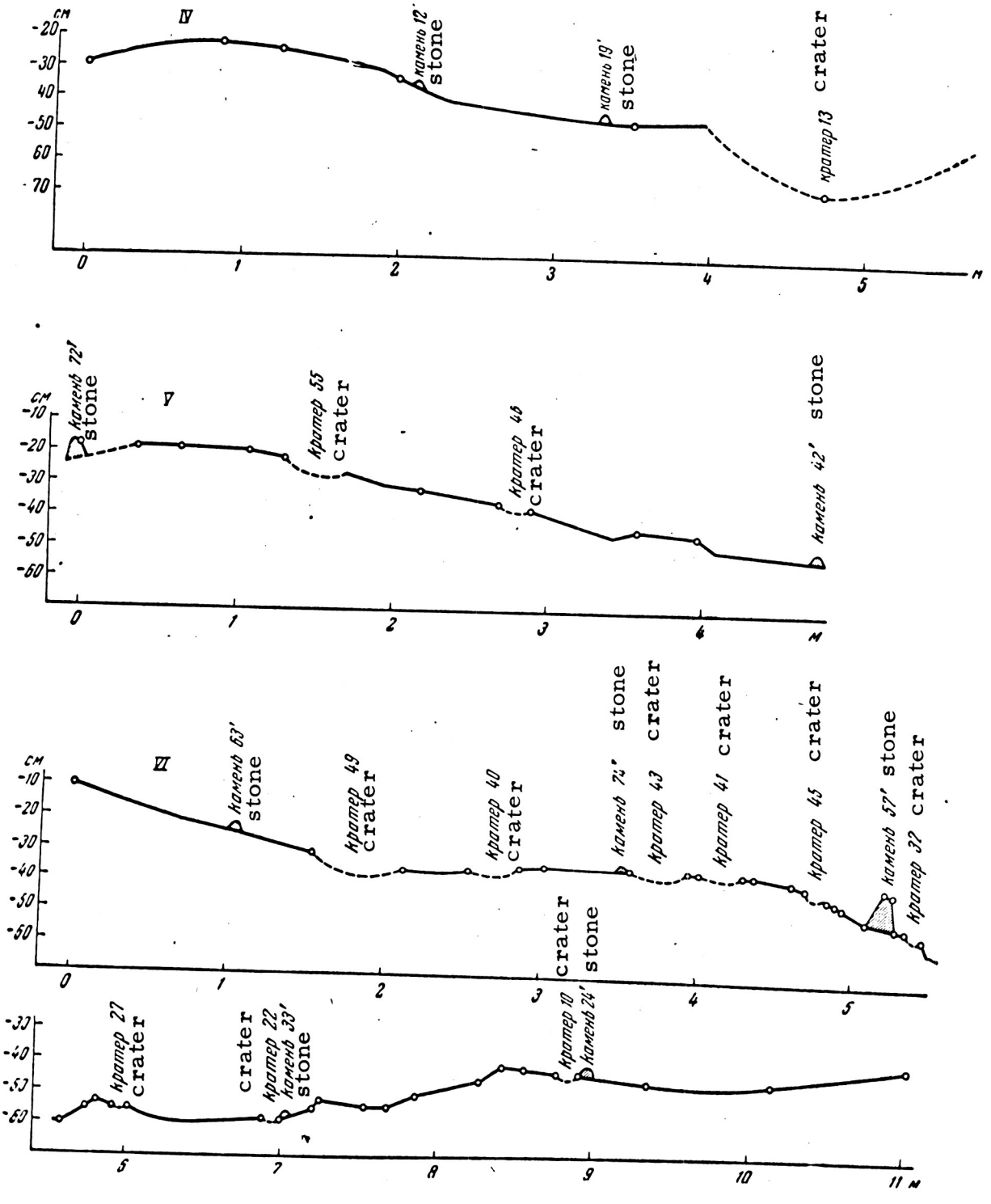


Fig. 24

Profiles of selected directions (end)

CHAPTER II

MORPHOLOGICAL PECULIARITIES OF THE LUNAR SURFACE

The first panoramas obtained by the station Luna-9 contain broad material for the study of morphological and geologic peculiarities of the landing site. Among the details visible on the panoramas, a series of characteristic type formations are exposed, which recur in the panoramas over and over again. The identity of the structure of the mutually remote details excludes the possibility of the observed forms being created by random illumination effects of by a casual disposition of elements not mutually connected; this refers also, in particular, to very tiny formations.

The investigation of the landscape surrounding the station may provide important information on the processes having taken place on the Moon's surface and on the properties of lunar matter.

In this chapter, particular attention is given to the development and the phenomenological description of the described forms. The references as to the nature of the surface and to the shape-producing processes will be limited to the most obvious aspects.

Comparison of the peculiarities of lunar landscape with the usual configurations of various terrestrial landscapes is to a great extent based upon the visual comparison. However, at such comparison there emerge difficulties, linked with the inclination of the television system's axis to the lunar vertical, as a result of which the panorama of the lunar surface acquires an unusual aspect, the horizon line inclination relative to the panorama frame being distinct in its various parts. An effort must thus be made, so as to lose the visual impression of a separately standing hill with comparatively steep slopes. This is why for a more correct perception of lunar landscapes, we brought out in Fig. 25 a panorama with a corrected horizon line, that is, disposed parallelwise to the frame.

For the transformation, realized with the aid of a phototransformer, panorama I was subdivided in fragments bounded by vertical lines distant

from one another by 12°. Each parcel was transformed separately in the assumption that within its bounds the image may be stustituted by a plane photograph constructed according to the laws of central projection. This did not introduce substantial errors. The greatest discrepancy of image details on the junctions in the lower part of the panorama did not exceed 0.5°.

In the panorama with the corrected horizon line the lunar landscape appears to be generally flat. The best expressed shapes of the positive relief, that is, the protuberances, are seen in the southwestern part of panorama I (230 - 270°). These are two hills with slope inclination of 12 to 14°.

On the basis of the consideration of images, of morphological comparison of monotypic details in various regions of the panorama, and of comparisons of panoramas, taken at different heights of the Sun above the horizon, it is possible to outline the following characteristic types of microsculptures, that is, of tiny details of surface structure.

1. - The lunes of craterlets appear as rounded out hollows of small dimensions, as a rule not having any, or having a hardly noticeable rim. The coarser ones will be called craters, as is customary for the well known lunar formations.

2. - The linear structures

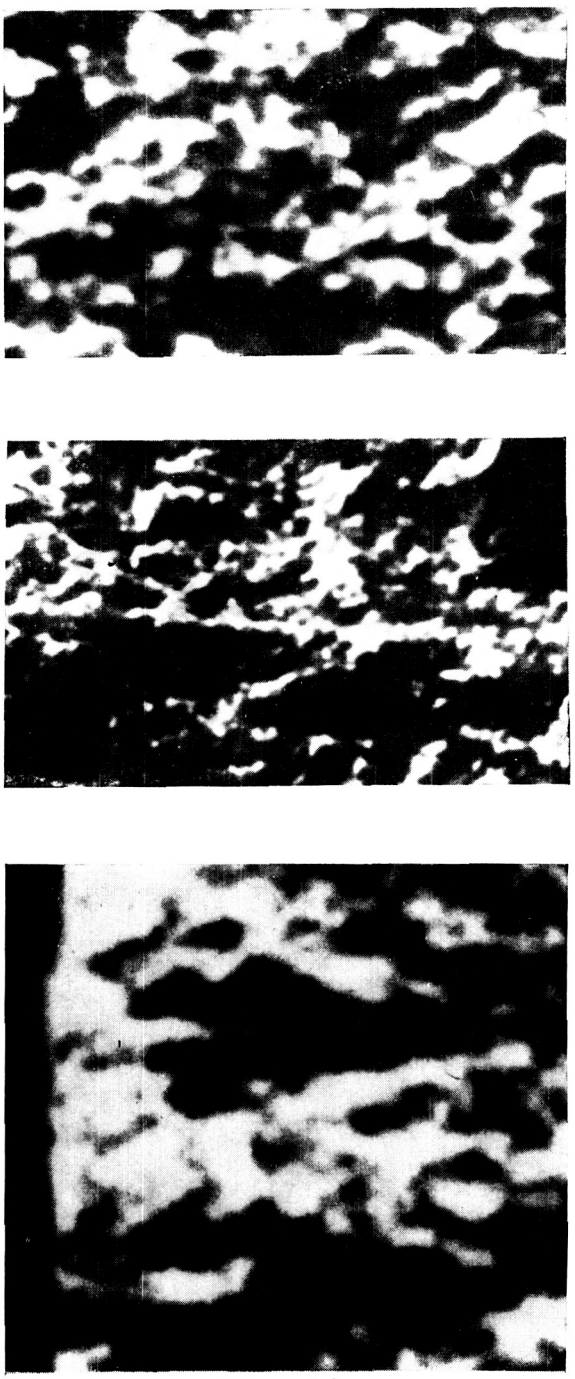


Fig. 26
Details of images with complex structure

of various types usually intersect one another in various directions, forming at time characteristic radial or forked (Y-shaped) formations, and

3.-Stones.

There are numerous portions with complex structures that lend themselves to different interpretations.

Aside from the clearly expressed forms above, intermediate, mixed and other details, devoid of any characteristic shape, and having apparently emerged as a result of multiple actions by various processes of either endogenous or exogenous nature, are revealed on the panoramas. The latter emerge as a result of meteorite and stone impacts, and also of solar wind particle action.

The predominating type of relief in the portion studied is constituted by negative shapes, having the aspect of circular pits, craters, funnels, craterlets typical of the entire surface of the Moon.

A detailed description of formations visible on the panoramas is presented below.

1. CRATERLETS

The coarsest craterlet in the right-hand part of panorama I (200 - 230°) has a diameter of about 2.8 m. – The tiniest among the clearly noticeable craterlets figured on the plan have a diameter of about 10 cm.

The statistical distribution by size of the craterlets, fixed in the central portion of the plan, is compiled in Table 6.

Here D is the diameter of the craterlet, N is the number of craterlets fixed in the plan, S is the area over which the count of craterlets was made; it is equal to 15 m^2. The distribution of craterlets by size may be approximated by the exponential function $N' = cD^{-n}$. The values computed by this formula at $n = 3.5$ are compiled in third column.

The craterlets located far away from the station are not included in Table 6. Eighty-eight craterlets are counted over an area of 50 m^2 on the topographic scheme.

The statistical data, presented above, have two essential shortcomings besides the scarcity of their number. First of all, tiny crater-

lets are poorly seen on the slopes of coarse formations or at great distances from the station, secondly, not all the craterlets were fixed in the plan, but only those to which the distance was determined with sufficient reliability by the stereoeffect, that is, the sorting of craterlets is incomplete.

TABLE 6

D, см	N	N'	$\frac{N}{S}$, $м^{-2}$
6—9	6		
10—12	11		
13—15	14	11,7	0,93
16—18	8	8,9	0,53
19—21	6	5,4	0,40
22—24	3	3,2	0,20
25—27	2	2,1	0,13
28—30	2	1,5	0,13
31—33	2	1,1	0,13
34—36	1		0,06
37—39	2		0,13
40—45	2		0,13

The minimum dimension of the observed craterlets is about 5 cm. It is comparable with the dimensions of the structural formations of the vesticular (honeycombed) lunar surface against the background of which the rounded shape of the craterlets is no longer perceptible, while the edges acquire ragged, irregular, contours. It is possible that this is due to massive craterlet superimposition. Only in rare cases can rounded craterlets with a diameter less than 5 cm be distinguished.

Separate craterlets are encountered everywhere on the panorama, including the slopes of larger scale craterlets, and possibly also on the surface of a series of stones on which portions are shown that resemble a conchoidal fracture and a fine pitting of the surface. Craterlets of small dimensions are often assembled. In these cases, they form ragged vesicular portions. Separate cells (honeycombs) within the group have usually edges of irregular shape, acquiring at times the character of a honeycomb structure.

Judging from shadows, the steepness of the inner slopes of craterlets with dimensions of more than one decimeter may, sometimes exceed 41°, which is well seen in Fig. 27, where fragments A and Б obtained during the complementary session of television transmission. In tinier craterlets, which merge with the cells, all possible inclinations are encountered, possibly including the negative angles of the inner soil voids.

Based upon the stereoscopic determinations of distances, we succeeded in measuring on the plan, the depths of five craterlets with 10 - 20 cm dimensions and a diameter to a depth ratio from 6 to 4, and one craterlet of 1.6 cm in diameter in which this ratio is 9.6. At the same time, in one case the inclination angle of the slope reached 55° on condition that we approximate the craterlet to a cone; this is because the craterlet in

Фрагмент А

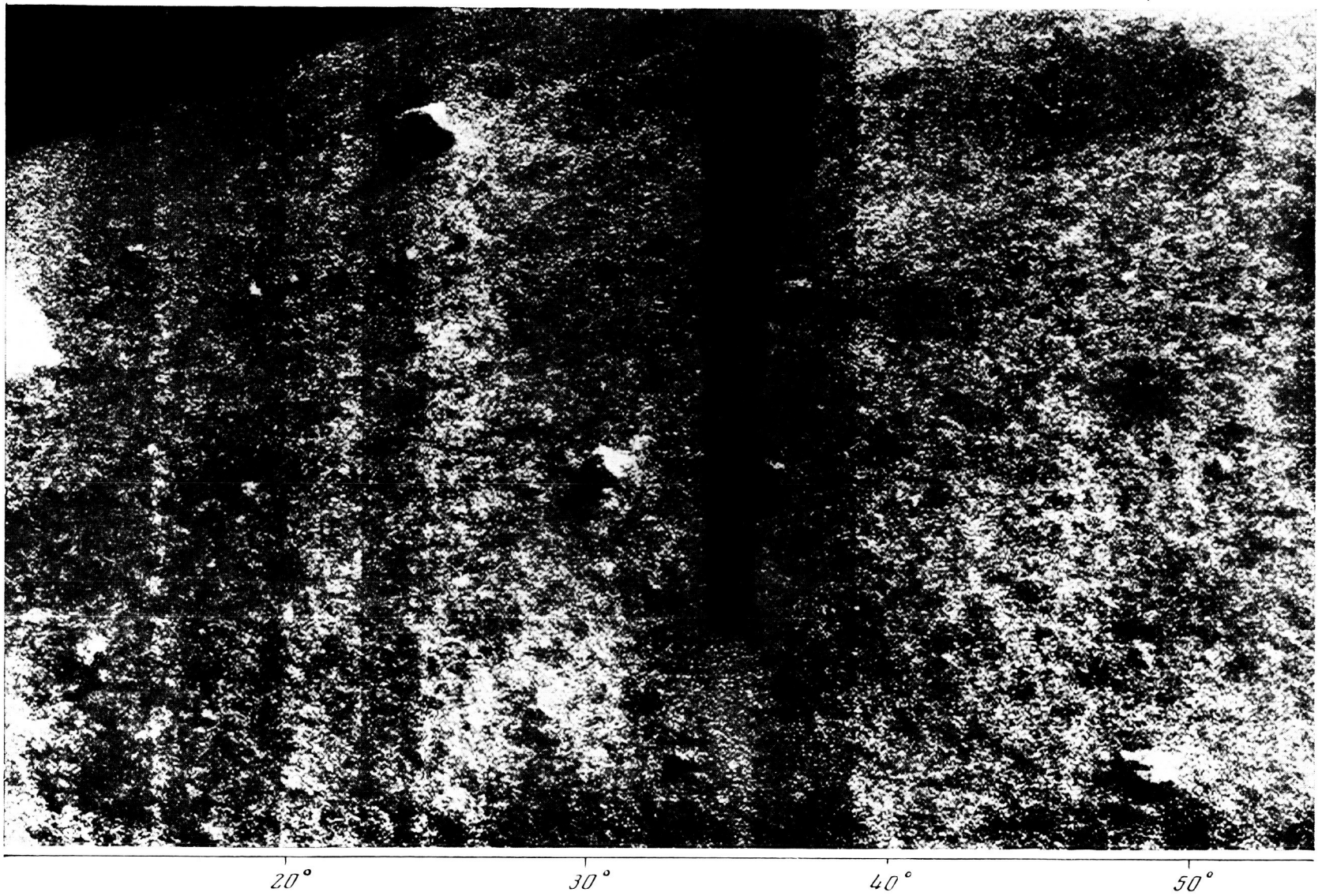


Fig. 27

Panorama fragments obtained in the course of the complementary session

question lies on a steep slope of another, coarser formation. In fact, numerous craterlets are cup-shaped and this is why the limit inclination angle may be still greater, which is evidence of sufficient soil tenacity. Plotted in Fig. 28 are the schematic cross sections of these craterlets. Shown near each cross section are: M—the scale, D—the diameter. D/h-the crater's diameter to depth ratio. We succeeded in plotting profiles for seven craterlets according to the variation in the position of shadow edges as the Sun rose over the horizon. Only the plane of the solar vertical passing through the center of the crater was then considered. We plotted in that plane a drawing, on which the points of the beginning and of the end of the shadows were marked according to the photographs of all the three panoramas. The scheme of Fig. 29 clarifies the dependence of the position and dimensions of the crater's shadows on its shape.

Further, having taken the diameter of the craterlet on the plan for the initial dimension, and assuming its axisymmetry, this drawing was superimposed with its mirror reflection and the missing portions of the contour were thus traced. In the case of unsymmetrical craters a non-correspondence could be obtained, as was apparently the case for the craterlet No. 15. The results are brought out in Fig. 30. The points correspond to actually determined values. They are joined by solid lines. The remainder of the profiles, constructed in the assumption of craterlet symmetry, was completed by dashed lines.

By stereoscopic examination of the panoramas, it may be seen that in a part of the craterlets and funnels, the inner edges do not indicate either cup-like or conical shapes, but widen upward and suggest by their shape the "trumpet" of a phonograph loudspeaker. This may be seen in Fig. 30 at craters No. 13 and 16. On the topographic plan, this property of craters is partly reflected as their confining to troughs (cavities) denoted by contour lines. The ascertaining of the true nature of funnels of such a shape, also noted on the Ranger-7 photographs, offers great interest. Such a type of funnel comes in particular at ground explosion in a case of sharp increase of strength with depth. At the level where the inclination of the funnels' slope varies abruptly, there takes place a substantial variation in the strength properties of the ground. The depth of this level is different for various craters, but is comprised within the range of a few centimeters.

The following remarks can be made relative to individual peculiarities of craterlets. No slight-produced loose material is usually noted in craterlets possibly because not all of them are fully examined.

Seen in a series of cases inside craterlets are orderly structural elements that can be linked either with the superimposition of two craterlets, or with the peculiarities of the inner soil structure. Conditioned by craterlet superimposition are probably the protruding barriers between funnels, sometimes acquiring annular structures, as may be seen in Fig. 31, ъ and possibly also in Fig. 32, б.

Another type of relief manifesting itself has a linear character and is linked with linear structures intersecting the craterlet; they are described below. Within the bounds of the general contour of craterlets, such formations are seen in Figs. 31, a and б, partly in 31, ъ and also in Fig. 32, б, ъ.

Usually the deepenings are devoid of a clearly expressed swell, which is sometimes noticed by a general increase in the illumination of the contour of the crater, and it is only seldom established with complete certitude as a result of favorable illumination conditions, even in the case of its insignificant development. A swell around the crater, may, for example, be observed in Figs. 31, a and д. In the latter case, a clot-like structure can be seen.

Finally, some of the formations should be referred to again, of which one is represented in Fig. 31e, ж (in a right lower angle), and the other like it, in Fig. 32 б, і (to the left above). These are small tubercles, resembling bulges with a deepening of the tubercles' upper part. The depth of the internal contour of pits is not examined and their structure is so far uncertain.

It is easy to have a representation on the dimensions of the entire formation by looking at Fig. 31, e, where alongside with it lies a tape 35 mm wide.

It is remarkable that no traces of structureless dust layer are noted anywhere within the limits of the panorama, including the slopes of funnels lying in the direct vicinity of the television head. All visible portions are characterized by clearly expressed structurally-bound formations, having probably emerged as a result of conglomeration of pulverized particles.

2. LINEAR STRUCTURES

By linear structures, we understand here the formations having for a common characteristic the fact that the principle element of their

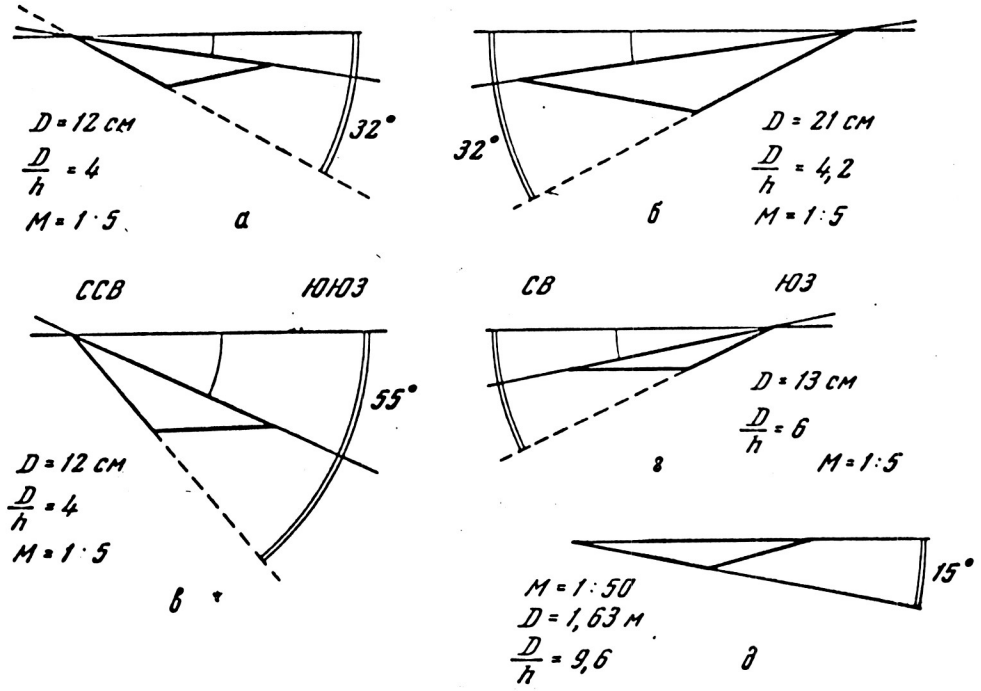


Fig. 28
Cross sections of craterlets according to togoraphic plan data

Craterlets NN 15 (а), 25 (б), 33 (в), 54 (г), 13 (д)

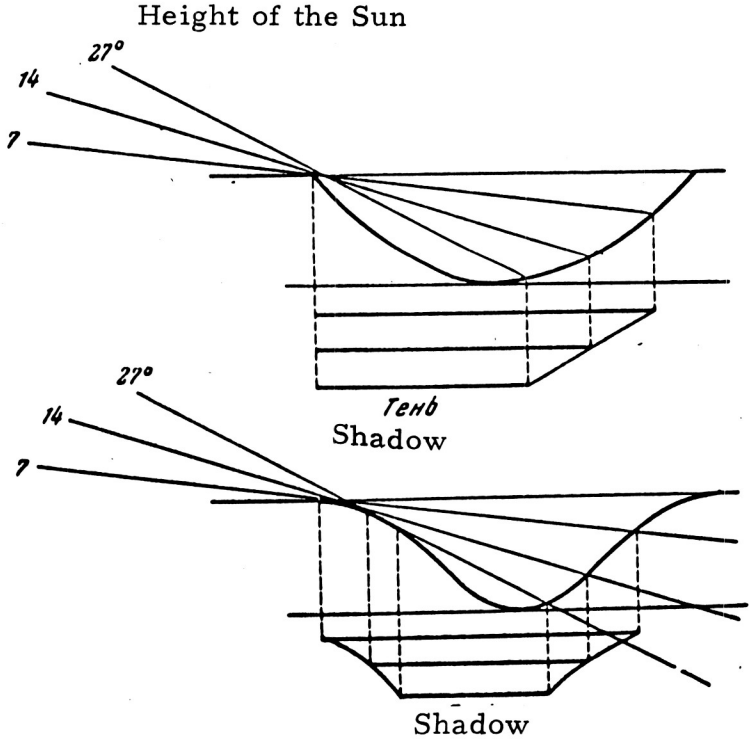


Fig. 29
Character of the variation of the darkened part of the funnel as a function of illumination conditions for various funnel's profiles.

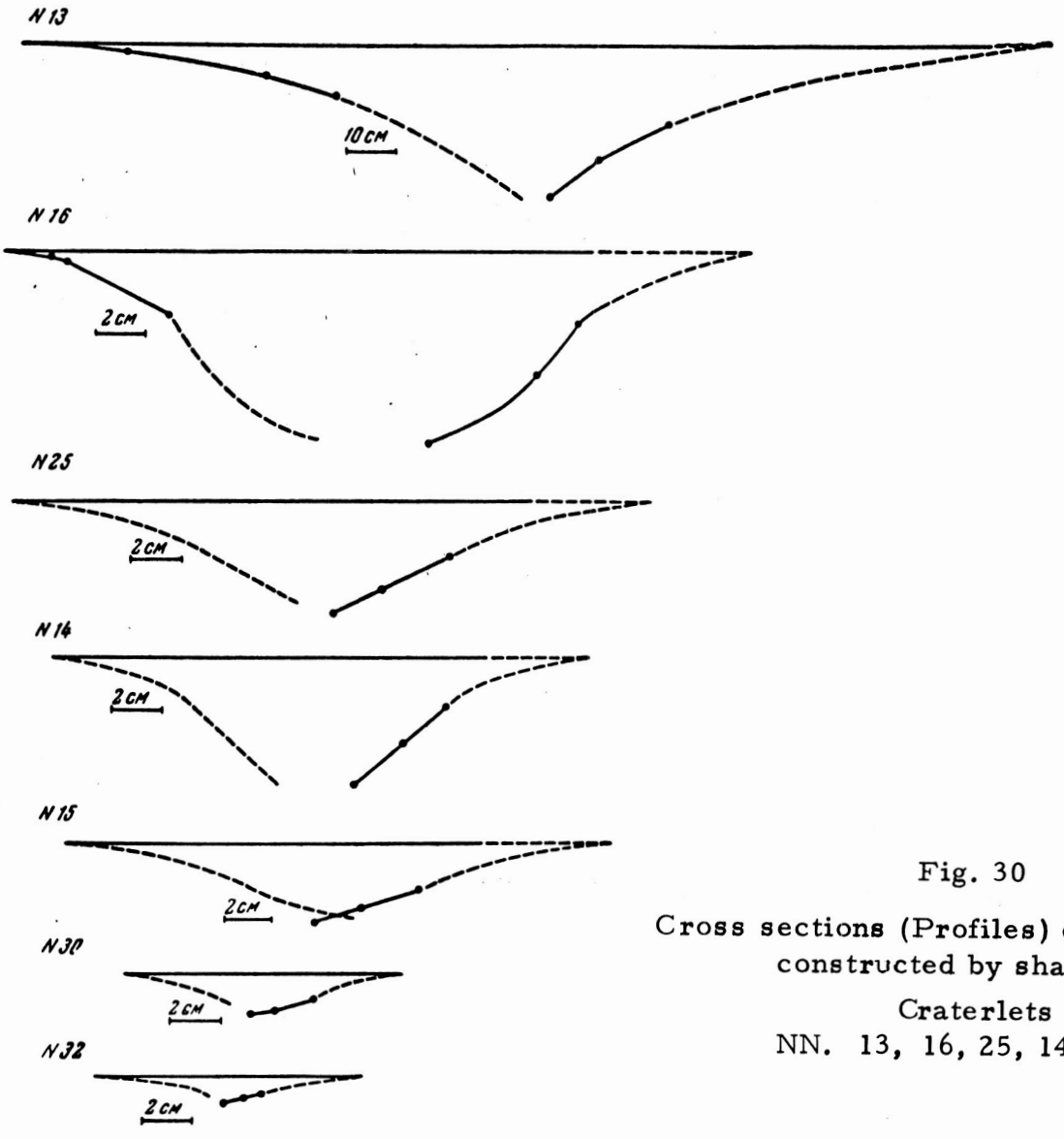
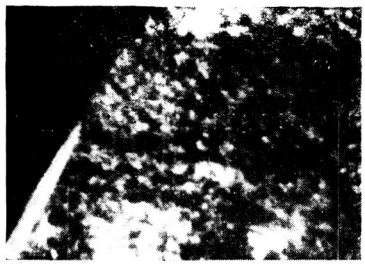


Fig. 30

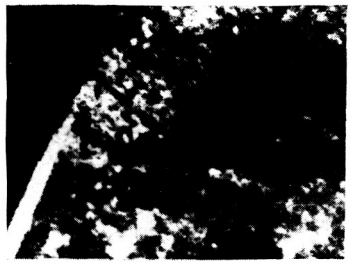
Cross sections (Profiles) of craterlets constructed by shadows

Craterlets
NN. 13, 16, 25, 14, 15, 30, 32

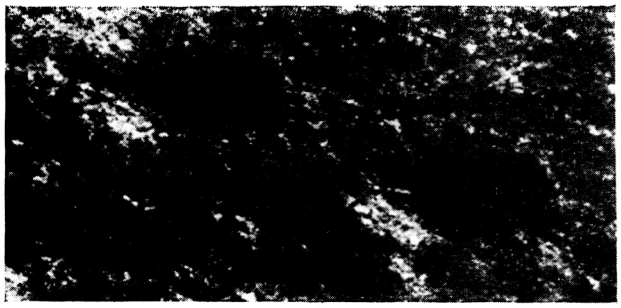
However, some sort of separately fallen-in stones or clots (Fig. 31, e), as well particle accumulations (Fig. 31 a, б) may be observed though rather rarely. The fine spongy structure of the illuminated part of the craterlet, situated within the resolution threshold of the television camera, can be well distinguished in Fig. 31 б, and may be set against the coarsely cellular structure of the lower craterlet in Fig. 31 в, which is brought out in a transformed planar form in Fig. 31 ж. -Two varieties at least can be outlined in the microsculpture of funnels' bottoms. In many cases, the slopes of the funnel resemble by their structure the surrounding rock. The character of structure, defining the irregular and ragged edges of the funnel, having a diameter of about 15 cm, can be expressedly seen in Fig. 31 ж.



а



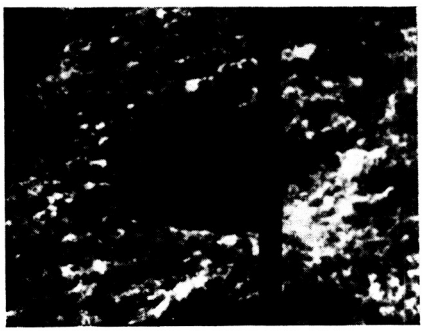
б



в



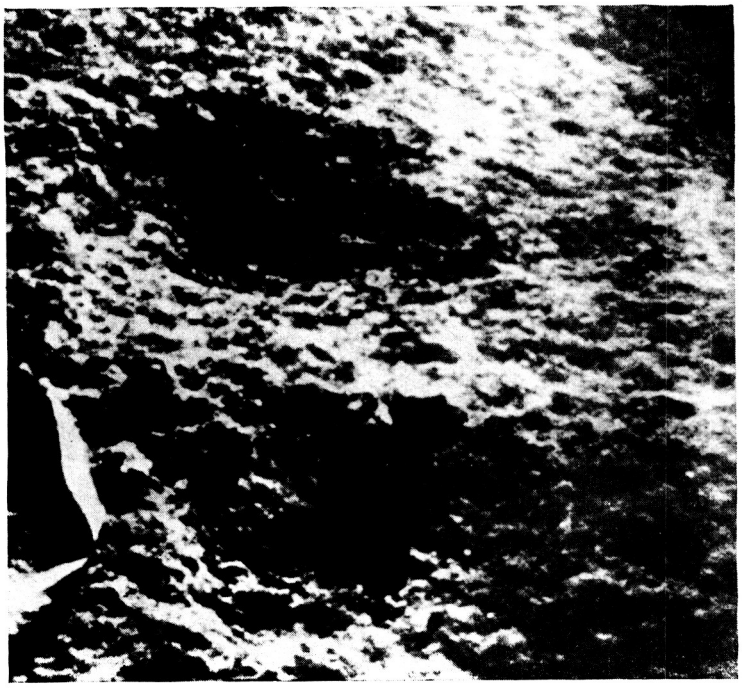
г



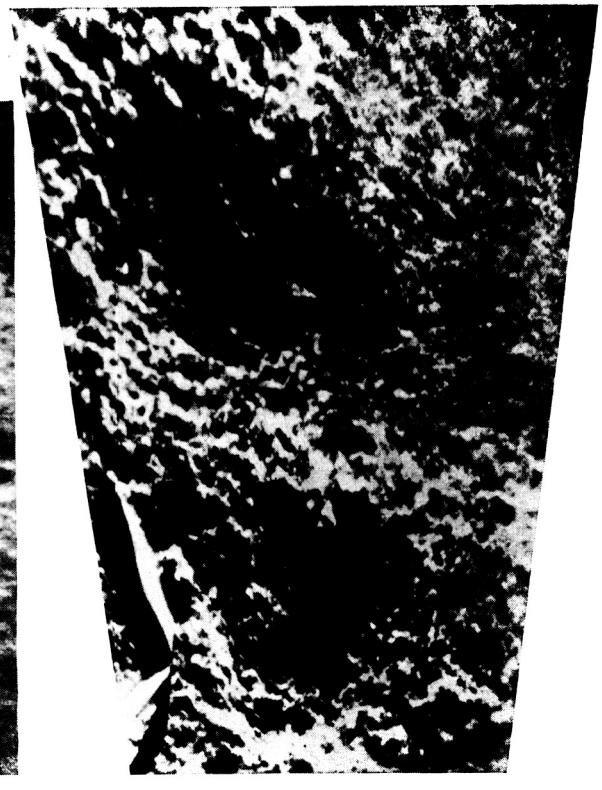
д

Fig. 31
Details of the panoramas

а — panorama III, $\gamma = 10 \div 20^{\circ}$; the frame is cut parallelwise to the horizon; б - same detail for panorama II; в - panorama II, $\gamma = 40 \div 50^{\circ}$; г - panorama III, $\gamma = 80 \div 90^{\circ}$; д - panorama II, $\gamma = 130 \div 140^{\circ}$; е - panorama III, $\gamma = 80 \div 90^{\circ}$; ж - transformed photograph of the same detail.



е



ж

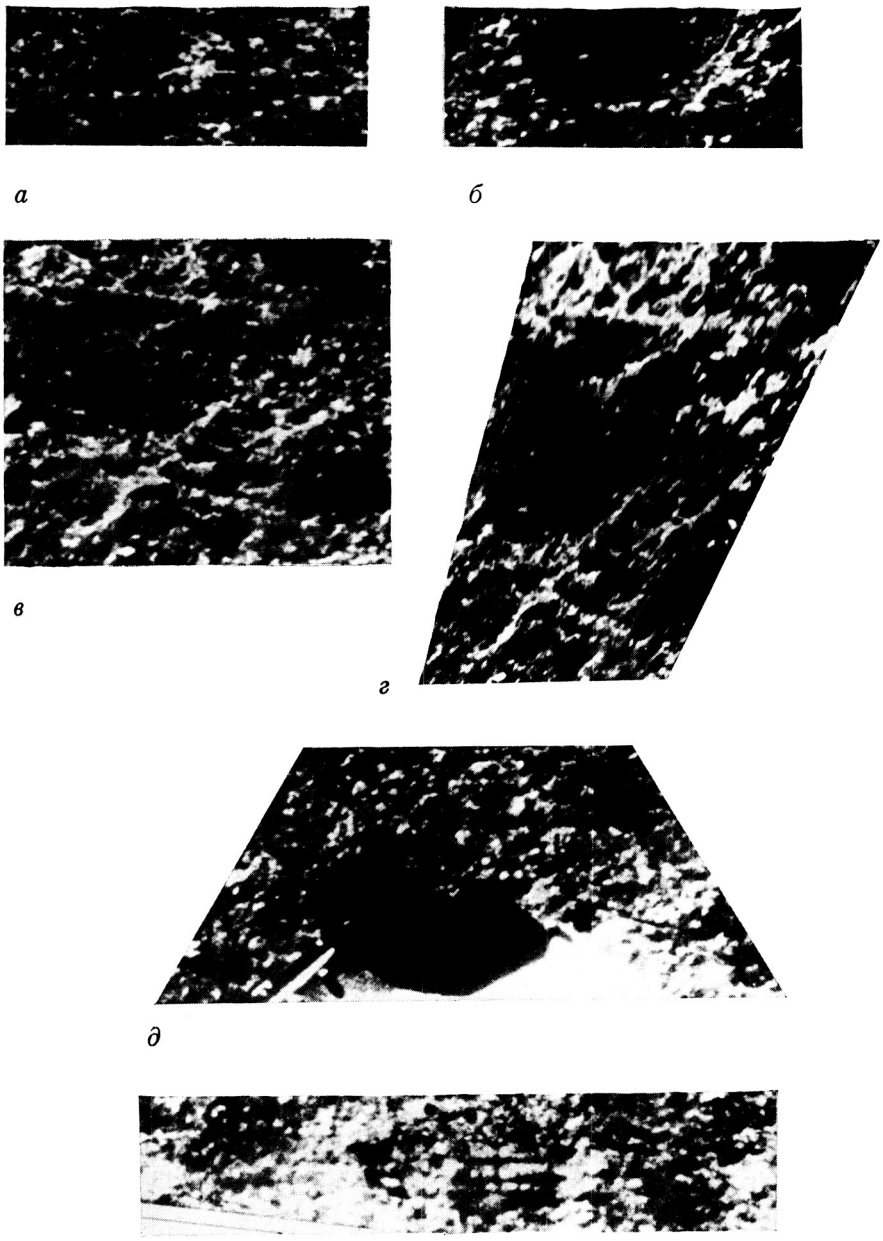


Fig. 32

Examples of linear structures

а, б — panorama III, $\gamma = 130 \div 140^{\circ}$; the frames of the photographs are parallel to the structure; в — panorama III, $\gamma = 130 \div 140^{\circ}$; г - transformed photo of the same detail; д - panorama III, $\gamma = 150 \div 160^{\circ}$; е — panorama III, $\gamma = 170 \div 180^{\circ}$; the frame of the photograph is parallel to the "laminar" structure.

shape is a straight line or a plane.

The basic types of linear structures are:

a) the linear sequences of monotypical protrusions forming nearly rectilinear structures;

b) the small, somehow plane areas ("facets"), interlocked into volumetric structures, that is, the complex "polyhedrons"; particularly often encountered are polyhedrons, suggesting parallelipipeds or forming an "indented structure";

c) small radial or Y-shaped forms (Fig. 32, б, в) fashioning at intersection points of linear structures and running in various directions;

d) structures, of which the details are not discernible; for a given illumination they suggest chains.

The detection of tiny linear structures is in principle a new fact, characterizing the essential peculiarities of the lunar surface.

Extended linear structures are noticeable on all the well examined portions of the lunar surface nearest the station; they attain a particularly sharp expression between the panoramic longitudes $140 - 150^{\circ}$. (See Fig. 33).

The small width of the linear structures (usually centimeters) and the insignificant relief allow their perception only at specific illumination conditions. At low position of the Sun they are hardly noticeable, being covered up by the long shadows of the irregularly disposed surface irregularities. A difficulty of a different character for reliable tracing of these structures arises from the natural tendency of the eye to assemble the disorderly scattered points into a system. Thus, despite the fact that the very presence of linear structures calls for no doubts, their incorporation into either system is not always trustworthy, and is only now and then subjective. to some extent.

One of such possible systems is presented in Fig. 33 with the view of showing how shorter, more clearly outlined portions of such structures may be united into a single smooth line passing through the place of questionable visibility and having a general length of several meters. When studying these lines, a stereoscopic effect was used, which increased the reliability of their tracing.

For more reliable linear structures of lengths from 20 to 30 cm a vectorial diagram of directions has been constructed. It shows that two

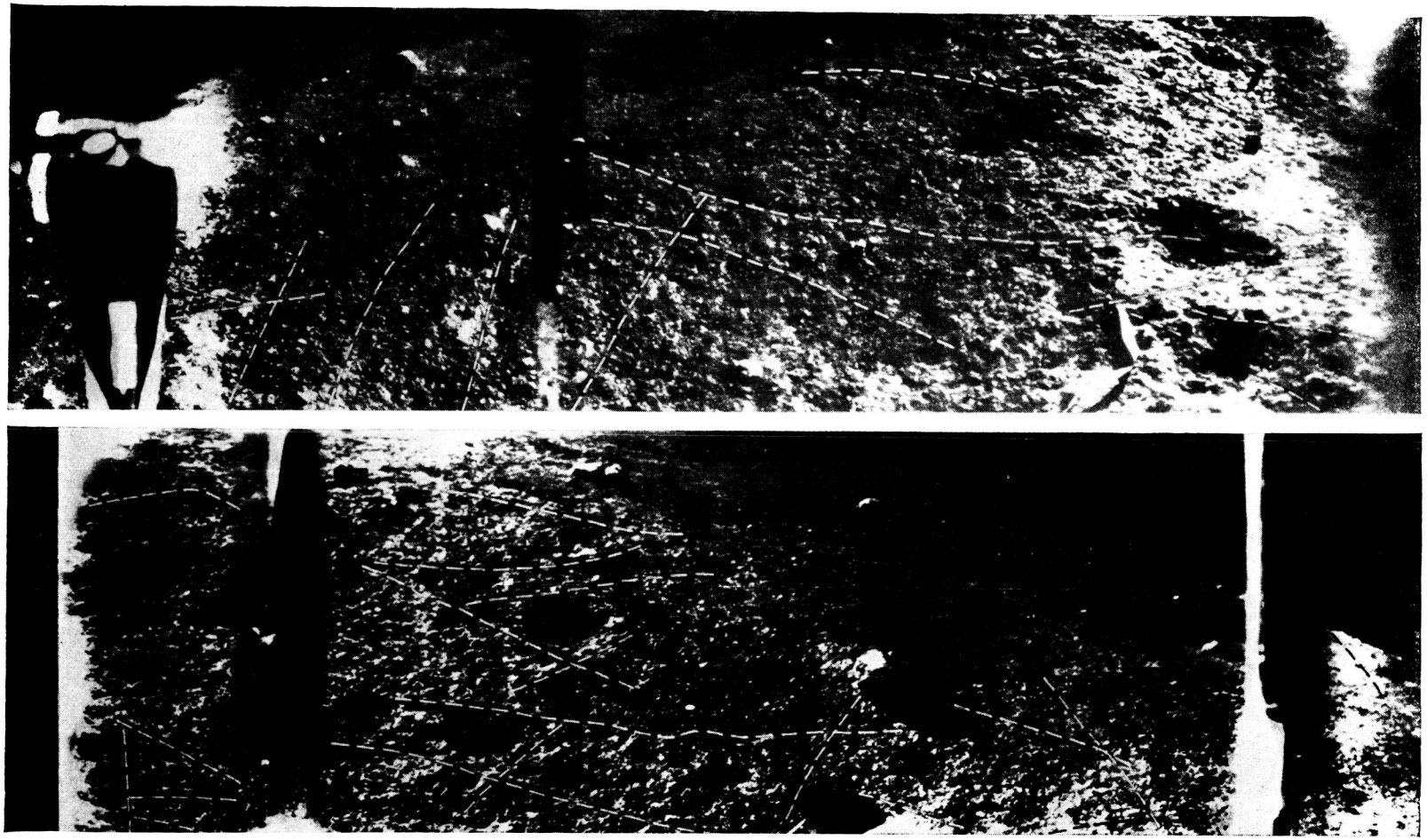


Fig. 33

Disposition of linear structures
in the panorama.

prevailing directions take place along the azimuth: 0 to 10° and 40 to 50°.

A direct measurement of intersection angles of two clear linear formations in transformed photographs of the photoplan (Fig. 32, ν) give the intersection angle of various structures at 40 and 70°. In the same drawing as in Fig. 32 a, δ a linear structure is visible crossing the craterlet. Apparently, it is stronger than the surrounding rock.

The relative strength of such structures is particularly clearly seen in Fig. 32, δ , and the protruding and thickened part of the structure disintegrates here perpendicularly to the course into a system of regular blocks, providing sharp shadows.

Another type of linear formation, resembles the one visible in Fig. 31, a, δ, and can be seen in Fig. 32, ϑ to the left. It looks like a deepening suggesting a filiform crevice (joint). Seen in Fig. 32, δ is a crack-patterned deepening along which clear points are disposed, gently protruding above the general soil surface.

Apparently, linear formations are stronger than the surrounding rocks, but they are disintegrating with comparatively greater ease into tiny structures in transverse directions. It is possible that these are outcrops of tiny veins as a result of superficial erosion; they have greater strength than the surrounding formations.

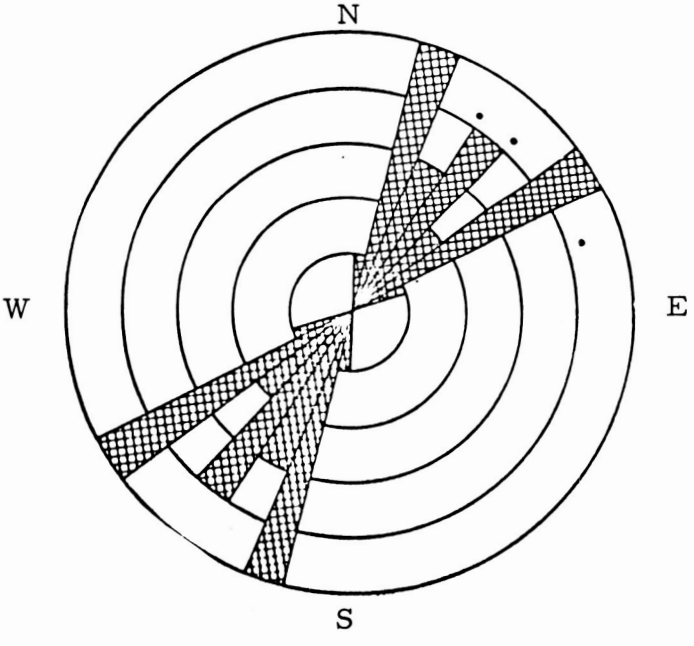


Fig. 34

Vectorial diagram of linear structures

3. STONES

It was already said above that the word "stones" was introduced as a conventional term. Being too indeterminate, this term is seldom used in geological literature, where it is substituted by narrower concepts, characterizing the nature and morphology of fragments of rocks. But precisely because of this uncertainty, this term is practical for denominating formations resembling stones on the lunar surface, at least until their more precise definition.

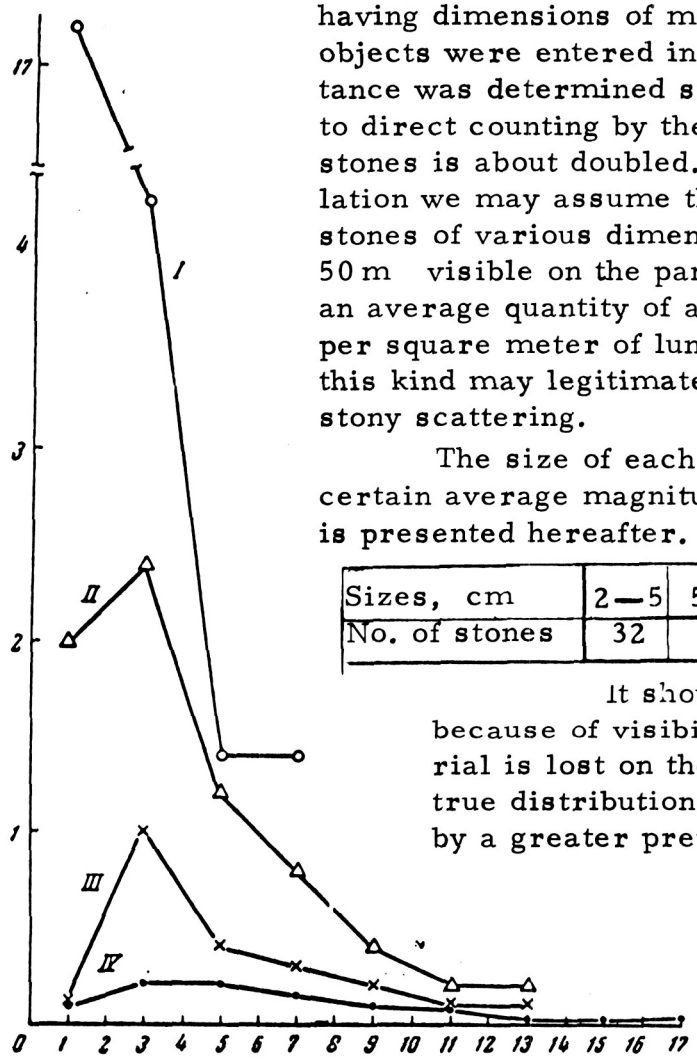


Fig. 35

Graph of the dependence of the number of visible stones on their dimension for various zones of the panorama

Seventy-five stones were entered on the plan, having dimensions of more than 2 cm. Only those objects were entered in the plan, to which the distance was determined stereoscopically. According to direct counting by the panorama, the number of stones is about doubled. For an approximate calculation we may assume that there are no less than 150 stones of various dimensions over an area of about 50 m visible on the panorama; this corresponds to an average quantity of about 3 stones pf such a type per square meter of lunar surface. A surface of this kind may legitimately be denominated as a stony scattering.

The size of each stone is characterized by a certain average magnitude. The distribution by size is presented hereafter.

Sizes, cm	2—5	5—10	10—15	15—20	20—25
No. of stones	32	31	4	6	2

It should be taken into account that because of visibility conditions, the tinier material is lost on the more remote plans, while the true distribution curve must be characterized by a greater prevalence of smaller size stones.

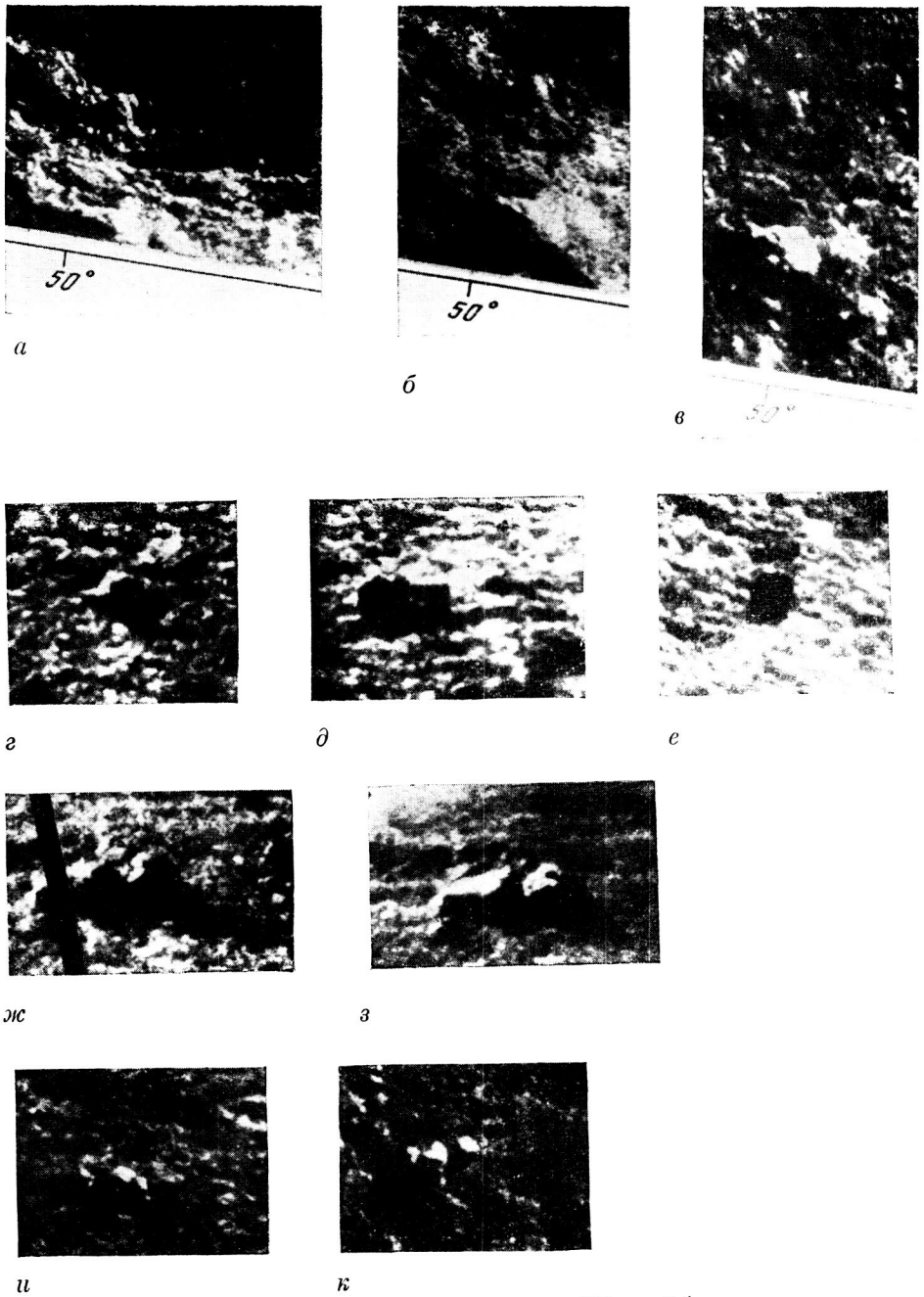


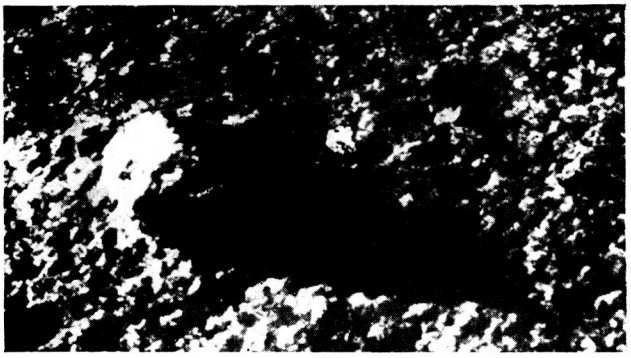
Fig. 36

Examples of stones and their groups

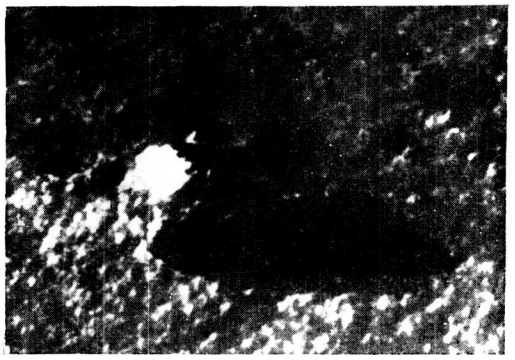
а, б, в, - stones at $\gamma = 50^{\circ}$ in various panoramas; the frame of the fragment is parallel to the horizon (а - panorama I, б - panorama II, в - panorama III); г, д, е - sharp angle fractures of various stones, panorama III (г, д - $\gamma = 120 \div 130^{\circ}$; е - $\gamma = 80 \div 90^{\circ}$); ж, з - group of stones $\gamma = 140^{\circ}$, possibly having formed from the disintegration of a monolithe (ж - panorama II, з - panorama III); и, к, — groups of stones, panorama III (и - $\gamma = 60 \div 70^{\circ}$, к - $\gamma = 55 - 60^{\circ}$)



а



б



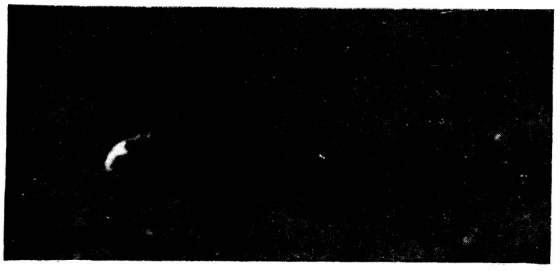
в



г



д



е

Fig. 37

Morphological peculiarities of stones

а, б, в - nearby stone at $\gamma = 160^{\circ}$ (а - panorama I, b - p. II; в - p. III)
г, д, е - shape variation of the remote stone at $\gamma = 160^{\circ}$ at different illumination (г - panorama I, д - p. II, е. - p. III)

Such dimensions fit the understanding of the term "detritus" under which stones with sizes from 1 to 10 cm are described. This term should be taken with reservation for it includes the representation of original form preservation in the rock's fracture (absence of toughness and of noticeable surface erosion of fragments), which is not quite applicable to the given case.

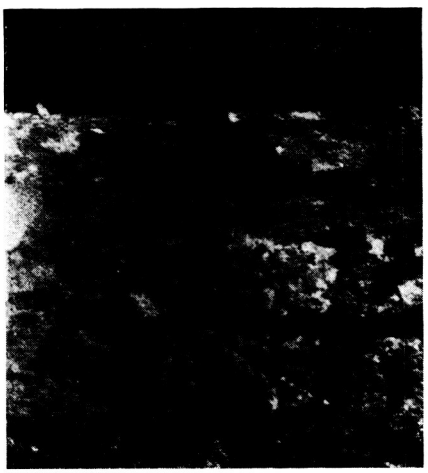
The distribution of visible stones as a function of their dimensions may be seen from the graphs of Fig. 35, where their count is given by various zones of panorama III, separated by lines of remoteness (see Fig. 22, б), drawn at every meter, so that the first zone corresponds to the distance of 1 m, the second from 1 to 2 m, the third from 2 to 3 m and the fourth from 3 to 6 m. The mean number of stones per m^2 for each zone is plotted in ordinate axis and the diameter of the stones in the abscissa.

Solitary stones predominate in the panorama; they lie between funnels, but are also encountered in groups giving the impression of fragments of one monolithe (Fig. 36, ж —k). Particular attention is earned by several chains of stones, disposed along a straight line. It is characteristic that the most clearly expressed range of stones (190 - 195°) extends in the direction of about 190° which is one of the most typical of the course of linear structures (Fig. 33). This line is also drawing attention by some of its external peculiarities allowing to assume here the passage of a denser structure, suggesting a disintegrated dyke or vein.

The observed relief, expressed by craters (craterlets) of various dimensions, may possibly have a meteoritic origin. However, it should be assumed that the enormous amount of observed stones can not be meteorite fragments. The number of lunar rock fragments on the surface must exceed the number of meteorites by several factors, and the detection of a meteorite on the panorama is of little probability.

Speaking of the character of occurrence of stones, it should be mentioned that some of them convey the impression of stones freely lying on the surface (see Figs. 36, 37, а— б) and even of stones having rolled down the craterlets (Fig. 31, а, в, е, ж and the others appear as if they were either having closer bindings with it, or being eroded in the process of soil disintegration (Fig. 36, а— в and 37). It is even possible that the row of stones at 190° longitude is the result of erosion.

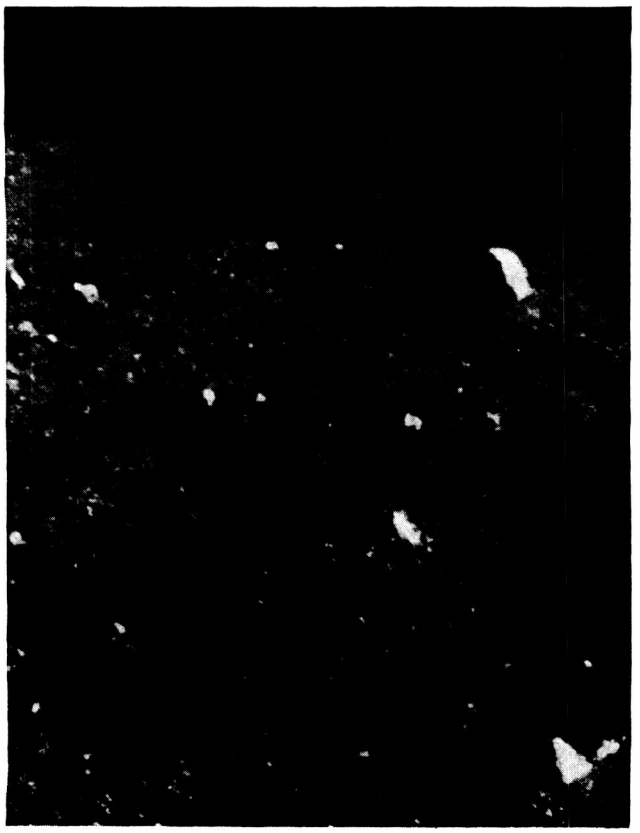
The surface of the stones often has a peculiar, unequal, "eaten" or corroded aspect, that suggests the eolian erosion of superficial dis-



а



б



в

Fig. 38

Panorama portion 15 - 30°

Frame parallel to horizon;
a - panorama I, - p. II, - p. III.

solution of certain terrestrial rocks. An irregularity of either the acting agent of of the formation's stability is usually clearly outlined in these processes.

Seen in Fig. 37, а—ґ are the details of a stone at different illumination. Attention should be given to what extent its external aspect is changing, and how one could easily be induced into error when estimating its shape. Quite curious also is the dented structure of the stone's crest, visible in all photographs.

Shell-like recesses are noticeable on the surface of numerous stones (Fig. 36, а, ѕ, and 37, ѵ, ѳ), that might be traces of micrometeorite impacts or a fracture of rocks, having a glassy structure.

An interesting spot at the base of the left-hand side of the stone is visible in Fig. 37, ѵ, ѳ; it may be interpreted as a certain accumulation of poured material at the time of the stone's disintegration or as erosion during the destruction of the bottom of the concealed parts of stones of large dimension.

Two stones are shown in Fig. 36, а, ѕ, of which one apparently lies freely on the surface while the other passes somehow unnoticed into the formation surrounding it, even by surface fracture. In this figure, as well as in Fig. 38, one may see that certain stones are raised, somhow finding themselves on some peculiar pedestal (this is seen in Fig. 38 in two places). The rise of a large stone is clearly evidenced by the distortion of the shadow in Fig. 38, ѕ. It is probably explained by the fact that the stone creates a peculiear protection of the soil over which it lies from the effects of erosion factors. This contributes to the preservation of the softer soil surrounding the stone. Turning back to Fig. 36, ѕ attention should be given to the tiny vesicular surface of the stone noticeable from its right-hand side. Apparently, an identical structure can be observed at the threshold of the image's resolution in Fig. 37, а; it is not noticeable at all under different illumination angles.

The small stones shown in Fig. 36, ѵ — е, which have clearer and sharper angular fracture surfaces, differ from the preceding by a somewhat different character of their surface. This may be explained by a fresher surface fracture as well as by the fact that the stones are relatively strong fragments, having fallen from linear formations of distinct petrographic character.

Fig. 36, ѫ — ѯ shows examples of group layout of stones, probably constituting the scattering of a single monolithe.

Certain stones have smoothed out round contours (Fig. 37) even at different illumination. However, considering the preceding figures, for example, Fig. 36, ж, з , one may see that the tiny details of surface structure may go quite unnoticed during contrast illumination of the lunar surface.

4. GENERALIZED MODEL OF THE LANDING SITE

The area swept by the station Luna-9 is small, and in order to judge on the nature of this area, a link must be found between the view of the panorama and the forms of the Moon's relief that are observed from Earth or photographed by other spacecrafts. In other words, a certain generalized model of the landing site must be obtained. Two paths for constructing generalized model of the locality are obvious: it is possible to average the heights by way of geodetical processing of pictures transmitted by Luna-9 and to obtain by the same token a smoothed out model, but one may also take another path, namely: to utilize the physical peculiarities of the investigated portion of the surface by correlating them with the well known lunar relief characteristics. The second way has certain advantages inasmuch as a reliable determination of the relief by geodetical methods is possible only near the station, where the stereoscopic effect manifests itself more tangibly.

When constructing a generalized model, we took advantage of the fact that aside from the true horizon there is seen in the panoramas some sort of a "second" horizon (see for example, Fig. 39), upon passage through which both the brightness and landscape saturation by tiny details change rather abruptly. The spherical coordinates of this second horizon in the system linked with the station, were found to be lying on a small circle. If we assume that the plane of this small circle is truly horizontal, the station's inclination relative to the local vertical will be only about 16.5° for the first panorama and about 22.5° for the third.

Knowing the station's inclination relative to the vertical, it is possible to project on the plane perpendicular to it the points located on the second horizon, that is, to obtain a planar image of this second horizon. It should, however, be noted that the plan will be dimensionless, inasmuch the measurement unit must then be the height of the center of the center of the scanning mirror above the projection plane. An example of a plan obtained in such a fashion from panorama I is presented in Fig. 40. It is not difficult to see that the points of the second horizon are quite satisfactorily represented in the plan by a circle, the center of which lies somewhat more northerly than the inclination plane of the camera. Taking in-

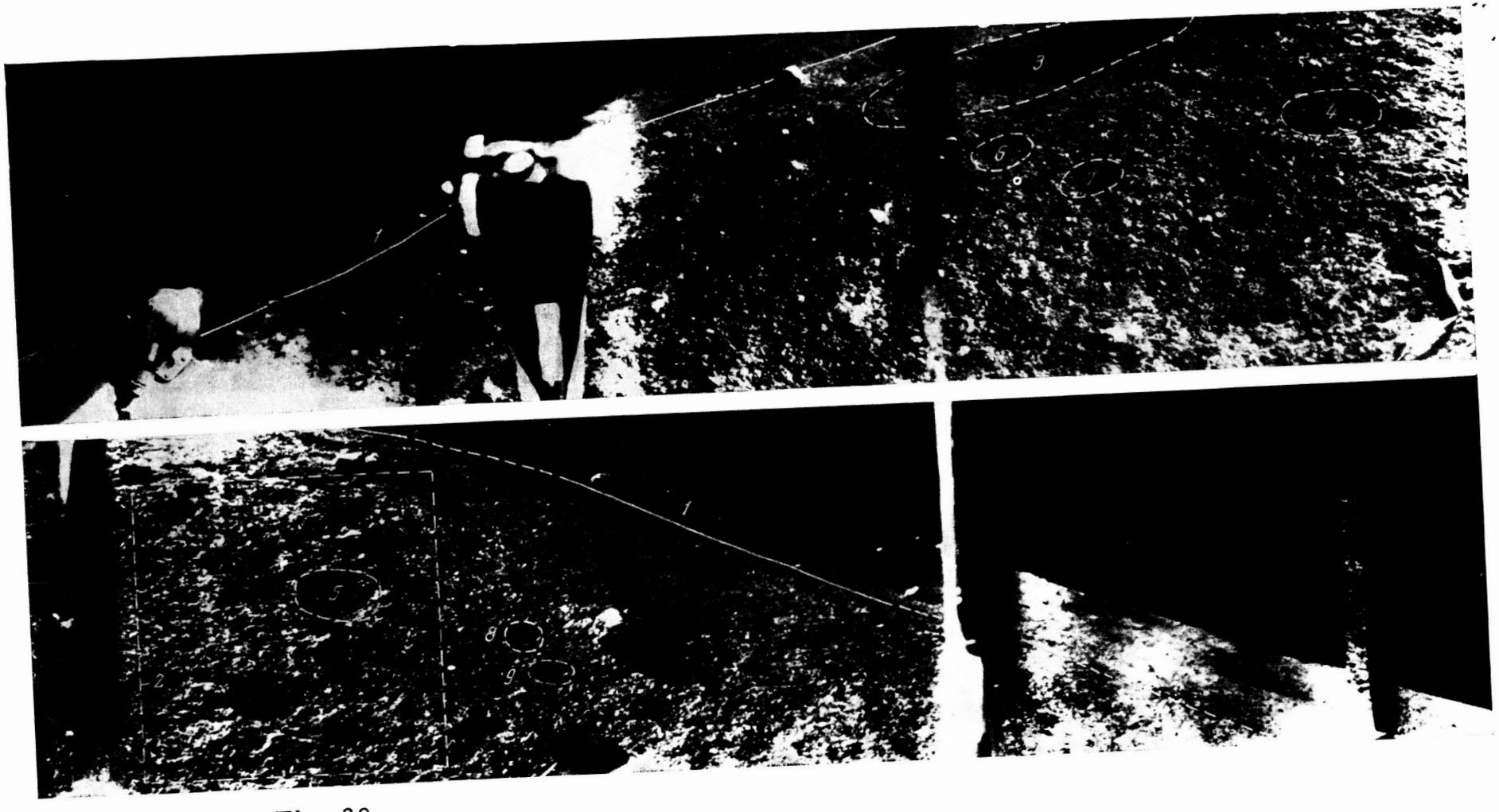


Fig. 39

Disposition scheme of the details of the relief

1 - "Brow" of the 15 m. crater;
2 - region of linear structures;
3 - 9 - craters, for which profiles were made by the shadow method

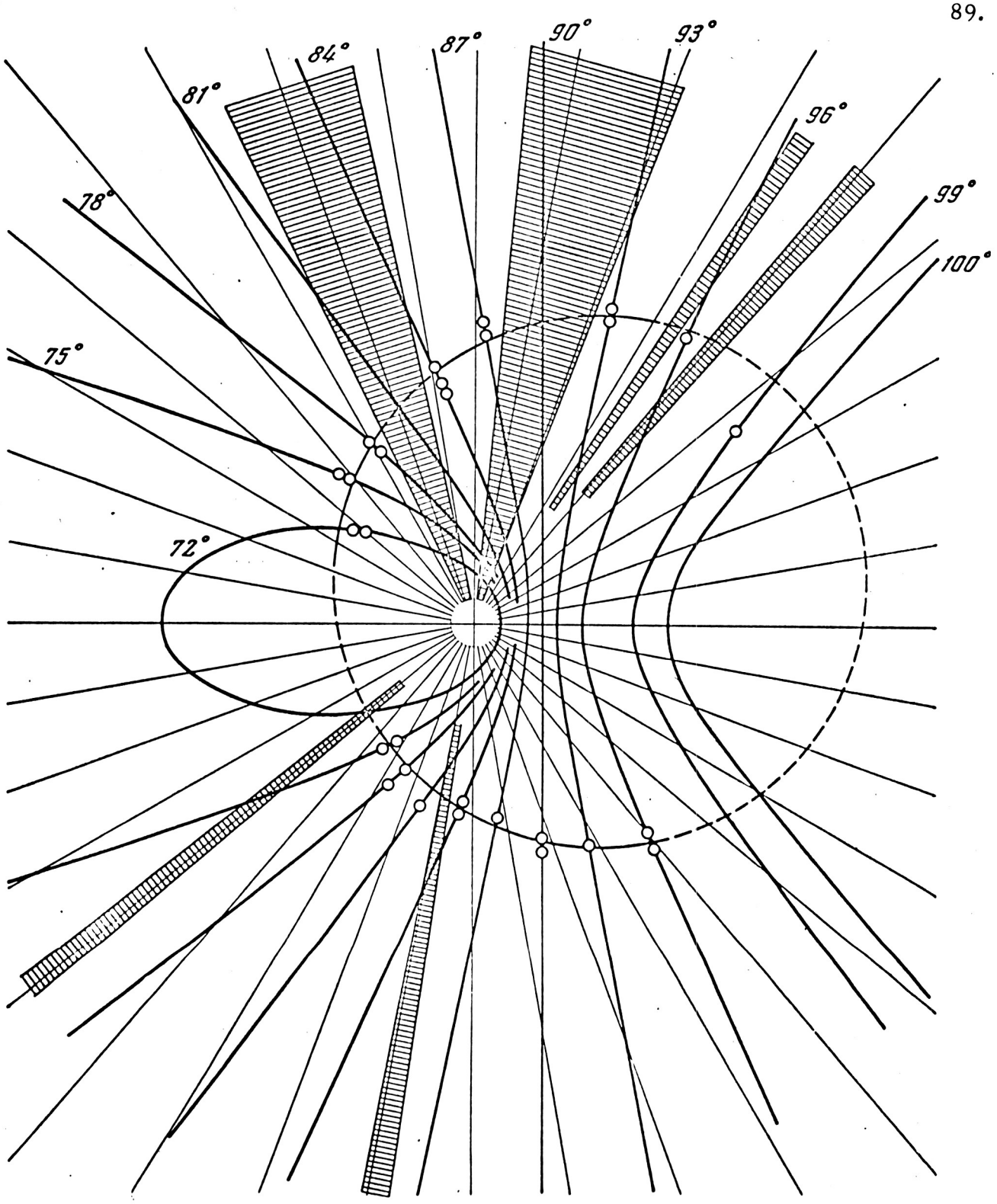


Fig. 40

Plan of the "brow" of the 15-meter crater

The rays correspond to lines of equal azimuths, the hyperbolas to lines of equal heights in the system of spherical coordinates linked with the station. The rings are the points of the brow taken down from panorama I.

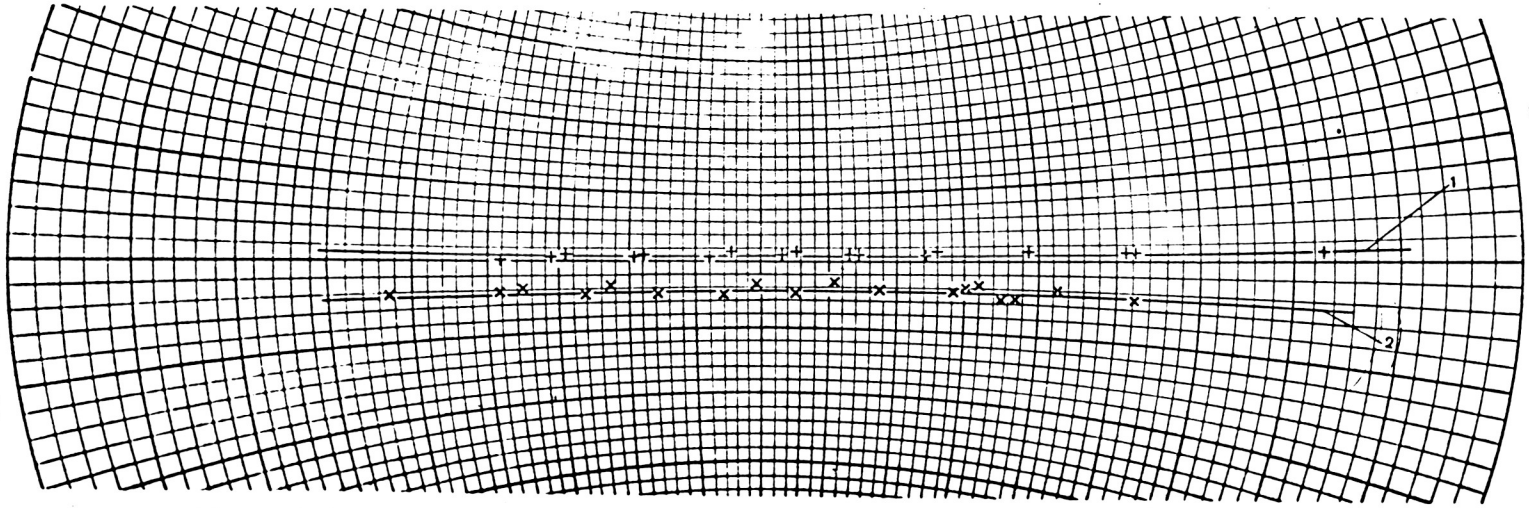


Fig. 41

Spherical coordinates of the visible horizon (1), of the 15 meter crater's brow (2) in the panorama I. During the transmission of this panorama the axis of the station was inclined at the angle of 16.5° to the E.

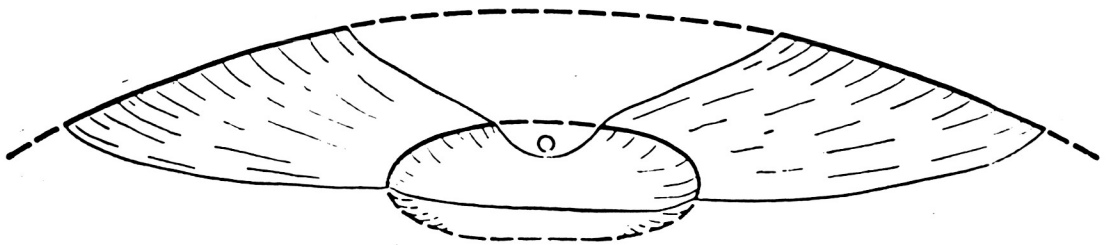


Fig. 42

A possible generalized scheme of the relief

to account that for the morphology of the lunar relief in any scale the overwhelming prevalence of round craters is typical, it was natural to assume is located on the western slope of the funnel and is inclined to its central part, that is, to the East.

In order to obtain a representation on the linear dimensions of this funnel, stereoscopic portions of the landscape obtained with the aid of the dihedral mirrors were utilized.

It was assumed that the internal path of the crater is closed in its shape to a spherical cup. Such a model was adopted only for a rough representation of the generalized relief and it apparently approximates it satisfactorily in the area observed from the station and lying inside the crater.

In the locality eleven points were identified by three images in the mirrors and by their coordinates in the system linked with the station; the position of the center and the radius of the approximating sphere were determined by the method of least squares. It was assumed that the center of the square lies above the center of the crater. The estimate of the position of the center and of the radius of the approximating sphere was made also by 15 points for which the distances and the heights relative to the center of the scanning mirror of the station were borrowed from the geodetic or, to be more precise, from the photogrammetric determinations (see the preceding chapter).

It was found that the radius of the approximating sphere constitutes about 25 – 30 m, while the center of the crater is located within a few meters from the station and to the Northeast of it.

Making use of the graph of the second horizon, it is possible to find that the depth of the crater apparently does not exceed 1 m, and the diameter is close to 12 – 15 m, which is in agreement with the estimates brought out on page 63. It should be remarked that, contrary to geodetic determinations, for which the stereoscopic effect created by the station's shift during operations was utilized, the determinations described in this paragraph independently from panoramas I and III, provided coinciding results and might have been conducted even in the absence of the station's shift.

The northwestern and southwestern slopes of the craters are also sharply outlined in the plan constructed by photogrammetric methods (see the third part of this book). The diameter and the depth of the crater, obtained by the geodetic data and found by the morphological characteristics, were found to be quite close.

As already pointed out, it is not known whether the site of landing is a mare or continental region. Serving as a criterion for the solution of this problem may be the results of photometric determinations of brightness of the landscape surrounding the station. According to the preliminary photometric data, the inner part of the crater, in which the station is located, belongs to the clear parts of the lunar surface.

A certain additional basis for such a conclusion is given by the circumstance that the horizon visible on the panoramas is not a great circle (Fig. 41). In panorama I the visible horizon is best represented by a small circle lying at about 1.5° above the mathematical horizon. This much rather speaks of the fact that the 15 m funnel is situated inside a substantially larger crater which still is much smaller than the crater's revealed during optical observations on the ground (Fig. 42).

Note that the infrared observations conducted by Shorthill and Sarri during the total lunar eclipse of 1964 point to a high heat conductivity of the surface for the lunar conditions in the landing region of Luna-9. In the course of these observations a high heat conductivity (to be more precise, a slow cooling of the surface, which is linked with heat influx from deeper layers and a greater heat conductivity per unit of volume of matter of the most superficial layer) was also noted for a series of "young" craters of which the bottom appears to be clear during optical observations. It is probably natural to assume that the region of increased heat conductivity at the landing site of Luna-9 is linked with the presence in that region of an accumulation of young craters. It is not ruled out that Luna-9 may be located in one of them.

It is customary to estimate that the bottom of young craters is characterized by a small thickness of heat insulating formation layer, and that at times, its total absence may be the case. In this regard particular attention is drawn by the linear structures clearly visible in the southeastern sector of the panoramas. In a series of cases, these structures intersect separate craterlets and extend over a distance of about 1 m. Inasmuch as in the region of linear structures, craterlets are seen with a diameter of a few tens of centimeters and depths of the order of several centimeters, the conclusion could apparently be derived that the depth of the freshly reworked layer does not exceed a few centimeters, at least in this panorama sector. The presence of linear structures opens certain possibilities for estimating the age of the crater, provided we understand by that the time interval having elapsed from the moment of the discovery of linear structures. This estimate may be based upon the fact that within the portion of the 15 m depression accesible to observations, in which the station is located, craters and funnels of smal-

ler dimensions occupy no more than 20% of the area.

The external shapes of the surface and the details of the microsculpture are linked with the erosion by exogenous processes in which, in particular, the impact of meteorites of various sizes play a substantial role. However, in the best observed lots the average thickness of the dust reworked layer apparently does not exceed a few centimeters. The superficial layer has a strongly "eaten up", spongy structure, which, generally speaking, agrees well with the existing concepts of the average character of the Moon's surface. This, in particular, is corroborated by the bell shaped appearance, inherent in numerous funnels whose width exceeds several centimeters and which is characterized by the accelerated role of craters' diameter as it draws nearer the surface. Apparently, as already mentioned above, such a crater shape is evidence of the variation of the strength of rocks along the vertical direction, inasmuch as in the final result, the diameter of the crater is determined at every level by the strength of the formation.

The presence of stones on the surface of the Moon is not in contradiction with the conclusion of the low strength of the soil's superficial layer, provided we take into account that in the portion of the surface observed there much rather exists a negative balance of mass. In this case, even with stones sunk down to a certain depth must gradually drop out and somehow "float up" or rise to the surface over the less resistant matter surrounding them. The very fact of the presence on the surface of relatively strong stones is naturally explained by their being ejected from the deeper parts of the soil during the formation of funnels covering the locality.

It should be stressed that within the few millimeter resolution of the image no traces of structureless dust or loose layer or of superficial processes of fusion were noted on the nearest plan.

A superficial disintegration process is difficult to visualize without the formation of dust-like, thinly-dispersed material. This is why one is led to believe that the pulverized matter forms as a result of conglomeration of specific structurally-bound aggregates, thus complicating the structure of the surface.

The inner structure of a more ancient formation manifests itself in this disintegration process. Among the less stable basic mass, denser linear formations, having a character of streaks or apophyses, intersecting at various angles, are detected in it. The presence of more powerful disintegrated veins and dykes, emerging in the linear disposition of separate rows of stones, is possible.

Evidently, the preceding is not sufficient to venture the judgment as to whether Luna-9 stands on the bedrock, "sprinkled" with a thin layer of soil reworked as a result of its disintegration, or on an accumulation of coarse fragments, "poured over" or interspersed by triturated soil. Nor is it clear to what extent this picture is typical of the Moon as a whole. It is possible that the considered layout is not very rare, in which case, basing ourselves on the radioastronomical data, it is possible to conclude that in order to assure a low heat conductivity and capacity to the superficial layers, a concept of interred, coarsely-fragmented layer, of which the density would accrue slowly with depth, would be sufficient.

The fact that linear structures are observed only over a limited portion of the surface may possibly constitute an argument in favor of the last hypothesis.

Even the consideration of the small portion of the Moon points to the difference in the formation time of the various elements of its surface and to the complexity of its geologic history, which can hardly amount to a one-type one-event process. A series of processes may be invoked, of which the conjunction in terrestrial conditions remains unknown. Their analogy should be searched for in entirely different geologic formations, or else these processes must be reproduced in laboratory conditions.

THE END

Contract No. NAS-5-9299
Consultants & Designers, Inc.
Arlington, Virginia

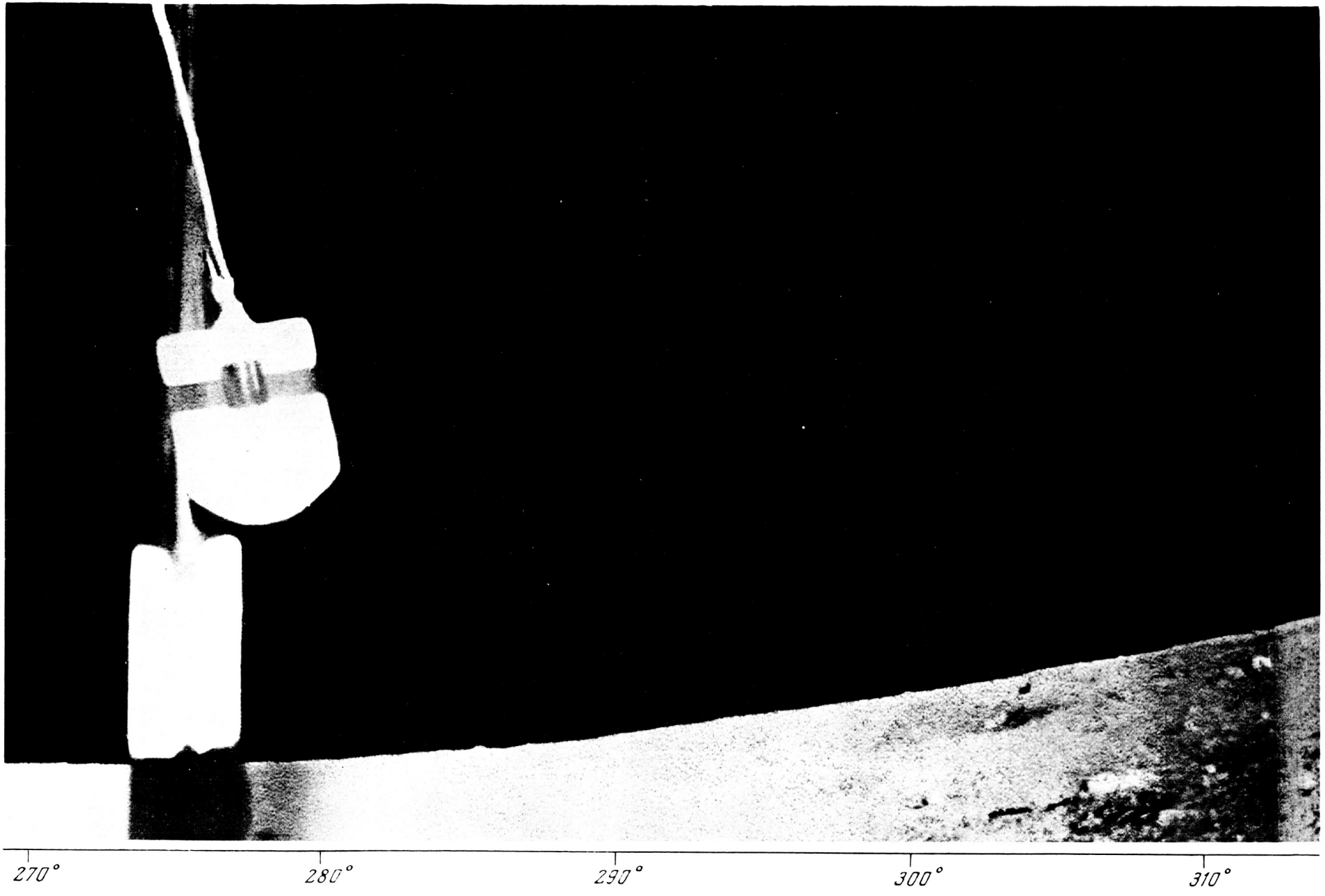
Translated by Andre L. Brichant
19 - 29 June 1966

PART III

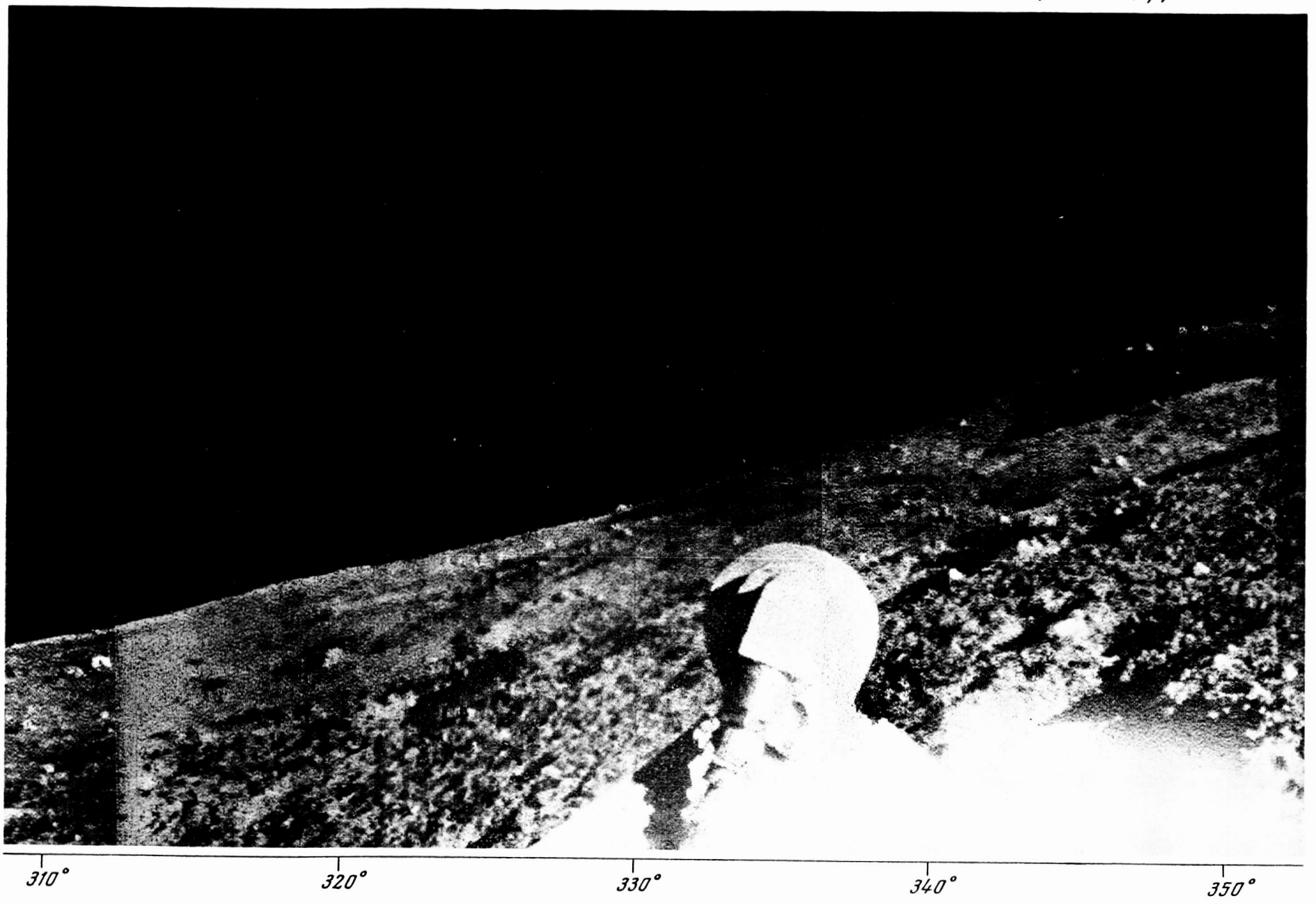
PANORAMIC PHOTOGRAPHS OF THE LUNAR SURFACE

PANORAMA I, Fragments 1 through 9
PANORAMA II, " 1 " 6
PANORAMA III, " 1 " 7
TRANSFORMED PHOTOGRAPHS
STEREOPAIRS, 1 — 12
TOPOGRAPHIC PLAN OF THE LANDING SITE
TOPOGRAPHIC SCHEME OF THE LANDING SITE
PANORAMAS I — III

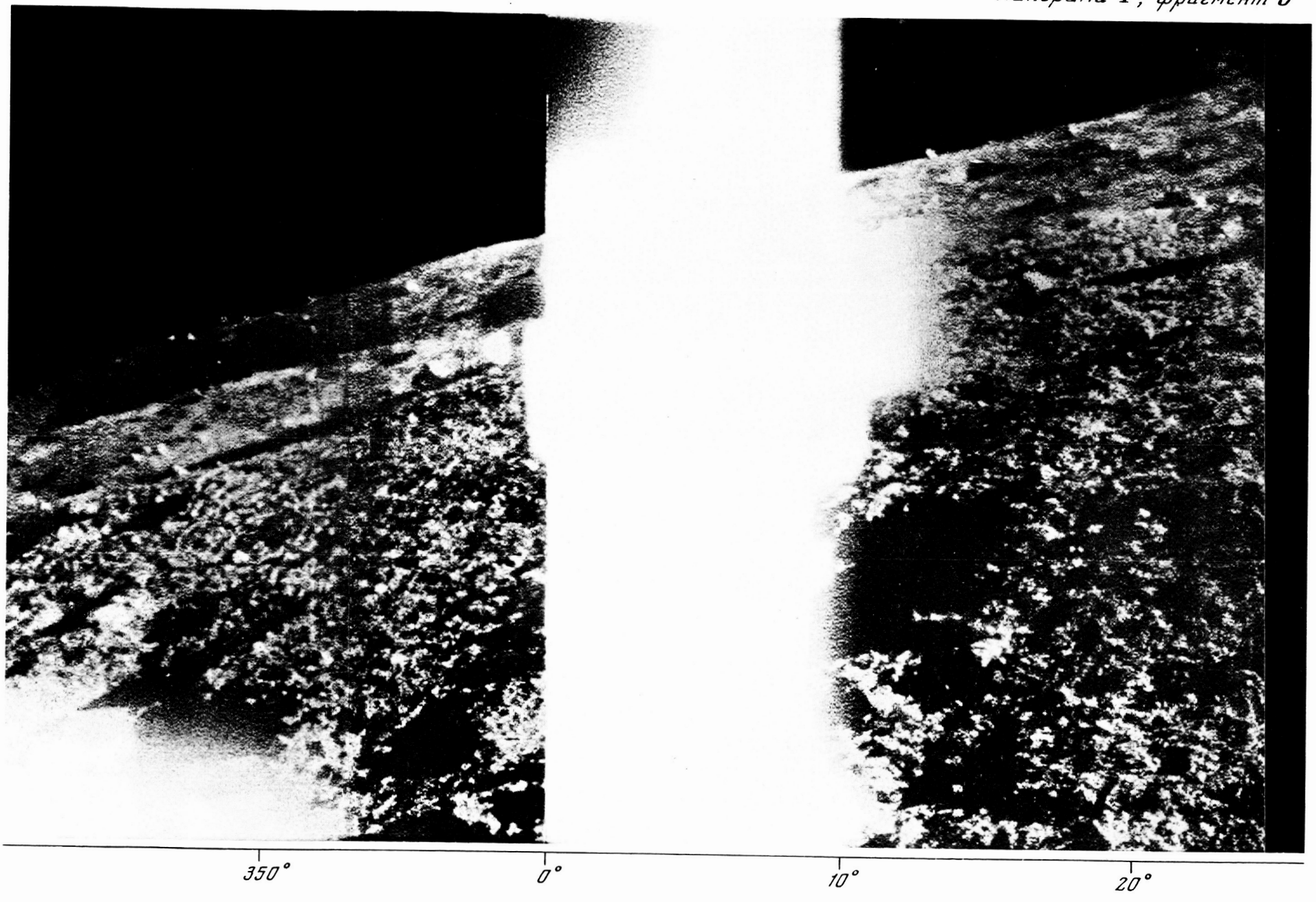
Панорама I, фрагмент 1



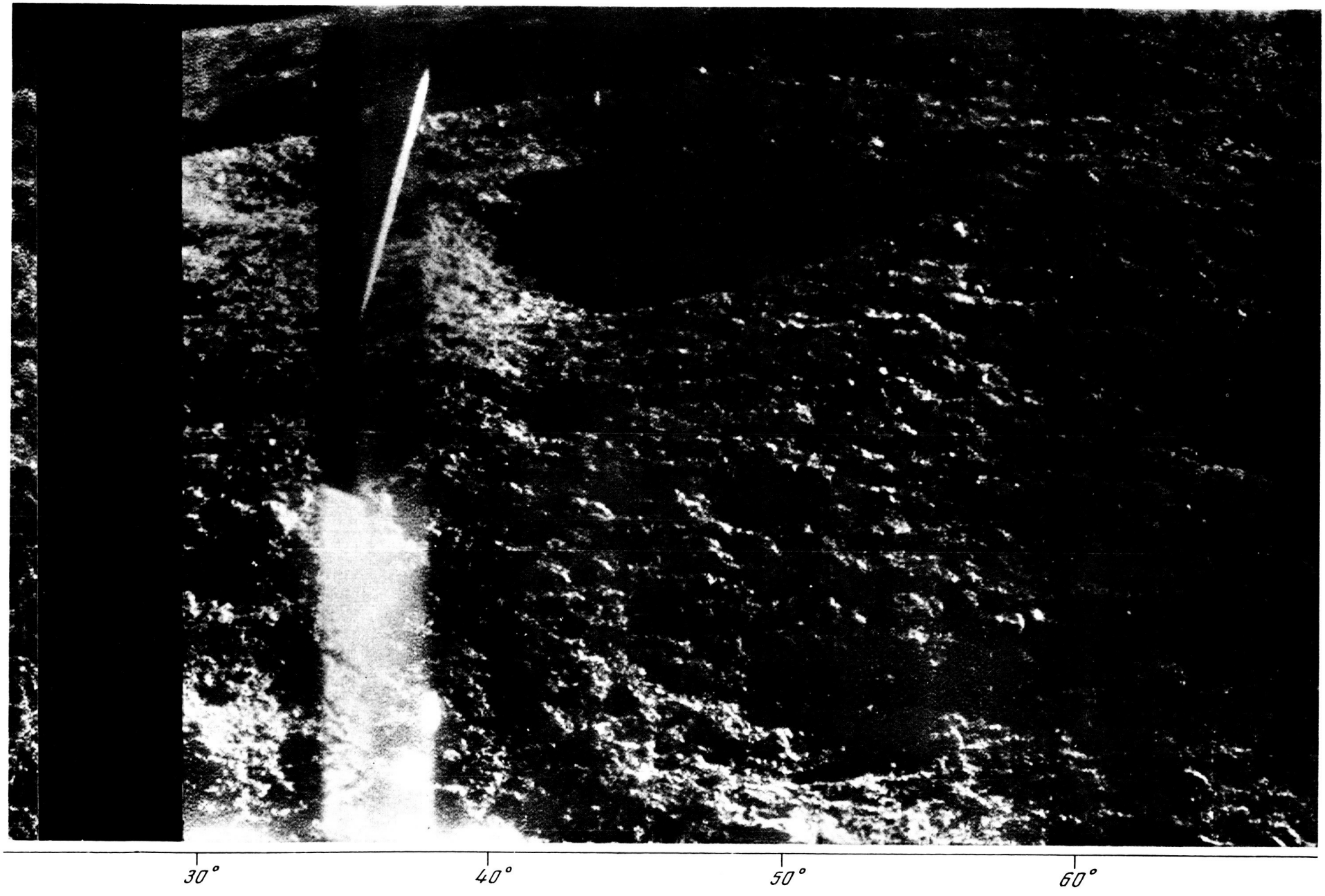
Панорама I, фрагмент 2



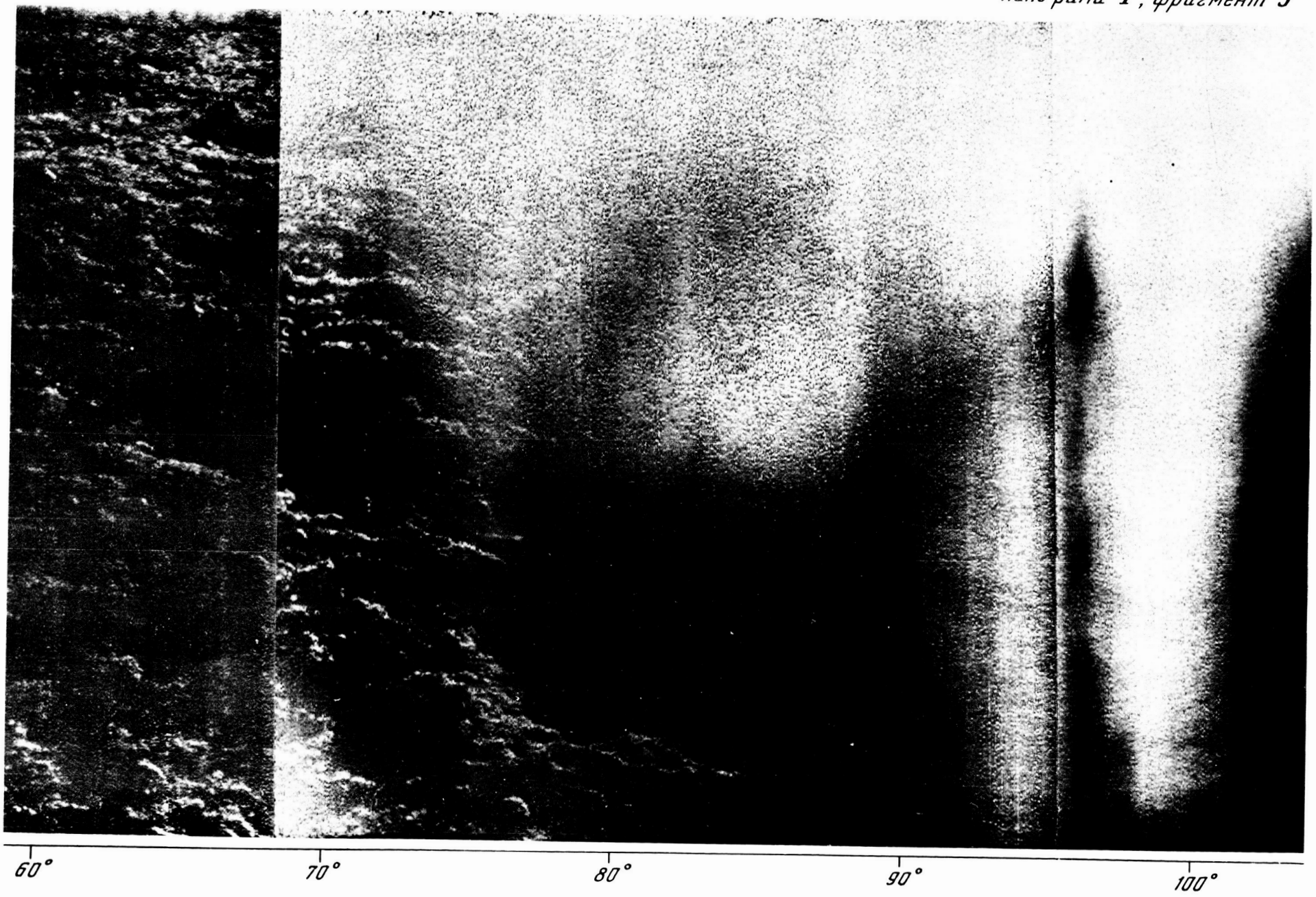
Панорама I, фрагмент 3



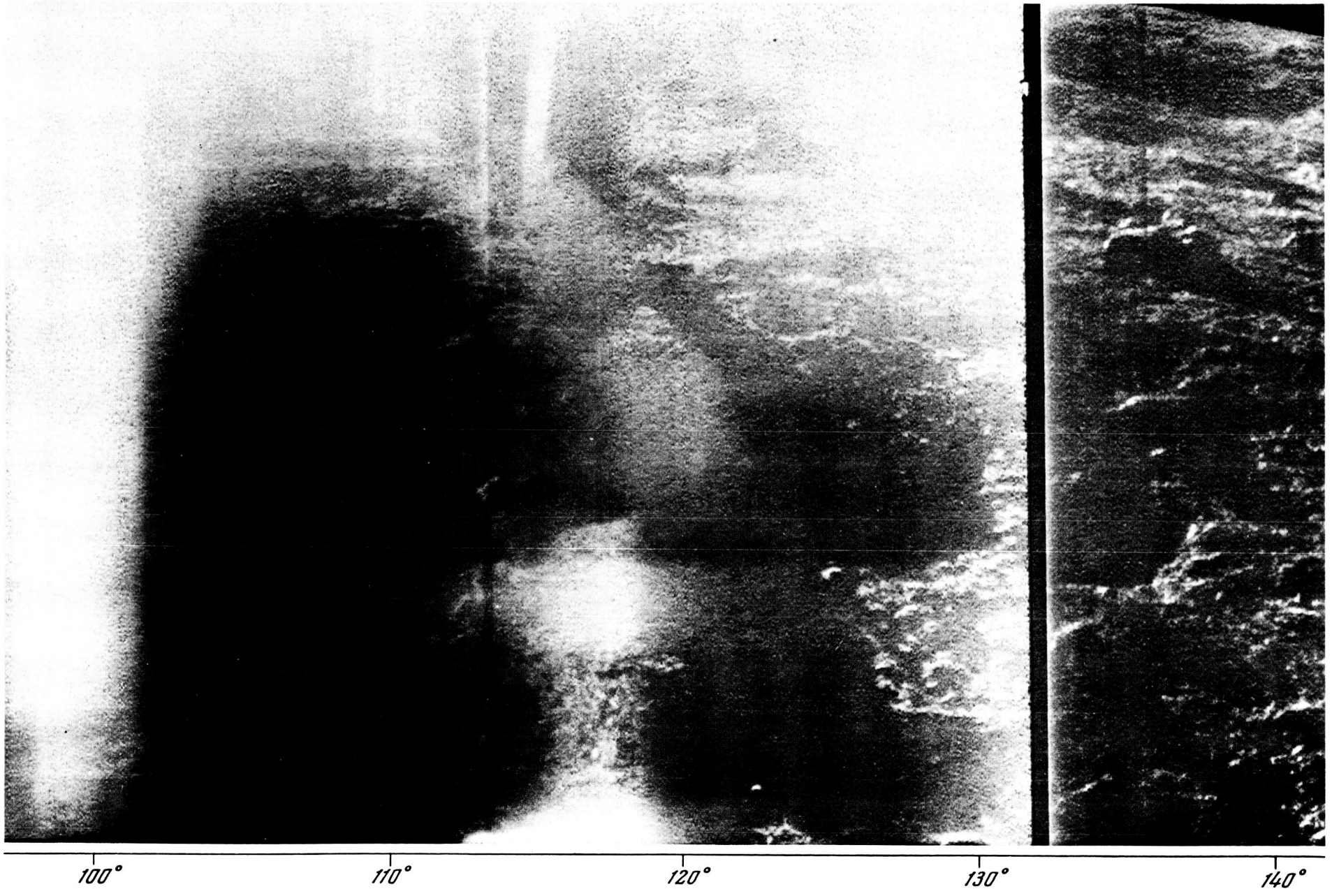
Панорама I, фрагмент 4



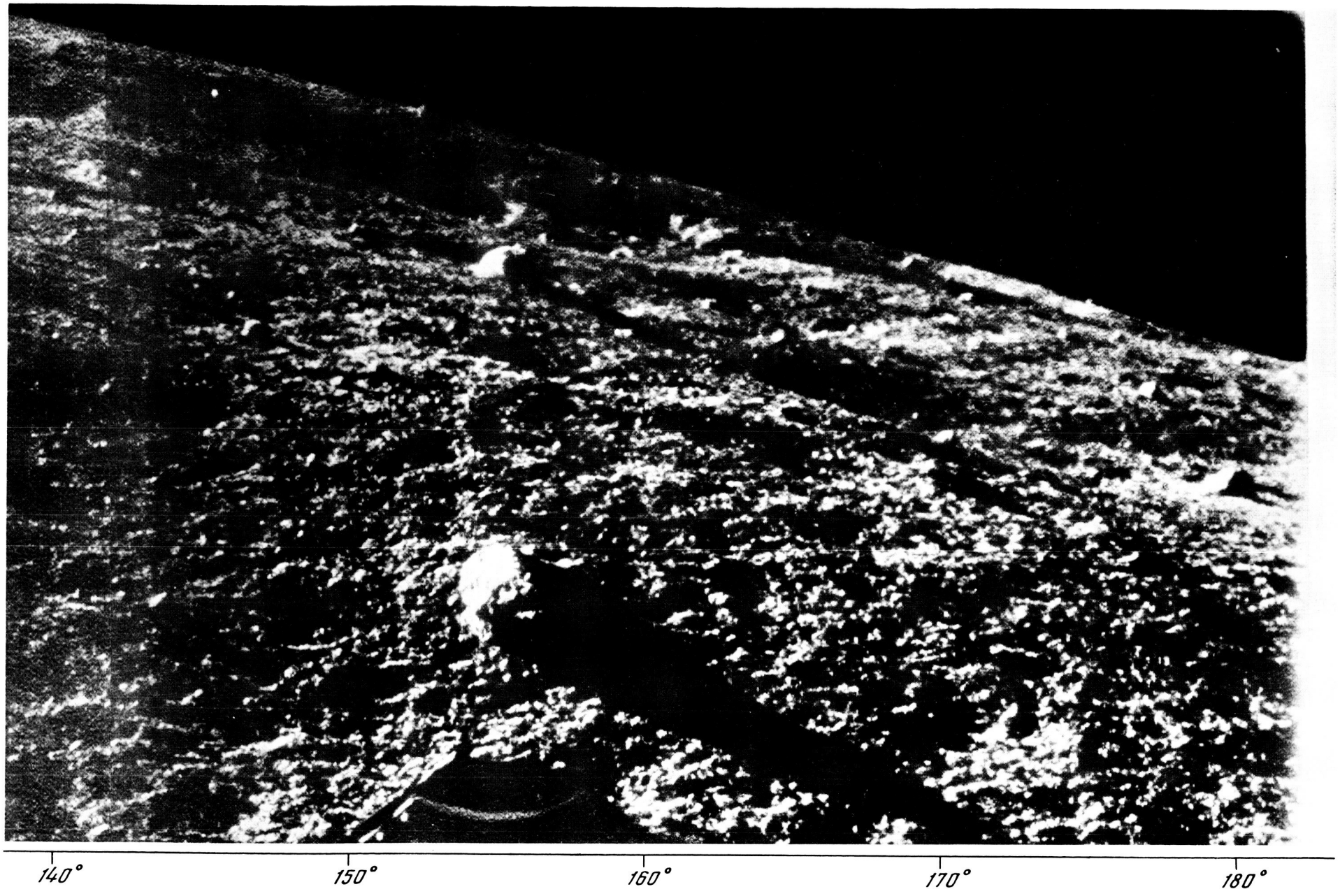
Панорама 1, фрагмент 5



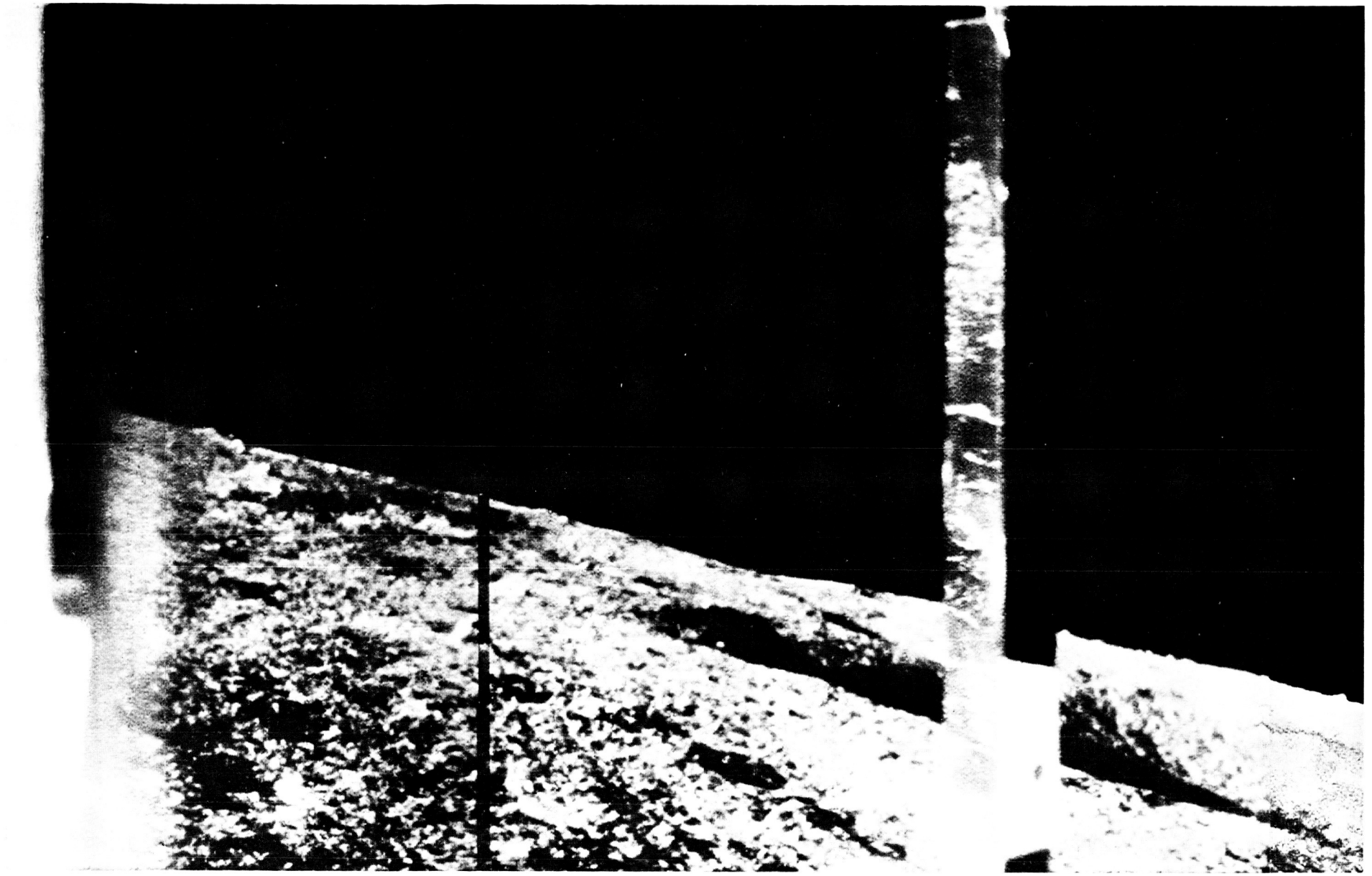
Панорама I , фрагмент 6



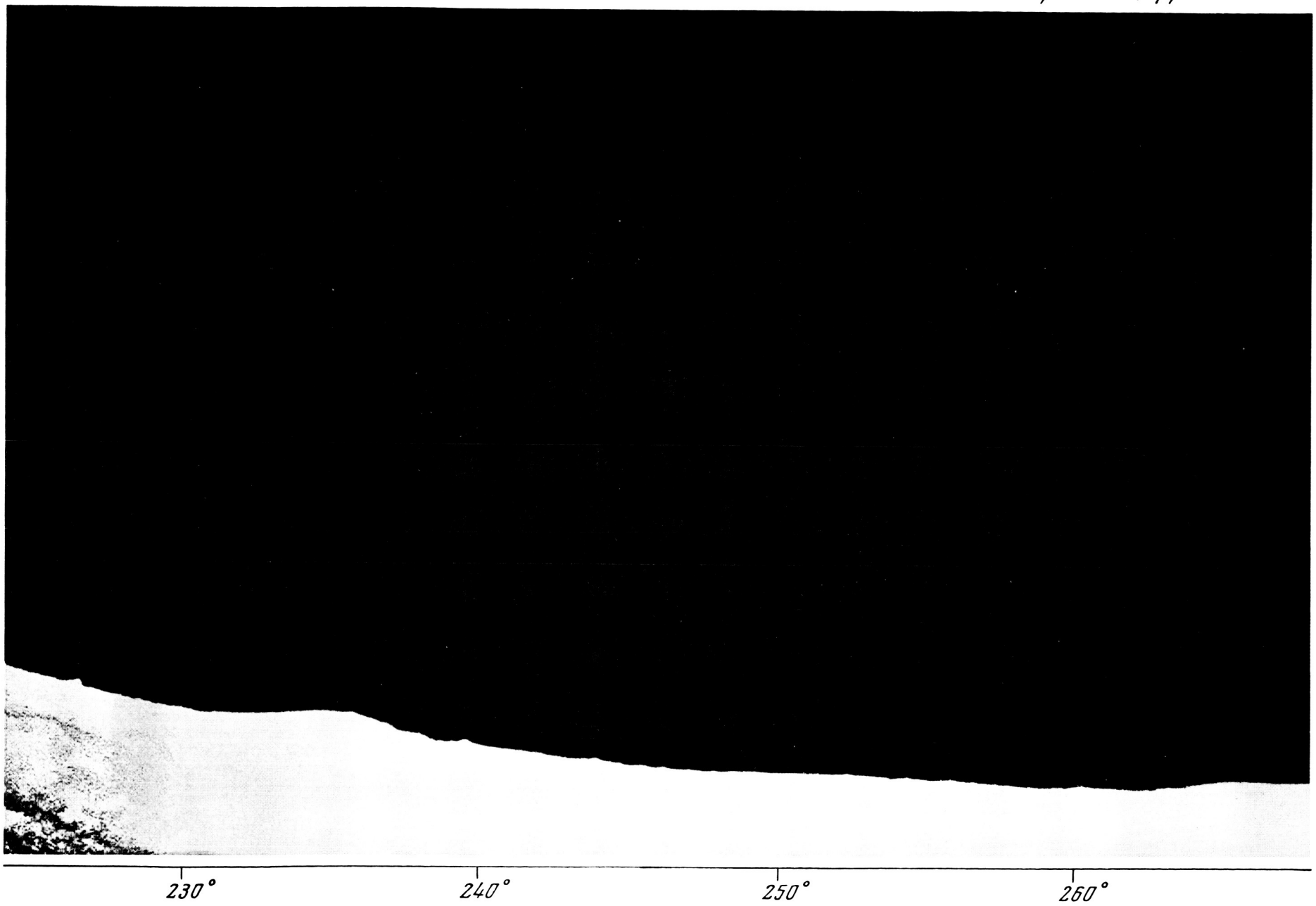
Панорама I, фрагмент 7



Панорама I, фрагмент 8



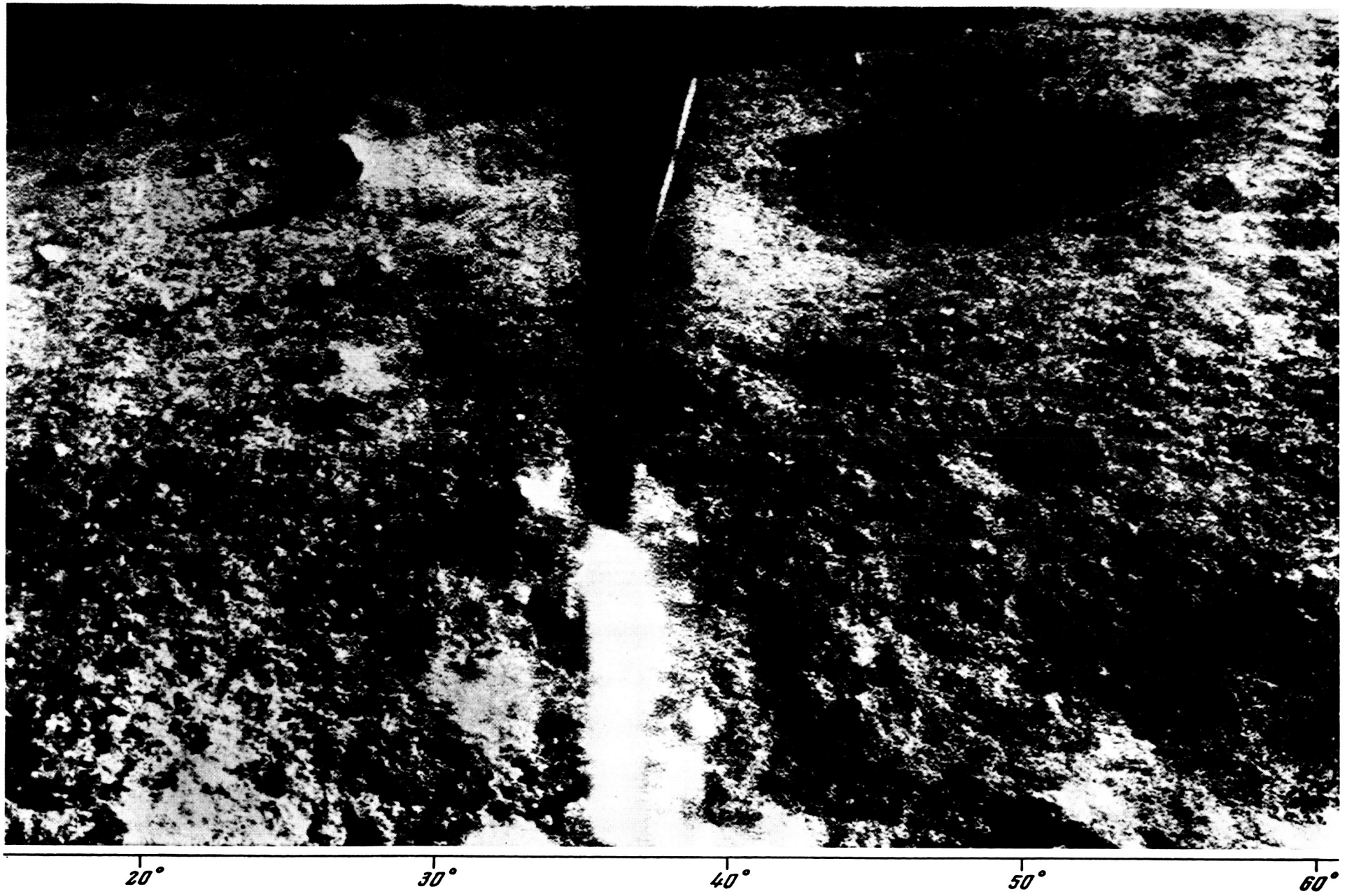
Панорама I, фрагмент 9



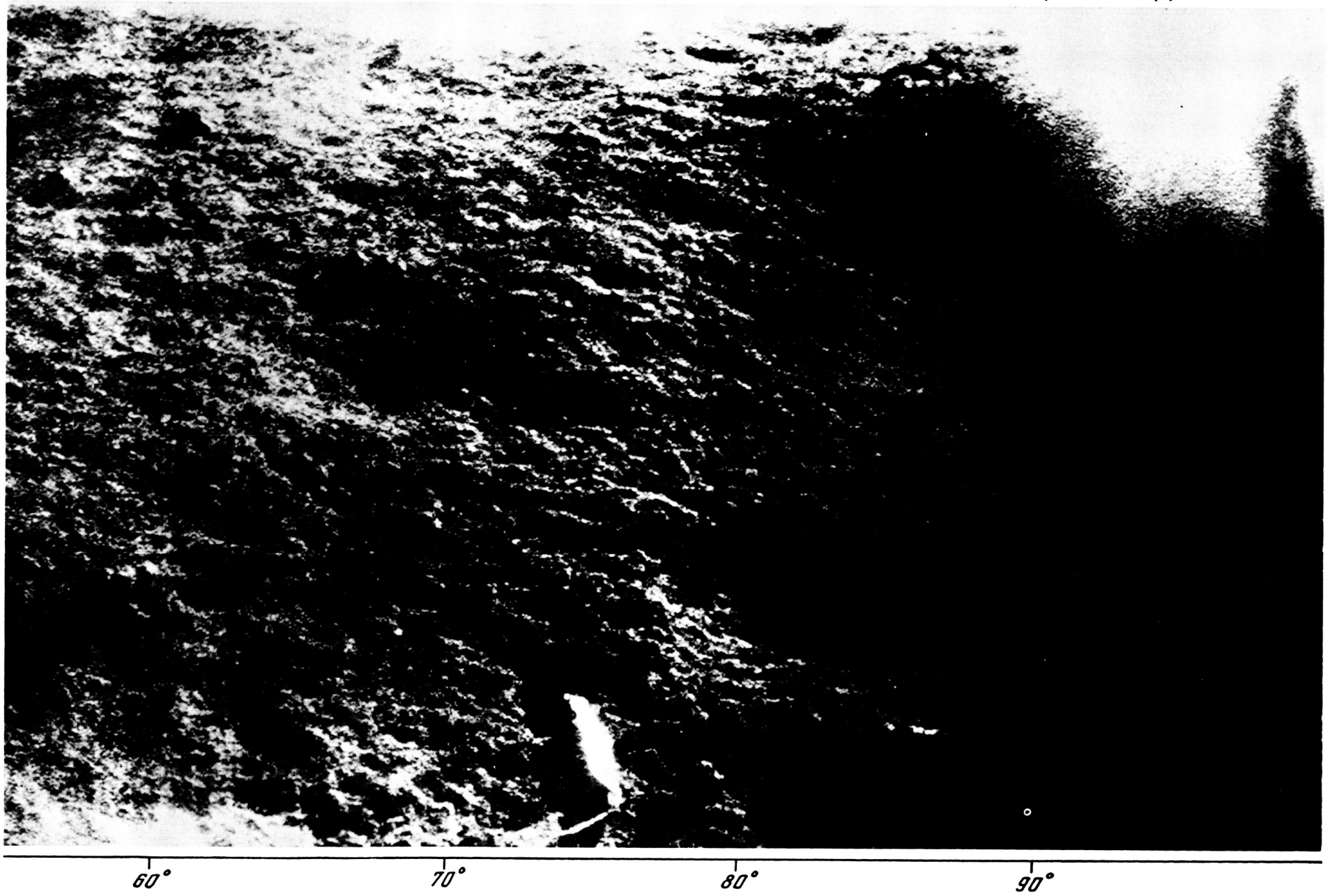
Панорама II, фрагмент 1



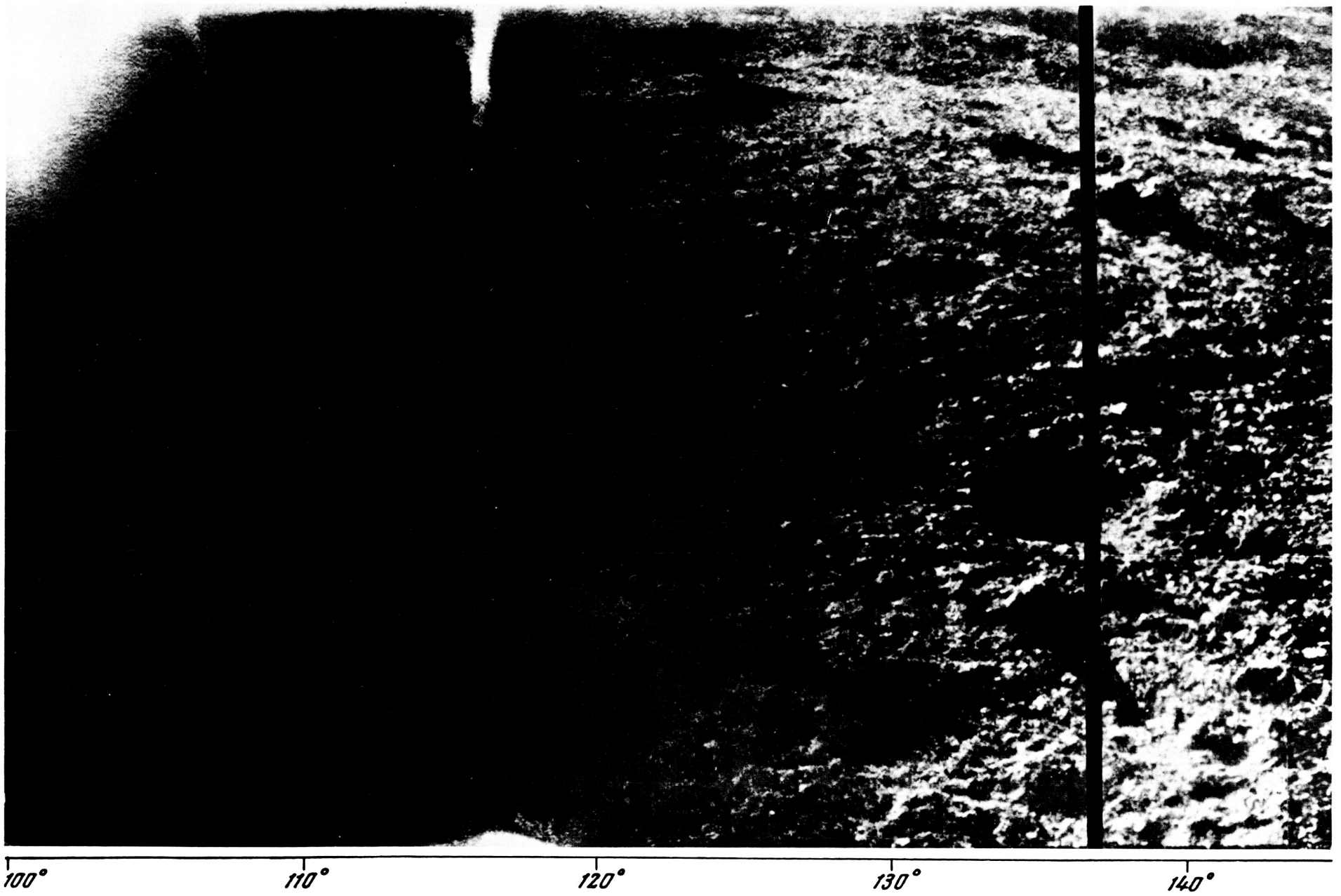
Панорама II, фрагмент 2



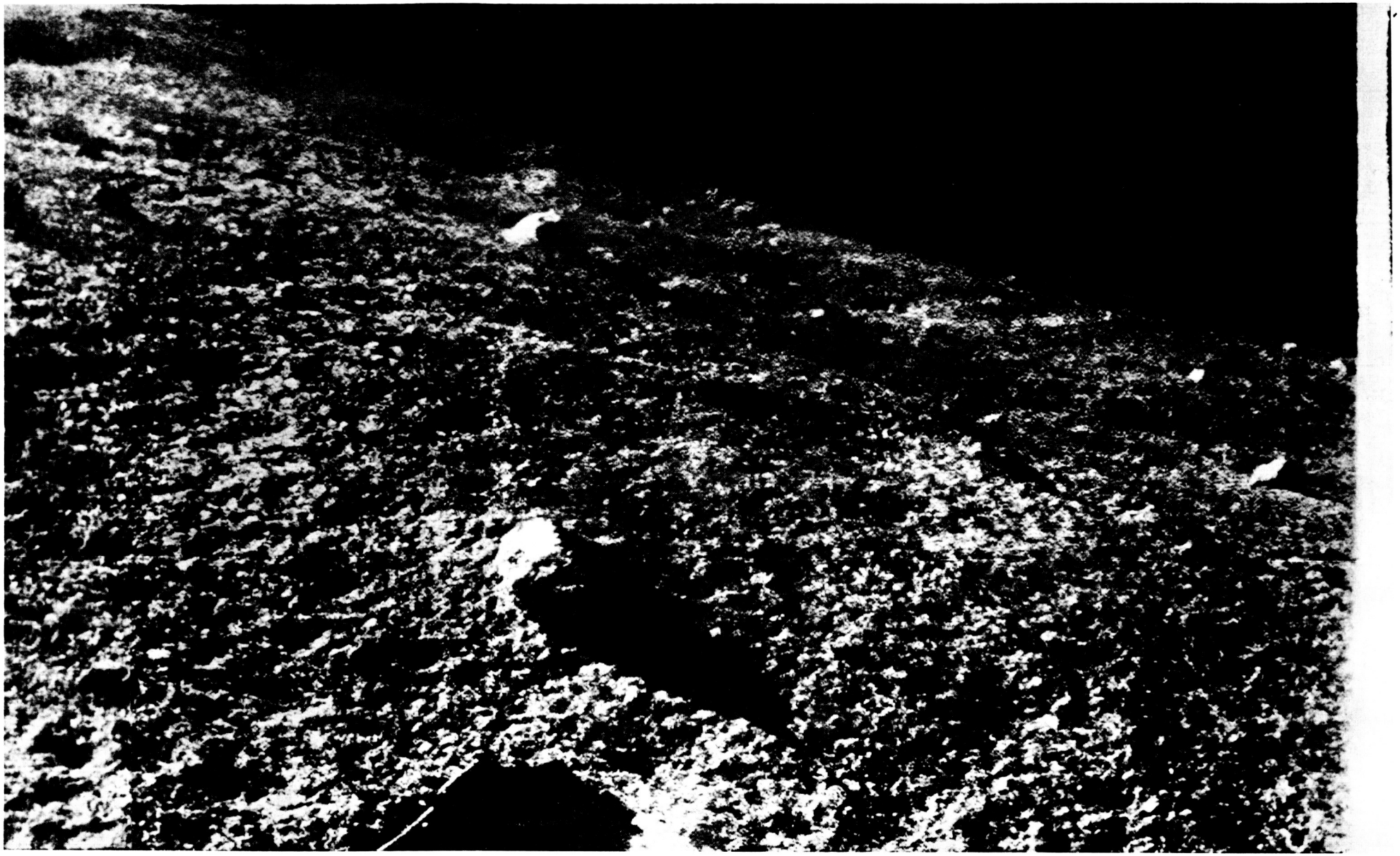
Панорама II, фрагмент 3



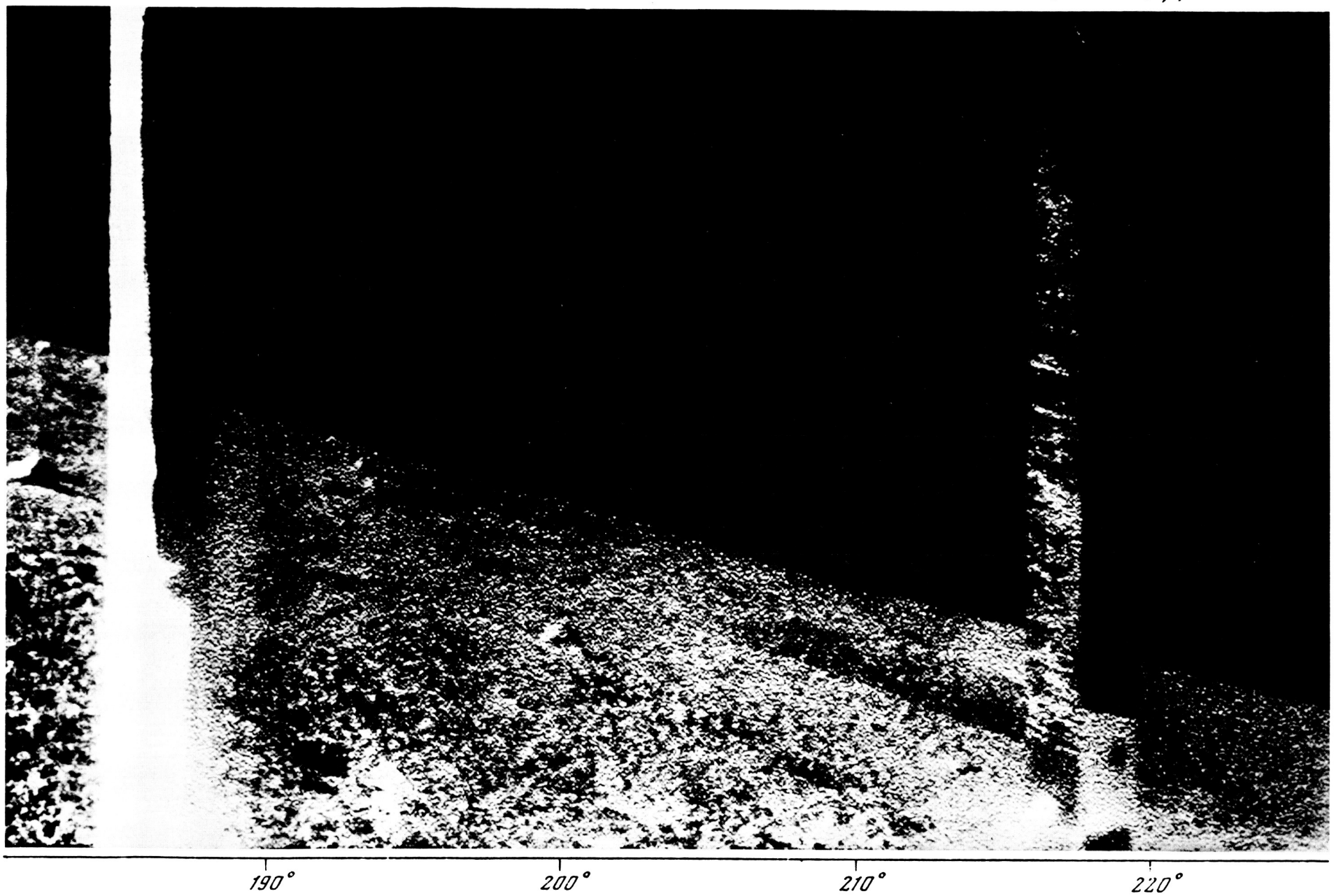
Панорама II, фрагмент 4



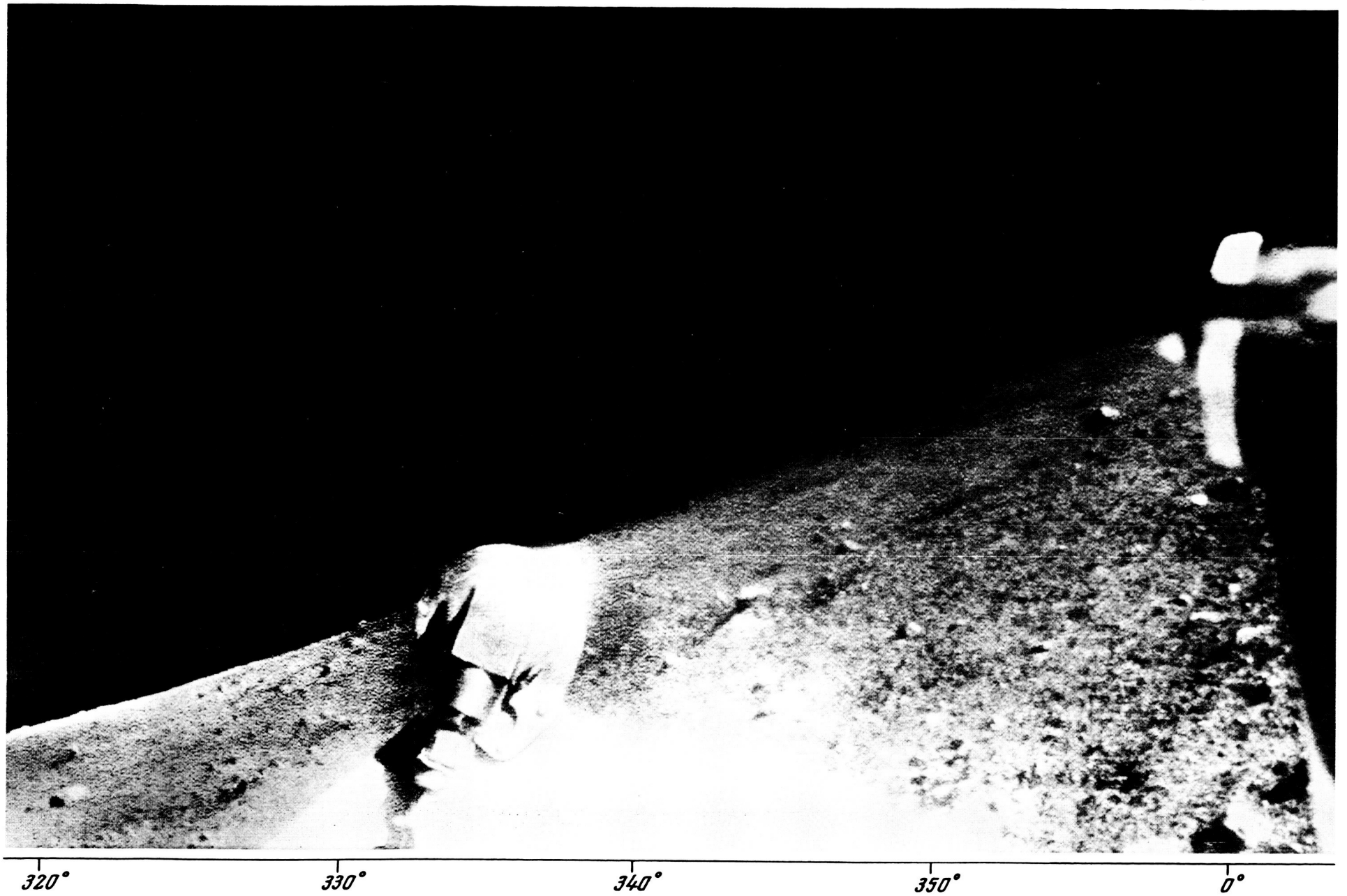
Панорама II, фрагмент 5



Панорама II, фрагмент 6



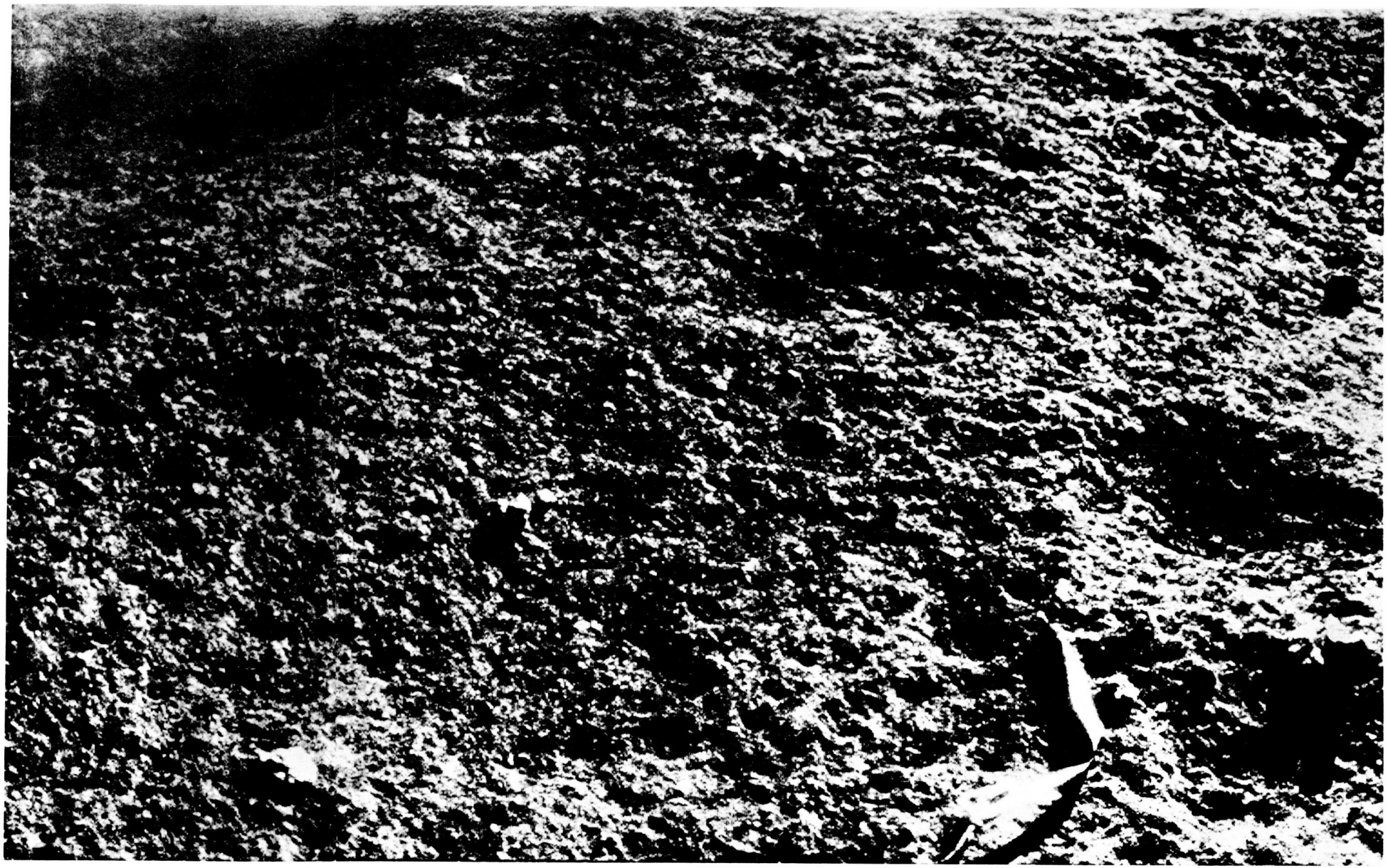
Панорама III, фрагмент 1



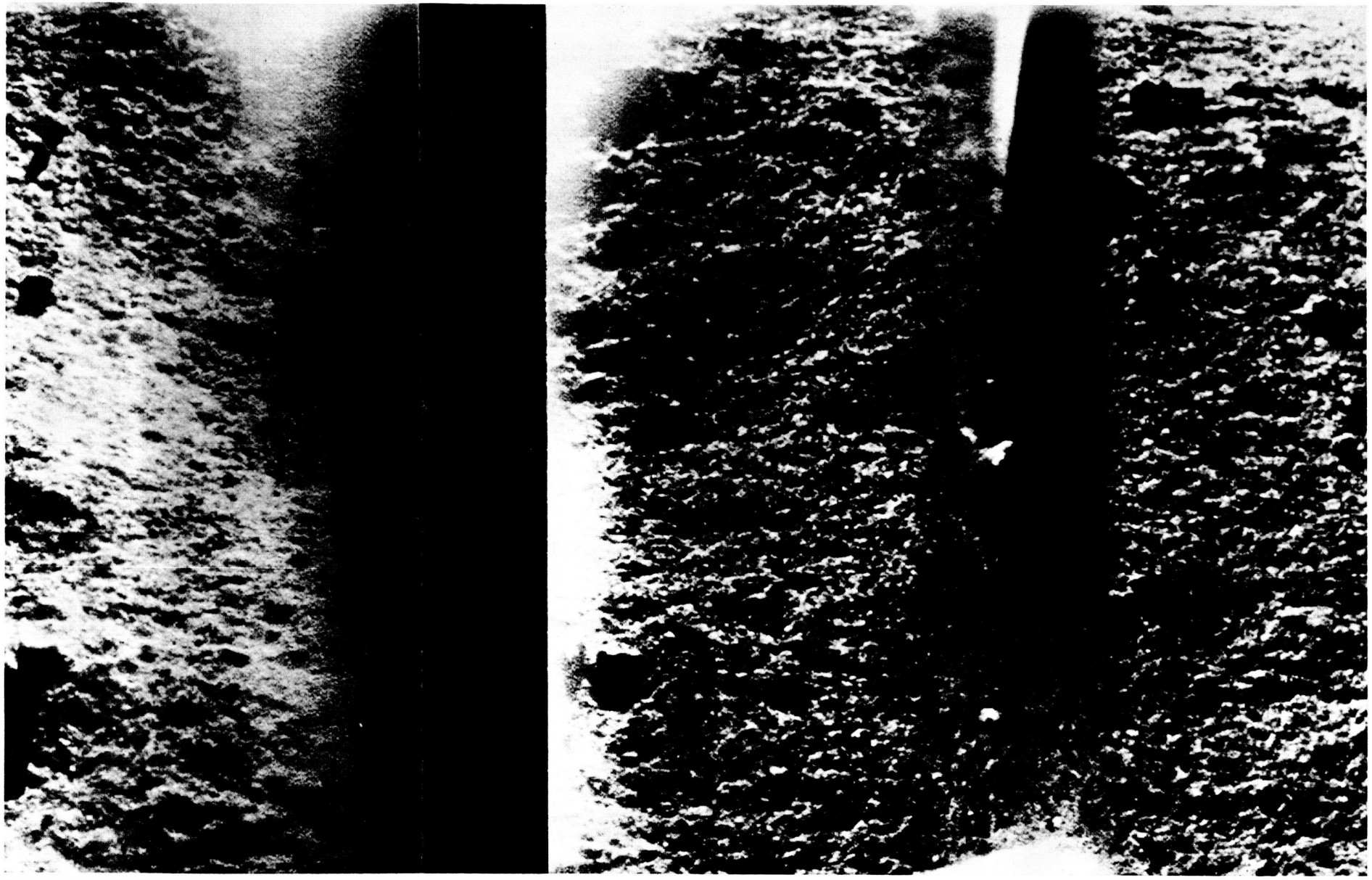
Панорама III, фрагмент 2



Панорама III, фрагмент 3



Панорама III, фрагмент 4



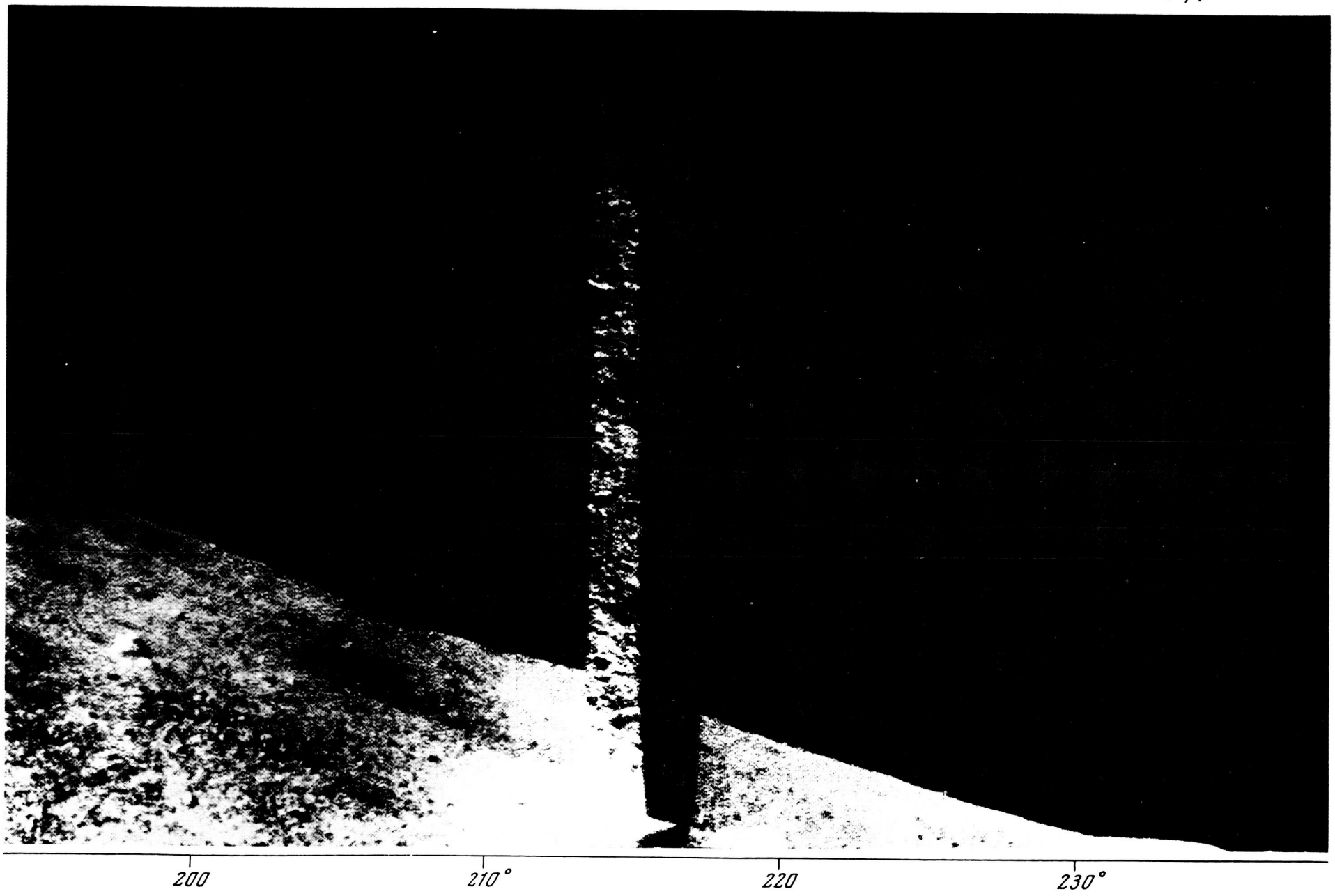
Панорама III, фрагмент 5



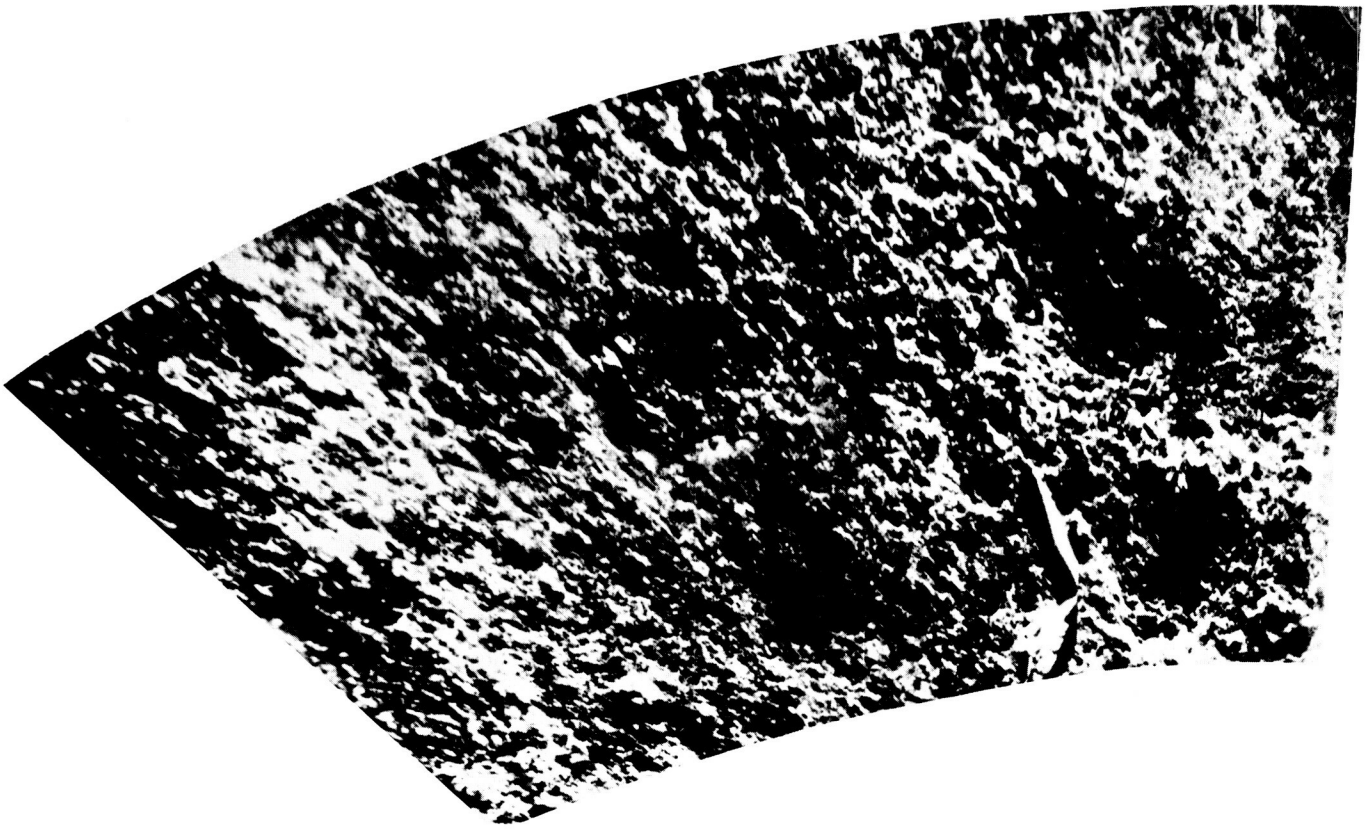
Панорама III, фрагмент 6

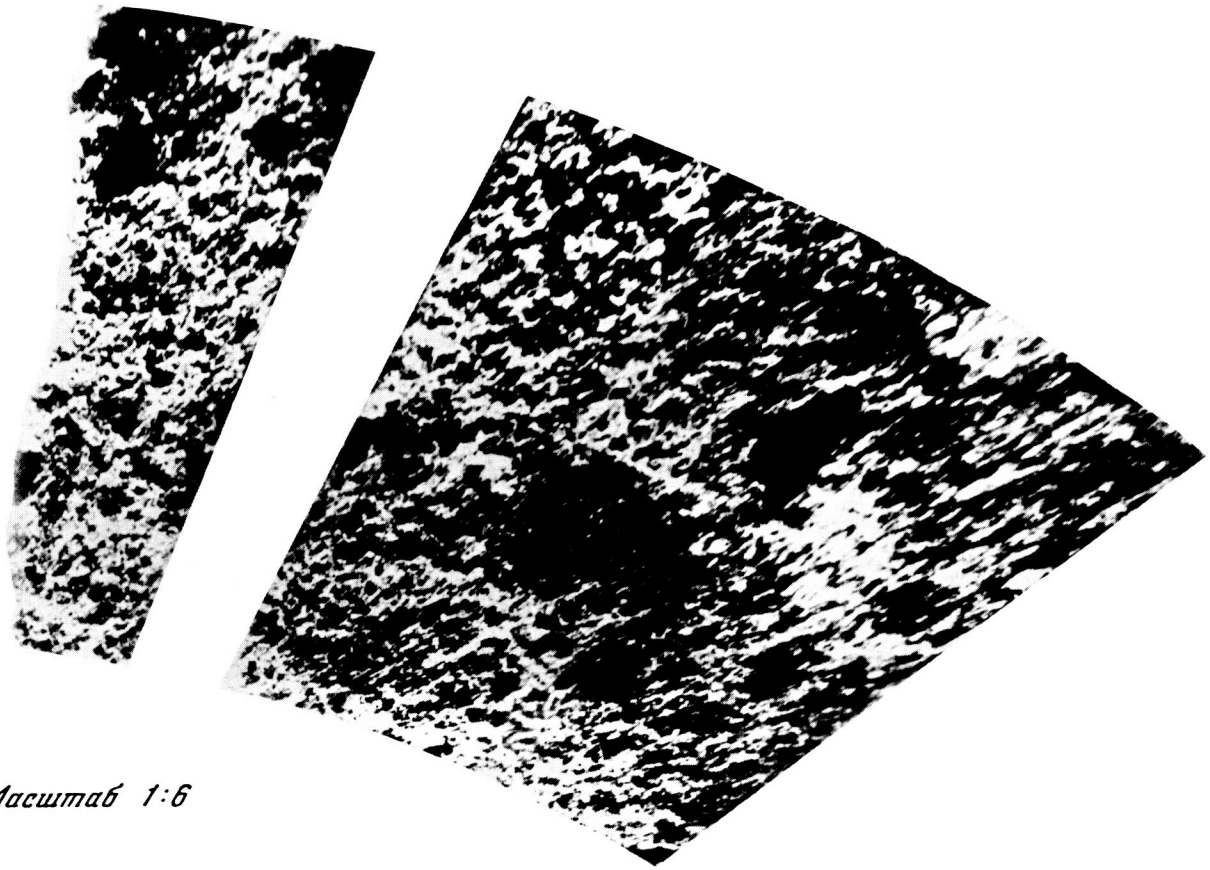


Панорама III, фрагмент 7



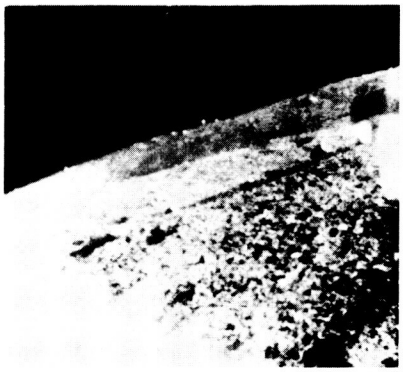
Трансформированные снимки





Масштаб 1:6

Стереопара 1

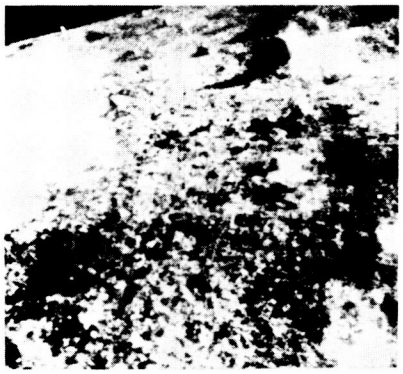


Панорама II

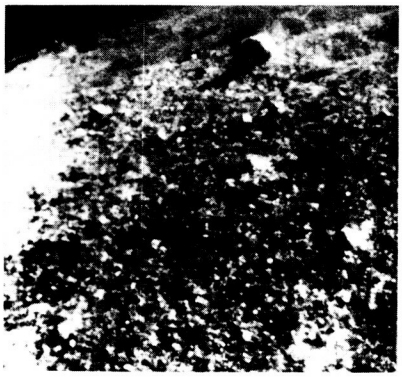


Панорама III

Стереопара 2

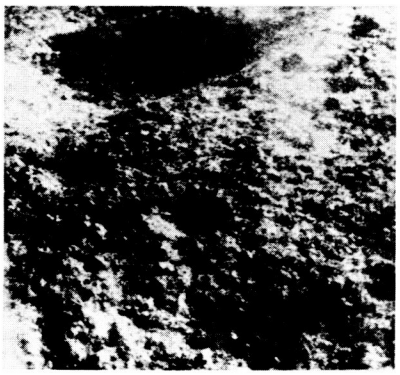


Панорама II



Панорама III

Стереопара 3



Панорама II



Панорама III

Стереопара 4

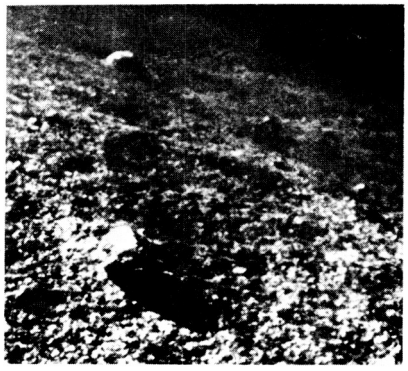


Панорама III

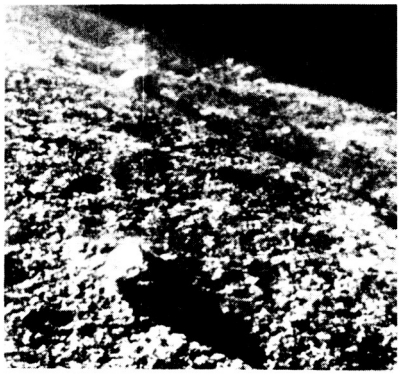


Панорама II

Стереопара 5



Панорама III



Панорама II

Стереопара 6

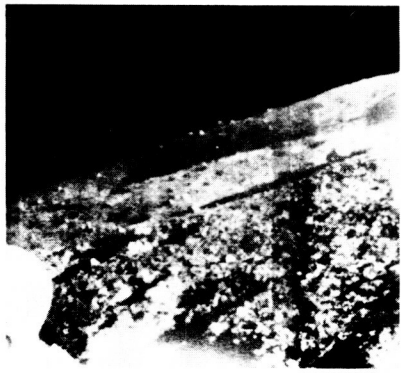


Панорама III



Панорама II

Стереопара 7

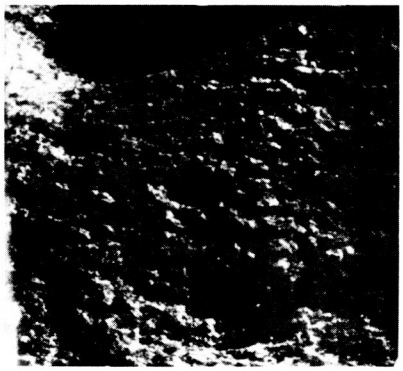


Панорама I

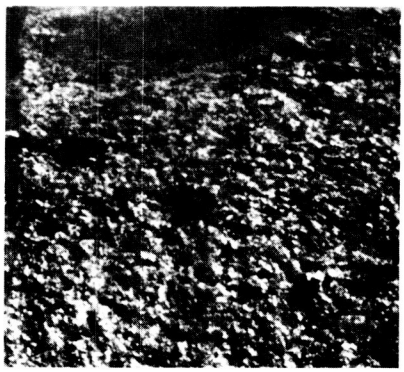


Панорама III

Стереопара 8



Панорама I

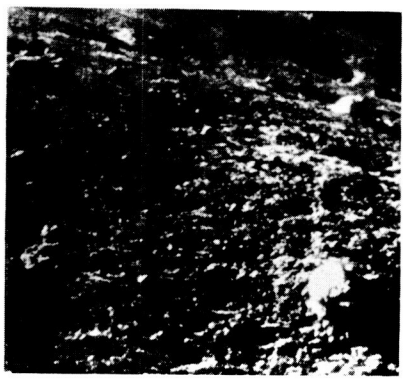


Панорама III

Стереопара 9

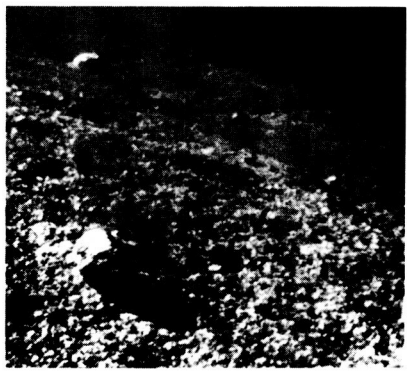


Панорама III

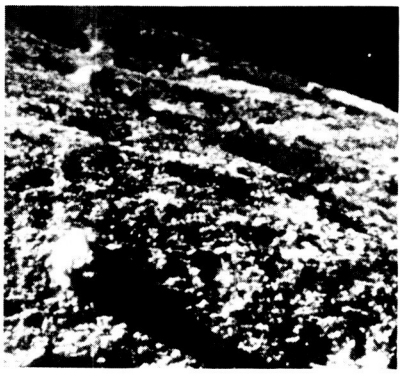


Панорама I

Стереопара 10



Панорама III



Панорама I

Стереопара 11

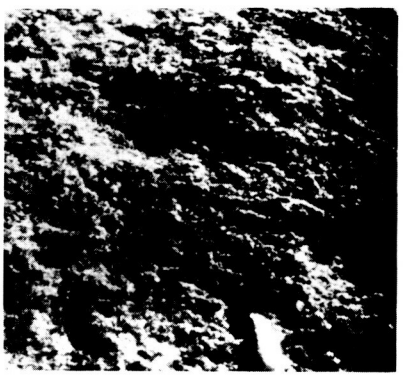


Панорама III



Панорама I

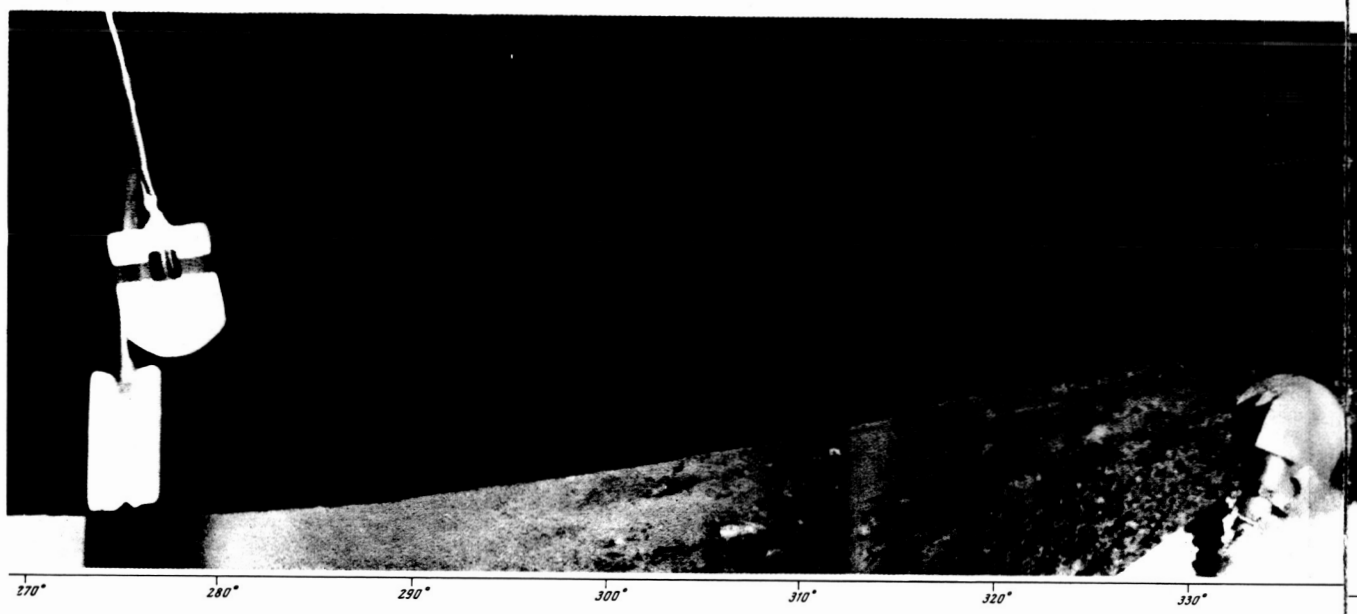
Стереопара 12



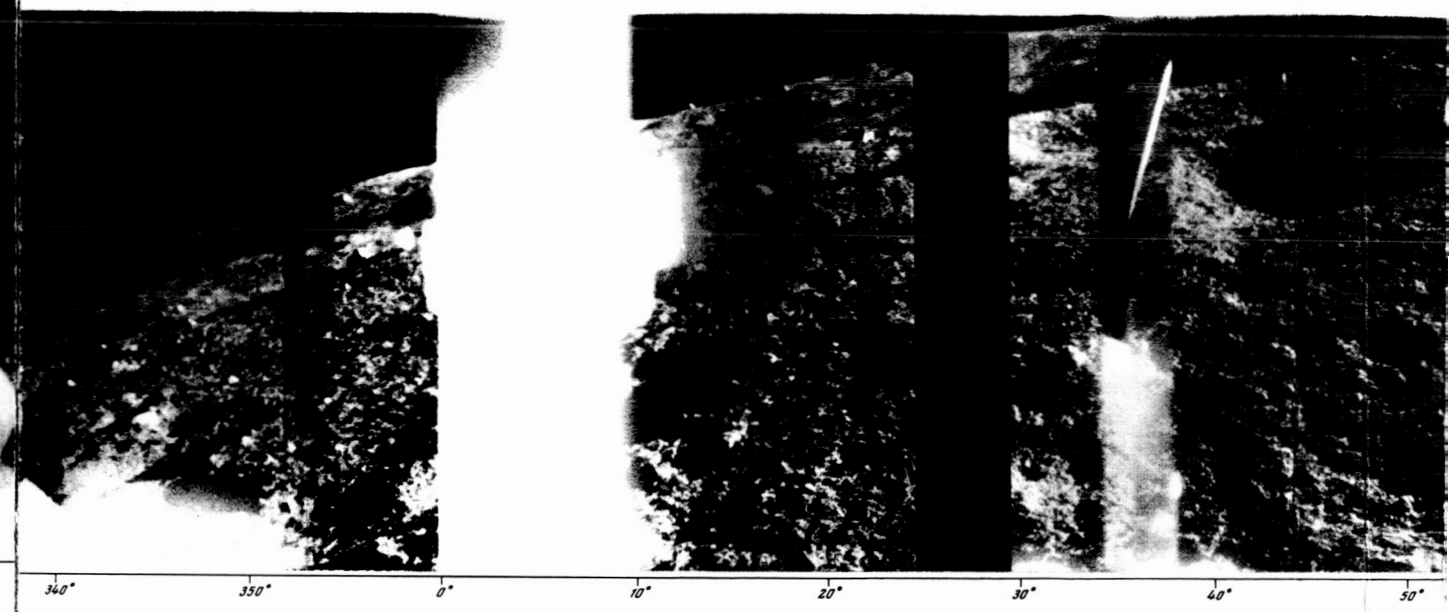
Панорама II



Панорама III

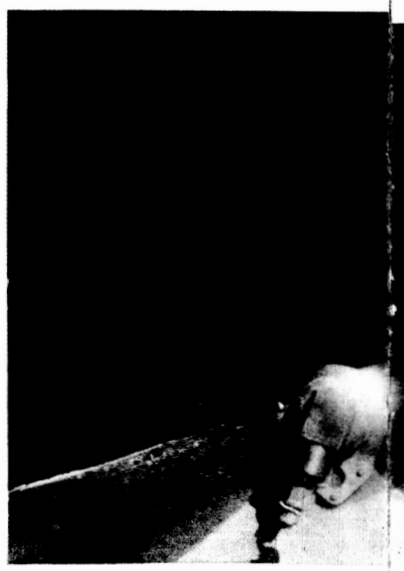


Панорама I





Панорама II

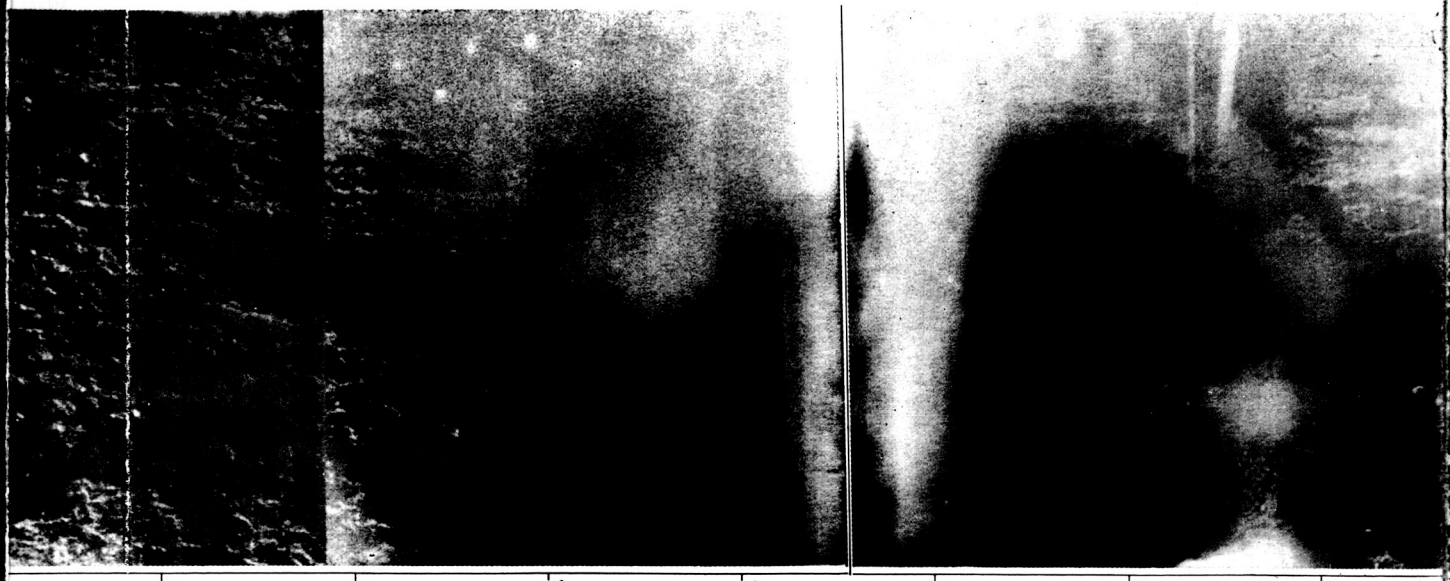


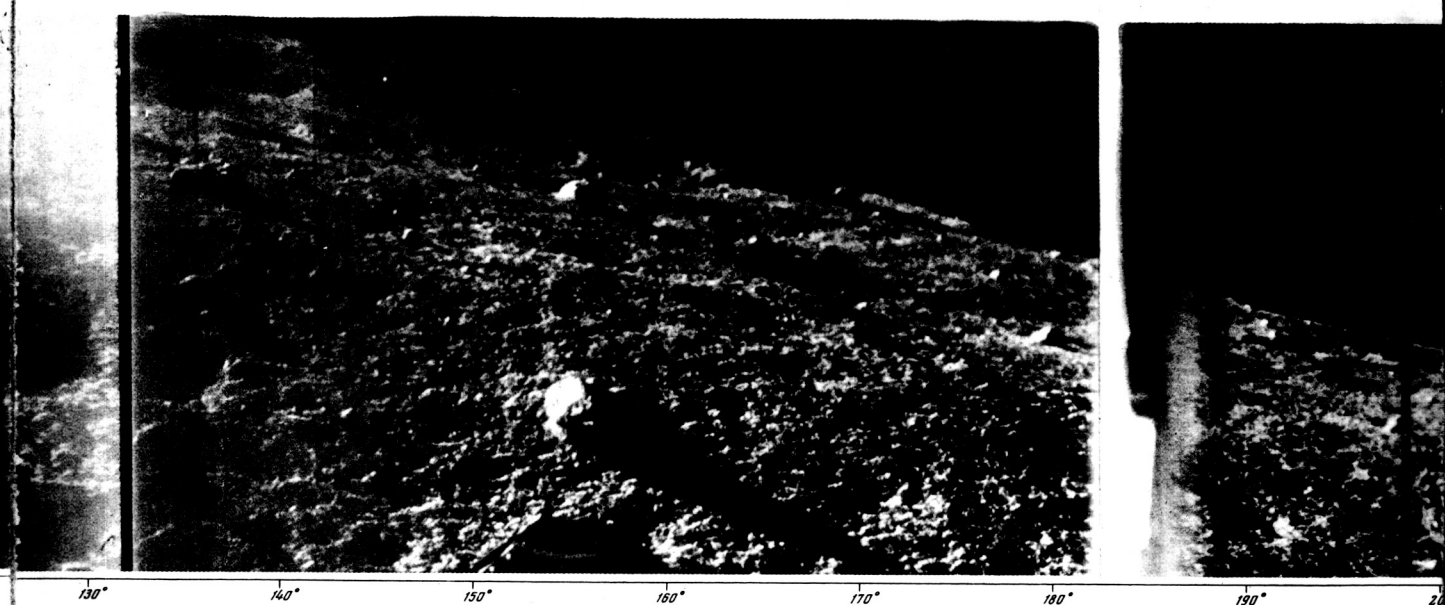
Панорама III



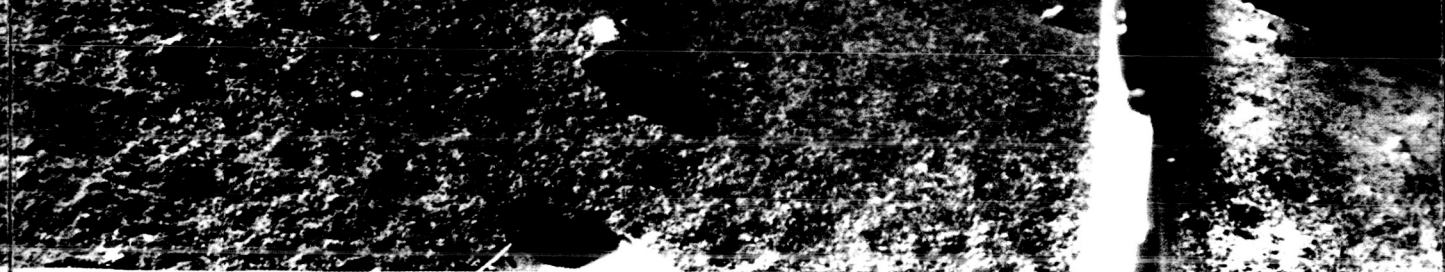
FOLDOUT FRAME 1

FOLDOUT FRAME 2



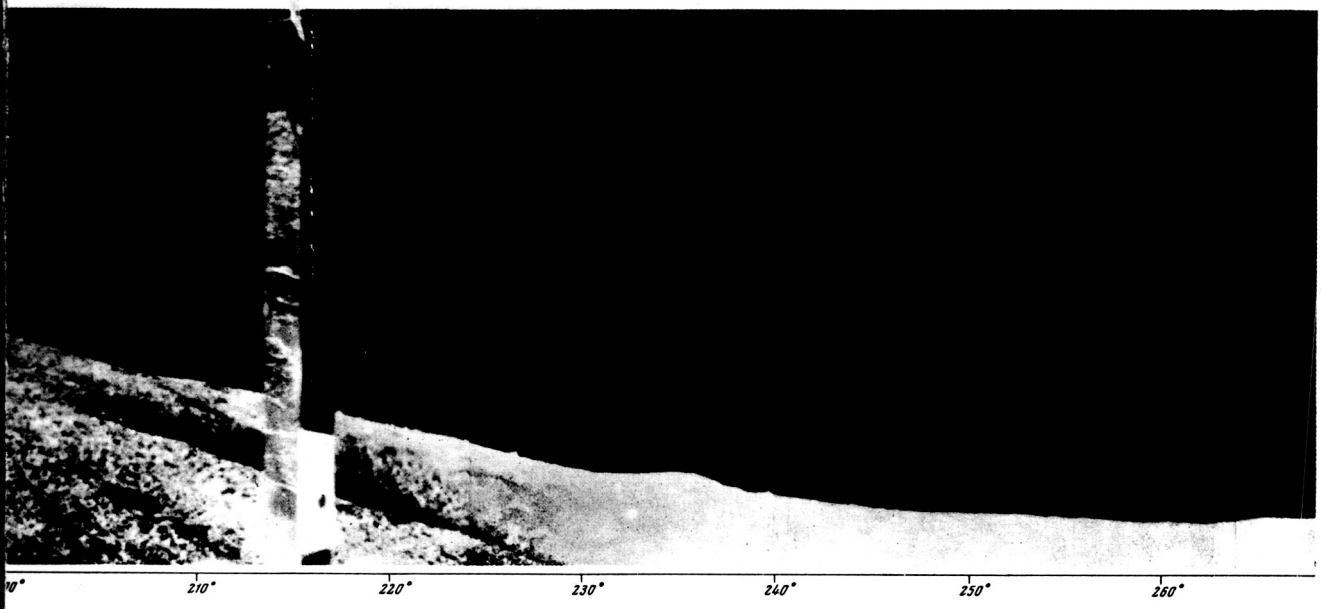


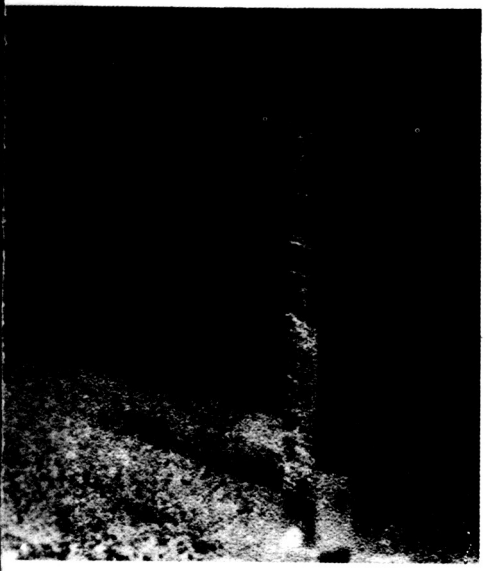




FOLDOUT FRAME 3

FOLDOUT FRAME 4







FOLDOUT FRAME 5

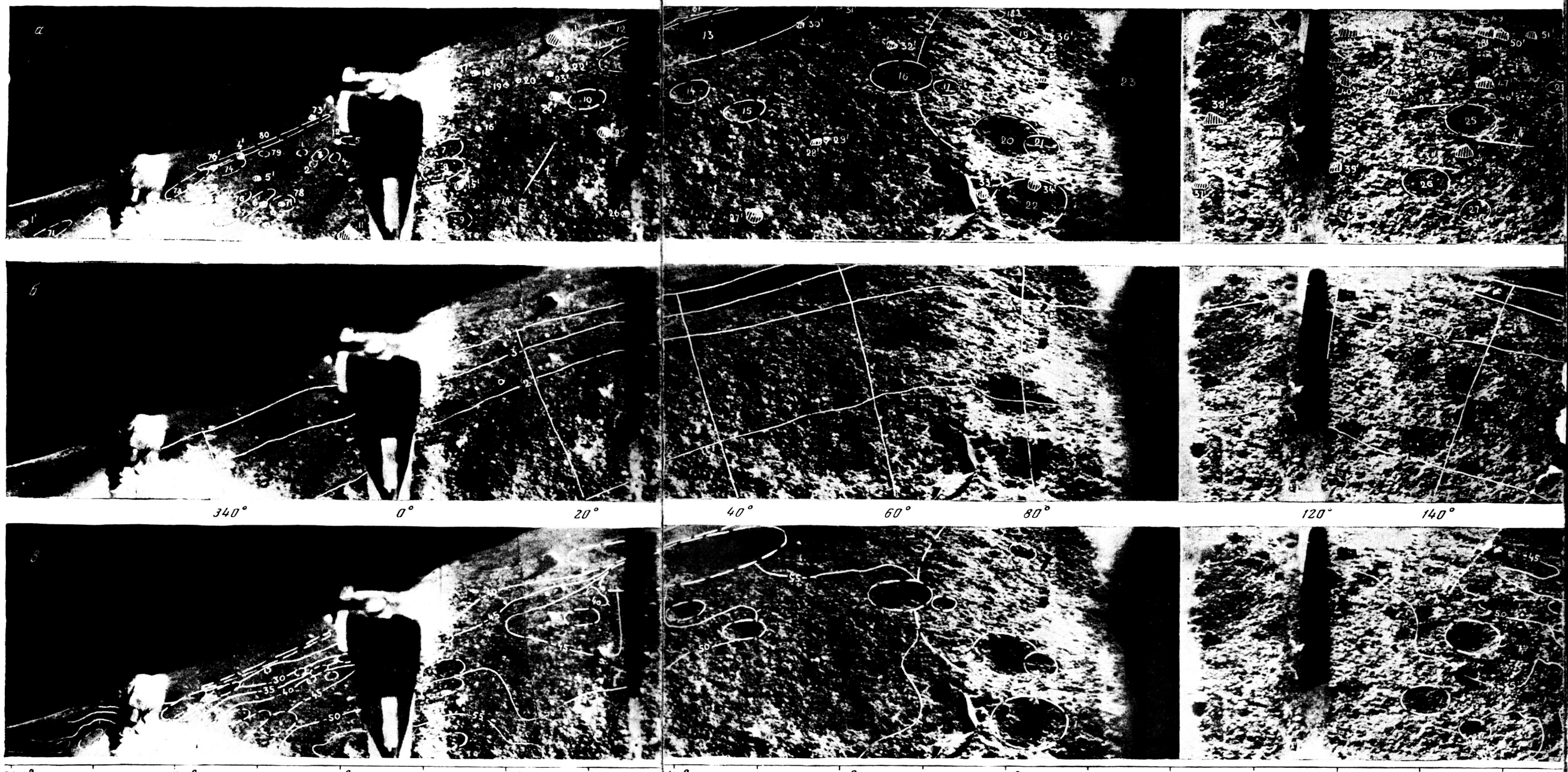


Fig 22 A

Fig 22 B

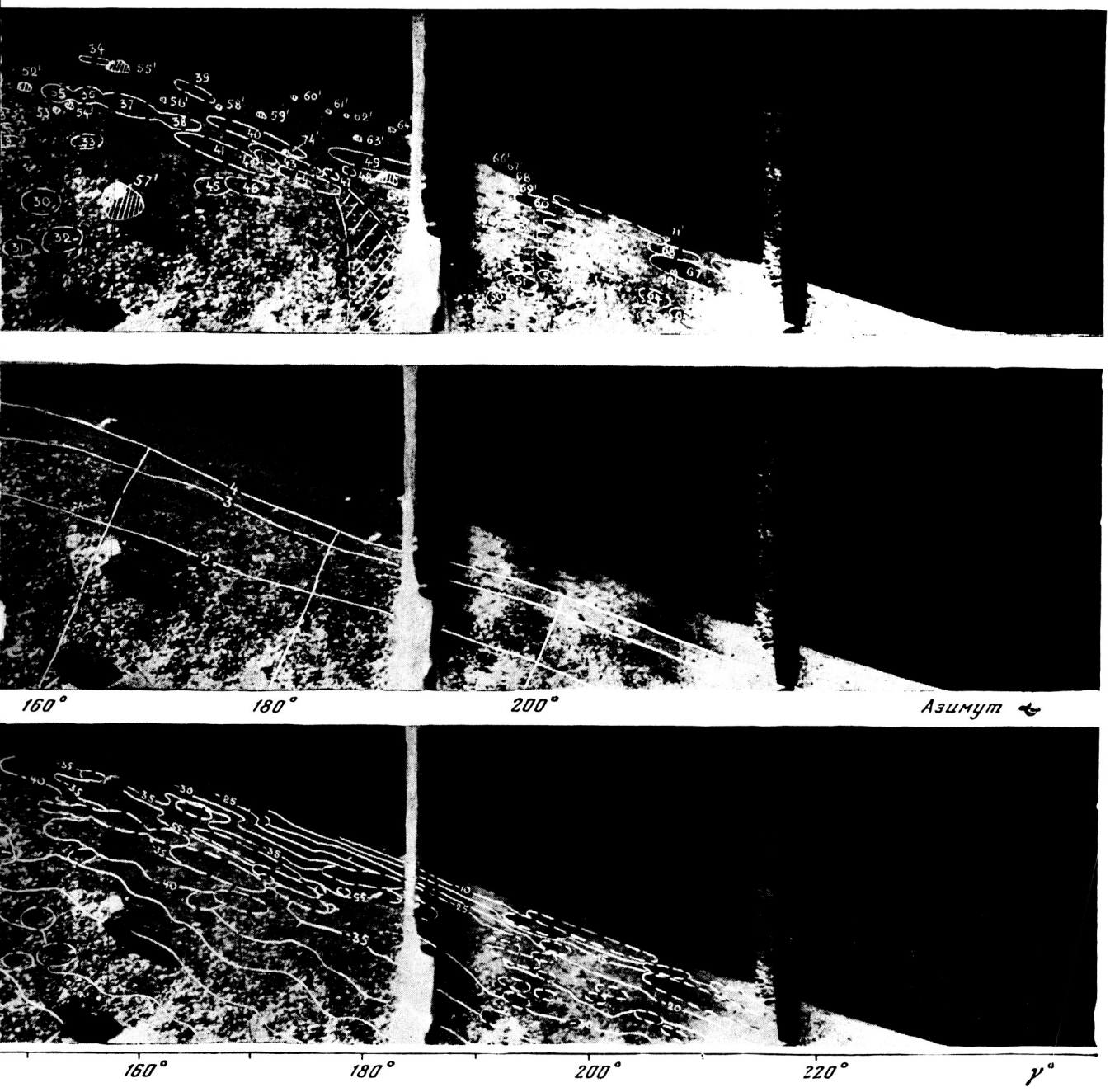


Fig. 22

а - Results of panorama deciphering
б - Image of range lines
в - Image of contour lines

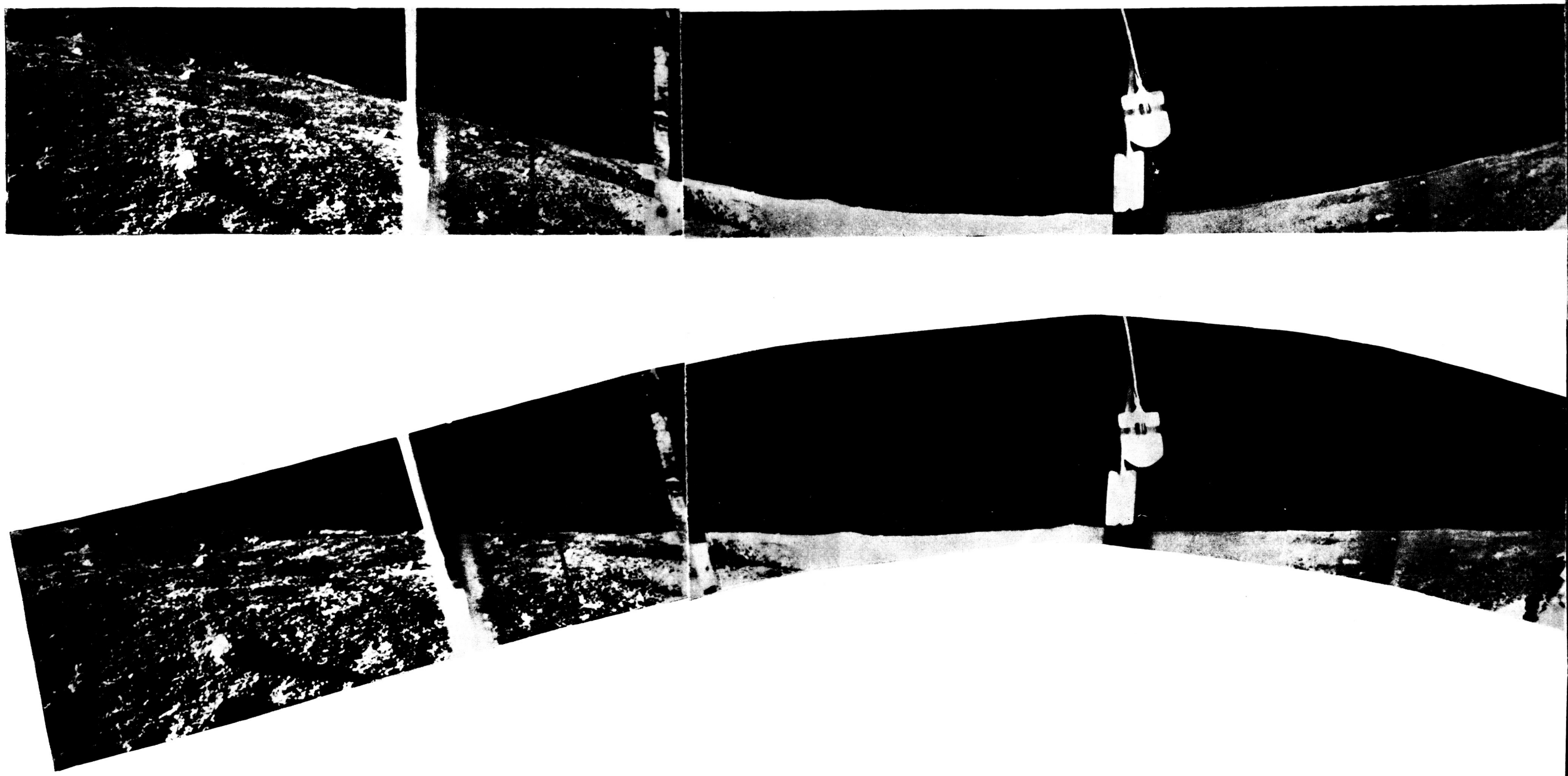


Fig 25. A

Fig 25 - B



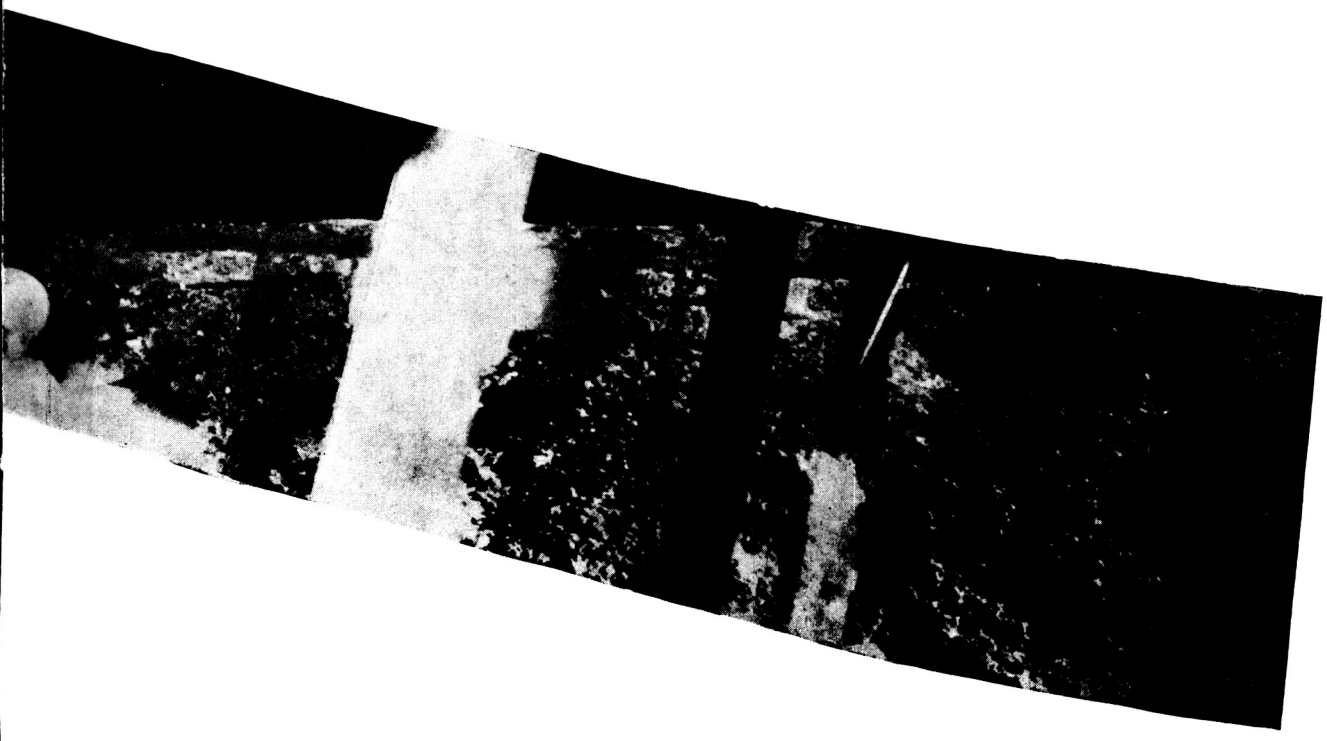
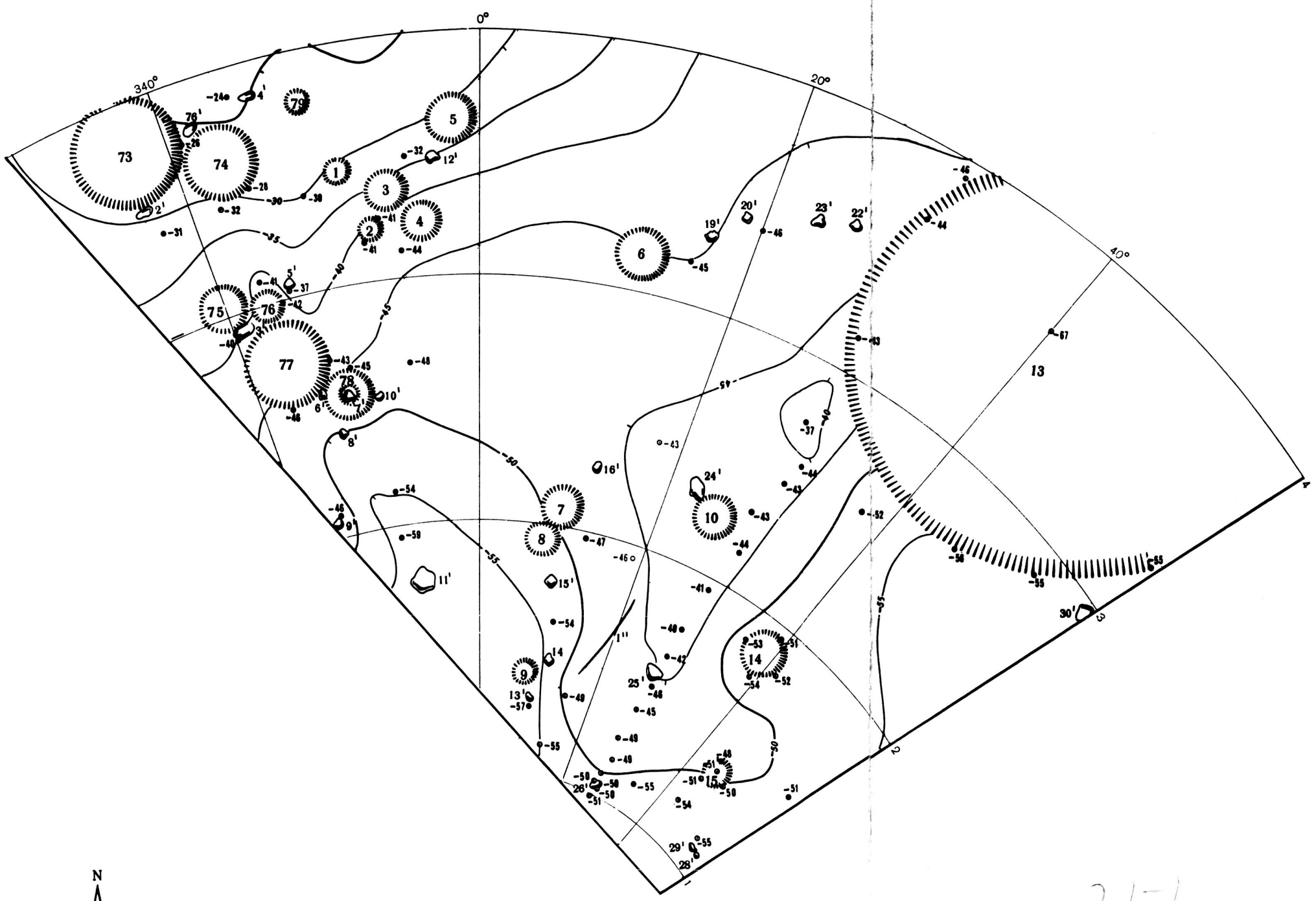


Fig. 25 C

Sweep and transformation of panoramic photographs
Above-panorama I, obtained at the station's inclinations at 16°;
Below-panorama I, transformed to the view at zero inclination

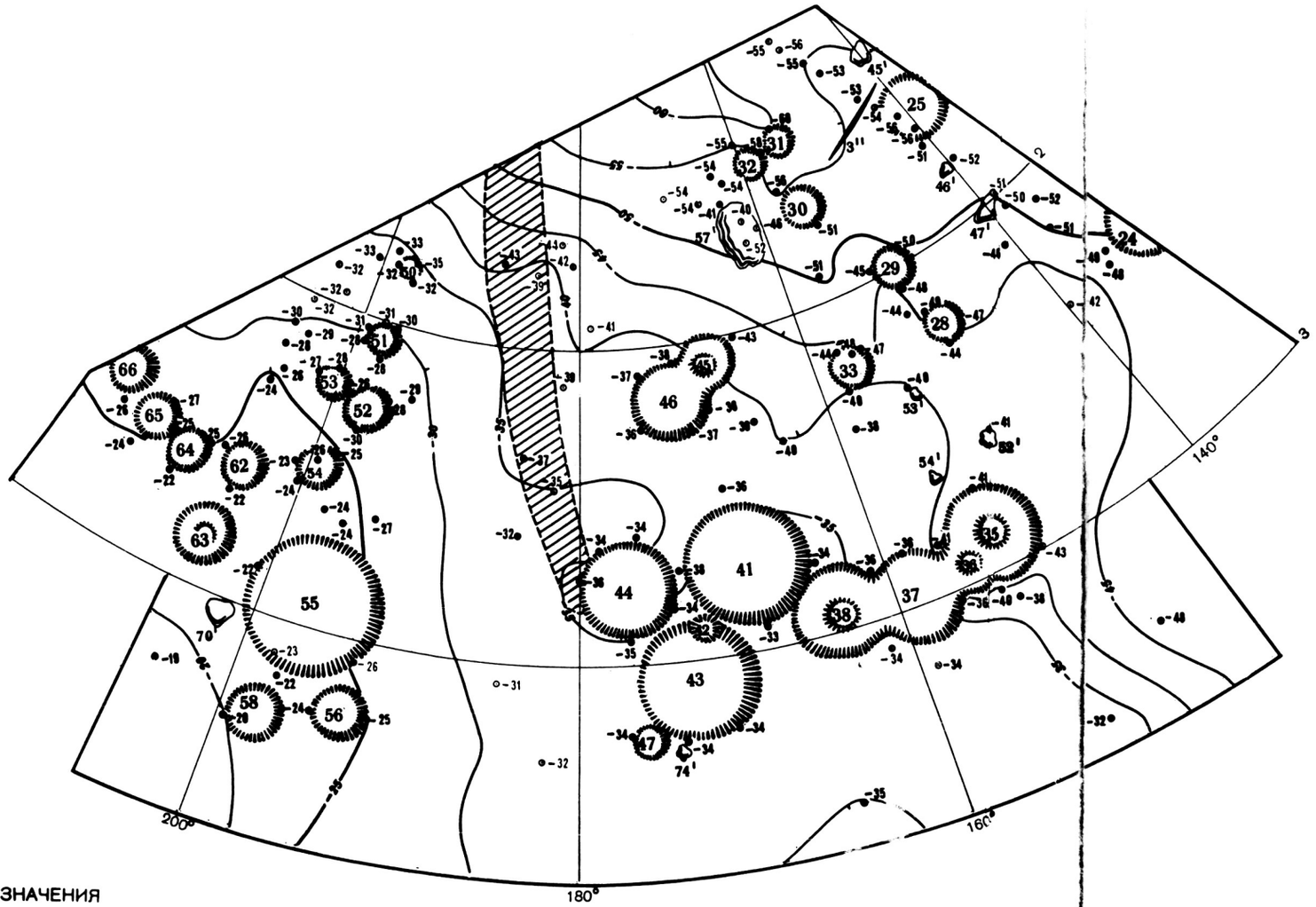
ТОПОГРАФИЧЕСКИЙ ПЛАН

МЕСТА ПОСАДКИ СОВЕТСКОЙ АВТОМАТИЧЕСКОЙ СТАНЦИИ "ЛУНА-9"



21-1

21-2



УСЛОВНЫЕ ОБОЗНАЧЕНИЯ

- •-47 — отметки высот (см)
- горизонтали
- (44) — кратеры
- 25' — камни
- 3'' — линейчатые образования, микрогряды
- 3 — линия дальностей (м)
- 80° 60° — линии азимутов

Масштаб 1:20

0,5 0 0,5 1,0 м

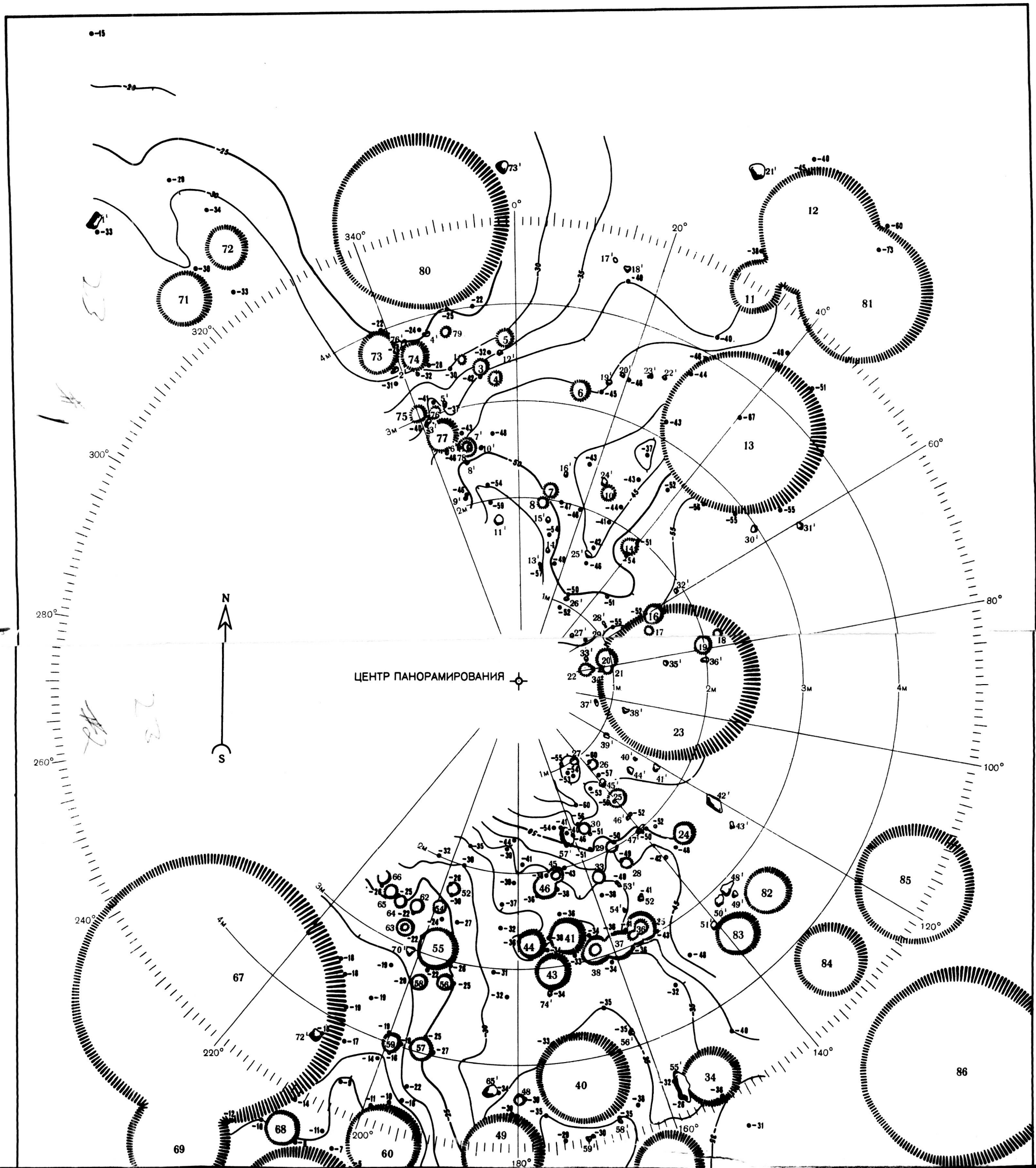
Сечение рельефа через 5

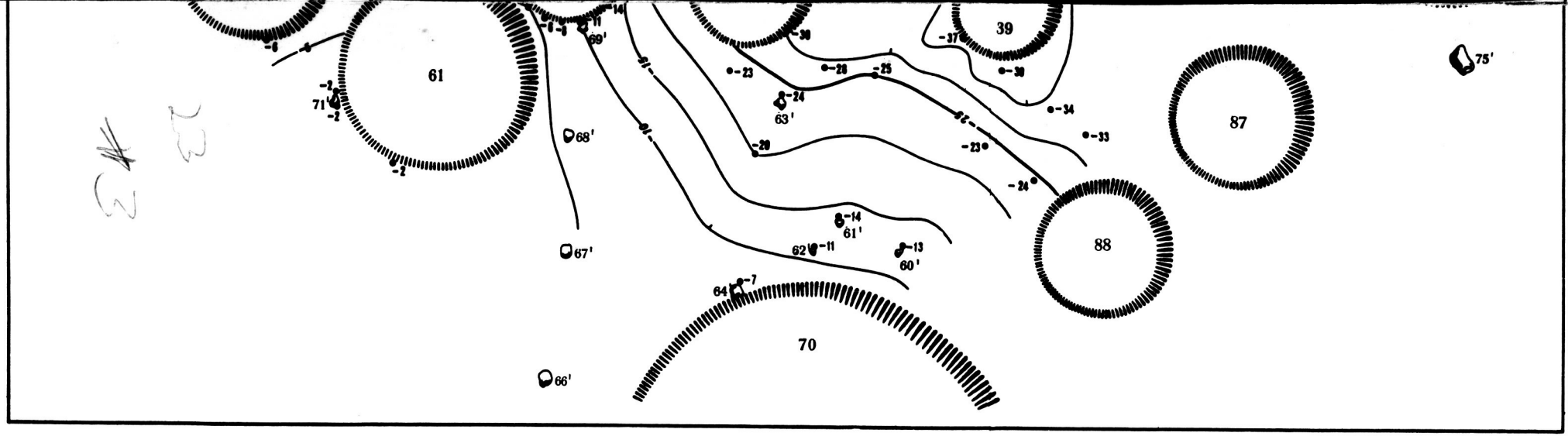
Отметки высот даны относительно центр[ь]ветьей панорамы

Топографический план составлен Московским институтом инженеров геодезии, аэрофотосъемки и картографии в 1966 году по материалам, полученным Советской автоматической станцией „Луна-9" 4 и 5 февраля 1966 года

ТОПОГРАФИЧЕСКАЯ СХЕМА

МЕСТА ПОСАДКИ СОВЕТСКОЙ АВТОМАТИЧЕСКОЙ СТАНЦИИ "ЛУНА-9"





Масштаб 1:40

1 0 1 2 м

Сечение рельефа через 5 см

Отметки высот даны относительно центра третьей панорамы

УСЛОВНЫЕ ОБОЗНАЧЕНИЯ

- отметки высот (см)
- горизонтали
- кратеры
- камни
- линия дальностей
- линии азимутов

Схема составлена Московским институтом инженеров геодезии, аэрофотосъемки и картографии в 1966 году по материалам, полученным Советской автоматической станцией „Луна-9" 4 и 5 февраля 1966 года